

THE PROCEEDINGS OF THE PHYSICAL SOCIETY

Section A

VOL. 63, PART 7

1 July 1950

No. 367 A

CONTENTS

	PAGE
Mr. SURAJ N. GUPTA. Theory of Longitudinal Photons in Quantum Electrodynamics	681
Prof. M. H. L. PRYCE. On the Energy of the Alpha-Particles from Radioactive Nuclei	692
Dr. W. E. MOFFITT. Excited Electronic Levels in Conjugated Molecules—IV: Symmetrical Cyanine Dyes	700
Mr. J. EWLES and Dr. C. CURRY. Resolution and Analysis of Low Temperature Luminescent Spectra of Bi and Pb Activated Solids of Simple Crystal Structure	708
Dr. A. A. SABRY. Influence of Dipole-Dipole Coupling on the Dielectric Constant of Dipolar Substances	716
Dr. P. WRIGHT. The Effect of Occluded Hydrogen on the Electrical Resistance of Palladium	727
Dr. R. S. TEBBLE, Dr. I. C. SKIDMORE and Dr. W. D. CORNER. The Barkhausen Effect	739
Dr. K. H. STEWART. Domain Wall Movement in a Single Crystal	761
Prof. A. RUBINOWICZ. Sommerfeld's Polynomial Method Simplified	766
Dr. M. W. FEAST. Investigation of the Spectrum of the High Voltage Arc in Carbon Dioxide: the CO Flame Spectrum	772
Letters to the Editor :	
Dr. F. D. S. BUTEMENT. Radioactive ¹⁶⁵ Er	775
Mr. E. R. RAE, Mr. J. G. RUTHERGLEN and Mr. R. D. SMITH. Proton Capture Radiation of Fluorine-19	775
Prof. H. FRÖHLICH. Isotope Effect in Superconductivity	778
Dr. A. G. GAYDON and Dr. H. G. WOLFARD. Excitation of Spectra in the Inner Cones of Flames	778
Corrigenda	780
Reviews of Books	780
Contents for Section B	783
Abstracts for Section B	783

Price to non-members 10s. net, by post 6d. extra. Annual subscription: £5 5s.
Composite subscription for both Sections A and B: £9 9s.

Published by
THE PHYSICAL SOCIETY
1 Lowther Gardens, Prince Consort Road, London S.W.7

PROCEEDINGS OF THE PHYSICAL SOCIETY

The *Proceedings* is now published monthly in two Sections.

ADVISORY BOARD

Chairman: The President of the Physical Society (L. F. BATES, D.Sc., Ph.D., F.R.S.).

E. N. da C. ANDRADE, Ph.D., D.Sc., F.R.S.
Sir EDWARD APPLETON, G.B.E., K.C.B., D.Sc.,
F.R.S.

P. M. S. BLACKETT, M.A., F.R.S.
Sir LAWRENCE BRAGG, O.B.E., M.A., Sc.D.,
D.Sc., F.R.S.

Sir JAMES CHADWICK, D.Sc., Ph.D., F.R.S.
LORD CHERWELL OF OXFORD, M.A., Ph.D.,
F.R.S.

Sir JOHN COCKCROFT, C.B.E., M.A., Ph.D.,
F.R.S.

Sir CHARLES DARWIN, K.B.E., M.C., M.A.,
Sc.D., F.R.S.

N. FEATHER, Ph.D., F.R.S.
G. I. FINCH, M.B.E., D.Sc., F.R.S.

D. R. HARTREE, M.A., Ph.D., F.R.S.

N. F. MOTT, M.A., F.R.S.

M. L. OLIPHANT, Ph.D., D.Sc., F.R.S.

F. E. SIMON, C.B.E., M.A., D.Phil., F.R.S.

T. SMITH, M.A., F.R.S.

Sir GEORGE THOMSON, M.A., D.Sc., F.R.S.

Papers for publication in the *Proceedings* should be addressed to the Hon. Papers Secretary,
Dr. H. H. HOPKINS, at the Office of the Physical Society, 1 Lowther Gardens, Prince
Consort Road, London S.W.7. Telephone: KENSington 0048, 0049.

Detailed Instructions to Authors were included in the February 1948 issue of
the *Proceedings*; separate copies can be obtained from the Secretary-Editor.

THE PHYSICAL SOCIETY

Founded 1874.

Incorporated 1878.

OFFICERS OF THE SOCIETY, 1950-51

President: Professor L. F. BATES, D.Sc., Ph.D., F.R.S.

Hon. Secretaries: C. G. WYNNE, B.A. (*Business*). H. H. HOPKINS, Ph.D. (*Papers*).

Hon. Foreign Secretary: Professor E. N. da C. ANDRADE, Ph.D., D.Sc., F.R.S.

Hon. Treasurer: A. J. PHILPOT, C.B.E., M.A., B.Sc.

Hon. Librarian: R. W. B. PEARSE, D.Sc., Ph.D.

SPECIALIST GROUPS

COLOUR GROUP

Chairman: W. S. STILES, O.B.E., D.Sc., Ph.D.

Hon. Secretary: R. G. HORNER, B.A.

LOW-TEMPERATURE GROUP

Chairman: Professor F. E. SIMON, C.B.E., M.A.,
D.Phil., F.R.S.

Hon. Secretary: G. G. HASELDEN, B.Sc., Ph.D.

OPTICAL GROUP

Chairman: A. C. G. MENZIES, M.A., D.Sc.

Hon. Secretary: K. J. HABELL, M.Sc.

ACOUSTICS GROUP

Chairman: H. L. KIRKE, C.B.E., M.I.E.E.

Hon. Secretaries: W. A. ALLEN, B.Arch.,
A.R.I.B.A., and A. T. PICKLES, O.B.E., M.A.

Secretary-Editor: Miss A. C. STICKLAND, M.Sc., Ph.D.

Offices and Library: 1 Lowther Gardens, Prince Consort Road, London S.W. 7.

Telephone: KENSington 0048, 0049

Now Ready

Metallurgical Applications of the **ELECTRON MICROSCOPE**

This book contains 13 papers presented at a Symposium on the subject, together with a report of a general discussion that took place upon them. Some of the papers summarize the present state of knowledge and experience in Great Britain, France, Germany and the United States, but others record the results of hitherto unpublished researches. The discussion contains important contributions from metallurgists and from leading authorities in the field of electron microscopy.

Besides being of value to all physicists and metallurgists working in this field, the book gives a most useful introduction to the subject for those who wish to know the potentialities and limitations of this comparatively new technique.

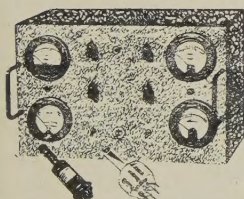
A comprehensive guide to the use of the electron microscope in metallurgy.


Cloth. 170 pages. 50 plates. $8\frac{1}{2} \times 5\frac{1}{2}$ in. 21s. or \$3.50, post free.

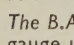
THE INSTITUTE OF METALS

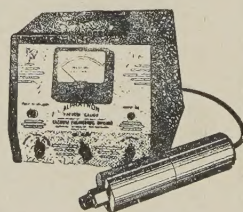
4 GROSVENOR GARDENS, LONDON, S.W.1

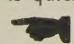
VACUUM LEAK DETECTION



 The B.A.R. Thermocouple-Ionisation Gauge Control. The newly developed Thermocouple-Ionisation Gauge Control, complete with Thermocouple and Ionisation Gauges, covers the pressure range from 2×10^{-7} mm. to 1 mm. Hg. Operation is dependable and simple. Ranges are 10^{-3} —1 mm. and 0—5, 0—10, 0—0.1 and 0—0.01 microns. The unit is removable from its cabinet for incorporation in a central panel.

 The B.A.R. Alphatron is an ionisation-type vacuum gauge using the ionising power of alpha particles from a radium source to measure total pressure of any gas, vapour or mixed atmosphere from 1 micron to 10 mm. Hg. with instantaneous linear response. The B.A.R. Alphatron is quickly available from batches now in production.



 The B.A.R. Thermocouple Gauge Control is a light, portable instrument that may be carried to any part of a plant or system for vacuum testing. It is compact, rugged and built throughout to withstand hard industrial use.

This unit gives pressure indications over a continuous range from 1 to 1,000 microns Hg. These pressures are read directly on the microammeter, which is calibrated both in microns and microamperes. By means of increased filament current and special calibration, the unit will indicate pressures up to 2 mm. Hg. The gauge is undamaged by operation at atmospheric pressure.

All of the above instruments are suitable for operating on a 230/250 volt, 50/60 cycle supply.

BRITISH AMERICAN RESEARCH LTD

(ASSOCIATED WITH NATIONAL RESEARCH CORPORATION, CAMBRIDGE, MASSACHUSETTS)

DESIGNERS AND MANUFACTURERS OF HIGH VACUUM GAUGES · VALVES · SEALS
DIFFUSION PUMPS · STILLS · FURNACES · COATING EQUIPMENT AND DEHYDRATION PLANT

NETHERTON ROAD · WISHAW · LANARKSHIRE



SCIENTIFIC BOOKS

Messrs. H. K. LEWIS can supply from stock or to order any book on the Physical and Chemical Sciences. Catalogues post free on request.

FOREIGN DEPARTMENT: Select stock. Books not in stock obtained under Board of Trade licence.

SECOND-HAND SCIENTIFIC BOOKS.

140 GOWER STREET.

An extensive stock of books in all branches of Pure and Applied Science may be seen in this department. Large and small collections bought.

Back volumes of Scientific Journals.

SCIENTIFIC LENDING LIBRARY. Annual Subscription from ONE GUINEA. Bi-monthly List of New Books and New Editions added to the Library sent post free on request. Prospectus post free.

STATIONERY DEPARTMENT. A Comprehensive range of Sectional Designers Papers, Graph Books and Pads. Sheets and Pads of Logarithmic—"Z" Charts—Circular Percentage—Reciprocal—Triple Co-ordinate—Polar Graph—Time Table (Gantt)—Daily, Weekly and Monthly Charts—Planning Sheets, etc., held in stock.

Telephone: EUSton 4282

Telegrams: "Publicavit,
Westcent, London"

H. K. LEWIS & Co. Ltd.

136 GOWER STREET, LONDON, W.C.1

Business hours: 9 a.m. to 5 p.m., Saturdays to 1 p.m.

BALDWIN 'Ionex' Ionization Meter

An Ionization measuring instrument of exceptionally high accuracy, which has the means for self-checking incorporated within it, and is therefore invaluable where there is no ready access to standards of ionization measurement.

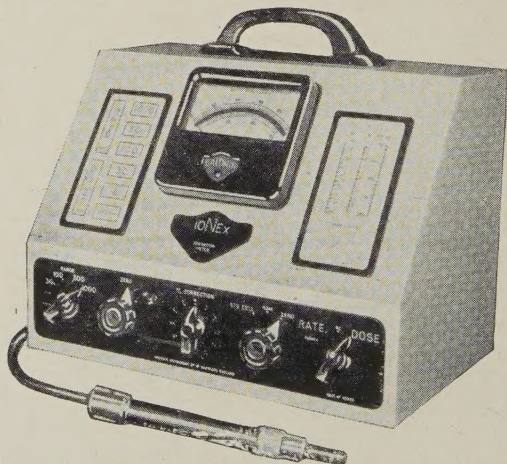
It measures either Dose or Dose-Rate.

In addition to the normal thimble chamber for X Rays, chambers are available for the measurement of Stray X and γ rays, soft X, α and β rays, radium needles and radon seeds, etc.

Ranges with thimble chamber are:—

Dose 30, 100, 300 & 1000 r

Dose-rate 30, 100, 300 & 1000 r/minute



Instrument with Thimble Ionization Chamber. Leaflet 118

BALDWIN INSTRUMENT CO. LTD., DARTFORD, KENT

Northern Agents: F. C. Robinson & Partners Ltd., 287 Deansgate, Manchester, 3

THE PHYSICAL SOCIETY

VOLUME XIII of the REPORTS ON PROGRESS IN PHYSICS

This Volume is to be published during July, and is a comprehensive annual review by specialist authors. The contents are as follows:

- M. P. LORD and W. D. WRIGHT. The Investigation of Eye Movements.
 L. GOLDBERG. Recent Advance in Infra-Red Solar Spectroscopy.
 W. G. PENNEY and H. H. M. PIKE. Shock Waves and the Propagation of
 Finite Pulses in Fluids.
 E. C. STONER. Ferromagnetism: Magnetization Curves.
 M. RYLE. Radio Astronomy.
 G. P. KUIPER. Planetary and Satellite Atmospheres.
 A. H. COOKE. Paramagnetic Relaxation Effects.
 J. H. FREMLIN and J. S. GOODEN. Cyclic Accelerators.
 C. F. POWELL. Mesons.

The price will be 50s. 0d. Members: One copy at 25s.

Further information can be obtained from

THE PHYSICAL SOCIETY

1 Lowther Gardens, Prince Consort Road, London S.W.7

BULLETIN ANALYTIQUE

Publication of the Centre National de la Recherche Scientifique, France

The *Bulletin Analytique* is an abstracting journal which appears monthly in two parts, Part I covering scientific and technical papers in the mathematical, chemical and physical sciences and their applications, Part II the biological sciences.

The *Bulletin*, which started on a modest scale in 1940 with an average of 10,000 abstracts per part, now averages 35 to 40,000 abstracts per part. The abstracts summarize briefly papers in scientific and technical periodicals received in Paris from all over the world and cover the majority of the more important journals in the world scientific press. The scope of the *Bulletin* is constantly being enlarged to include a wider selection of periodicals.

The *Bulletin* thus provides a valuable reference book both for the laboratory and for the individual research worker who wishes to keep in touch with advances in subjects bordering on his own.

A specially interesting feature of the *Bulletin* is the microfilm service. A microfilm is made of each article as it is abstracted and negative microfilm copies or prints from microfilm can be purchased from the editors.

The subscription rates for Great Britain are 4,000 frs. (£5) per annum for each part. Subscriptions can also be taken out to individual sections of the *Bulletin* as follows:

	frs.	
Pure and Applied Mathematics—Mathematics—Mechanics	550	14/6
Astronomy—Astrophysics—Geophysics	700	18/-
General Physics—Thermodynamics—Heat—Optics—Elec- tricity and Magnetism	900	22/6
Atomic Physics—Structure of Matter	325	8/6
General Chemistry—Physical Chemistry	325	8/6
Inorganic Chemistry—Organic Chemistry—Applied Chemistry—Metallurgy	1,800	45/-
Engineering Sciences	1,200	30/-
Mineralogy—Petrography—Geology—Paleontology ..	550	14/6
Biochemistry—Biophysics—Pharmacology	900	22/6
Microbiology—Virus and Phages	600	15/6
Animal Biology—Genetics—Plant Biology	1,800	45/-
Agriculture—Nutrition and the Food Industries ..	550	14/6

Subscriptions can be paid directly to the editors: Centre National de la Recherche Scientifique, 18, rue Pierre-Curie, Paris 5ème. (Compt-chèque-postal 2,500-42, Paris), or through Messrs. H. K. Lewis & Co. Ltd., 136, Gower Street, London W.C. 1.

PROCEEDINGS OF THE PHYSICAL SOCIETY

ADVERTISEMENT RATES

The *Proceedings* are divided into two parts, A and B. The charge for insertion is £18 for a full page in either Section A or Section B, £30 for a full page for insertion of the same advertisement in both Sections. The corresponding charges for part pages are:

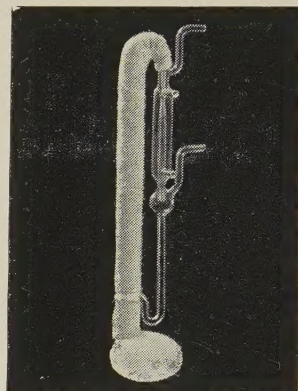
$\frac{1}{2}$ page	£9 5 0	£15 10 0
$\frac{1}{4}$ page	£4 15 0	£8 0 0
$\frac{1}{8}$ page	£2 10 0	£4 5 0

Discount is 20% for a series of six similar insertions and 10% for a series of three.

The printed area of the page is $8\frac{1}{2}'' \times 5\frac{1}{2}''$, and the screen number is 120.

Copy should be received at the Offices of the Physical Society six weeks before the date of publication of the *Proceedings*.

VITREOSIL MERCURY VAPOUR PUMPS



This new M.V. Fore Pump will operate from an ordinary water filter pump, and when used in conjunction with our Single-Stage or Two-Stage Pump, pressures less than 0.00002 mm. Hg. are attained.

Write for descriptive leaflet

THE THERMAL SYNDICATE LTD.

Head Office: Wallsend, Northumberland
London Office: 12-14 Old Pye Street, S.W.1

REPORTS ON PROGRESS IN PHYSICS

Volume XII (1948-1949)

Mass Spectrometry, by H. G. Thode and R. B. Shields.
Nuclear Paramagnetism, by B. V. Rollin. *Phosphors and Phosphorescence*, by G. F. J. Garlick. *Spontaneous Fluctuations*, by D. K. C. MacDonald. *Recent Nuclear Experiments with High Voltage X-Rays*, by W. Bosley and J. D. Craggs. *Linear Accelerators*, by D. W. Fry and W. Walkinshaw. *Viscosity and Related Properties in Glass*, by G. O. Jones. *Theory of the Oxidation of Metals*, by N. Cabrera and N. F. Mott. *Fracture and Strength of Solids*, by E. Orowan. *Multipole Radiation in Atomic Spectra*, by A. Rubinowicz. *Collisions between Atoms and Molecules at Ordinary Temperatures*, by H. S. W. Massey. *Low Temperature Physics*, by K. Mendelssohn. *Slow Neutron Absorption Cross-sections of the Elements*, by M. Ross and J. S. Story. *Molecular Distribution and Equation of State of Gases*, by J. de Boer.

Price £2 2s., postage and packing 1s.

Orders, with remittances, should be sent to the publishers:

THE PHYSICAL SOCIETY
1 Lowther Gardens, Prince Consort Road
London S.W.7

HANDBOOK OF THE PHYSICAL SOCIETY'S 34th EXHIBITION OF SCIENTIFIC INSTRUMENTS AND APPARATUS

1950

5s.; by post 6s.

Orders, with remittances, should be sent to

THE PHYSICAL SOCIETY
1 Lowther Gardens, Prince Consort Road,
London S.W.7

THE PROCEEDINGS OF THE PHYSICAL SOCIETY

Section A

VOL. 63, PART 7

1 July 1950

No. 367 A

Theory of Longitudinal Photons in Quantum Electrodynamics

BY SURAJ N. GUPTA *

Dublin Institute for Advanced Studies, Dublin, Eire †

*Communicated by W. Heitler; MS. received 20th June 1949 and in final form
13th December 1949*

ABSTRACT. The radiation field is quantized by introducing four types of photons—two transverse, one longitudinal, and one scalar. The scalar photons are treated by using an indefinite metric, and it is found necessary to modify the usual supplementary condition slightly. The present theory offers a justification for the symmetrical treatment of the four components of the electromagnetic potential, recently applied by a number of authors, and proves to be very convenient in applications. The results of physical interest, however, are the same as obtained from the ordinary formulation.

§ 1. INTRODUCTION

IN quantum electrodynamics usually the longitudinal part of the electromagnetic field is separated from the transverse part and replaced by the Coulomb interaction, which not only destroys the relativistic appearance of the interaction but is also inconvenient in application. It has been shown by Majumdar and the present writer (1947) that the self-energy of an electron may be easily obtained by treating the longitudinal field in the same way as the transverse field, and more recently the same device has been used by Feynman (1948). In some applications, Schwinger (1949) and Tomonaga and co-workers (Tati and Tomonaga 1948) have also adopted a symmetrical treatment for the four components of the electromagnetic potential. But so far no satisfactory justification for this procedure has been given. We, therefore, give a theory of quantizing the radiation field by introducing four types of photons corresponding to the four components of the electromagnetic potential. Two of these photons are transverse, one longitudinal and one scalar. Owing to the change in sign in the commutation relations for scalar photons, it has often been proposed to reverse the rôles of emission and absorption operators for scalar photons (see Dirac 1947). But this destroys the symmetry in the treatment of the four types of photons, and leads to difficulties (Ma 1949). Therefore we treat the scalar photons by using an indefinite metric and modify the usual supplementary condition. The use of an indefinite metric for the scalar photons does not raise any difficulty of physical interpretation. For, as a consequence of the supplementary condition,

* State Scholar of the Government of India.

† Now at the Cavendish Laboratory, Cambridge.

only transverse photons are observable, while the longitudinal and the scalar photons exist only in virtual states. For simplicity, the familiar momentum representation is used, and to show the advantage of the present treatment some applications are also given.

In the present paper the following notations will be used: Latin indices take the values 1, 2, 3, while Greek indices take the values 1, 2, 3, 4. A repeated Greek index is to be summed over all the four values. We shall often (explicitly) use the index 0 instead of 4, the relation between the two being $A_4 = iA_0$. For convenience, a Greek index will be used also for the quantity α_μ , where $\alpha_1, \alpha_2, \alpha_3$ are the Dirac matrices, and $\alpha_4 = i$ or $\alpha_0 = 1$. An asterisk denotes a complex conjugate or a Hermitian conjugate, while a dagger denotes an adjoint (for an indefinite metric the two concepts are different). We use natural units, i.e. we take $c = \hbar = 1$.

§ 2. QUANTIZATION OF THE RADIATION FIELD

For the reason already mentioned, the present treatment will differ from the usual one in the following two respects:

(1) We take the electromagnetic 4-potential A_μ to be a complex 4-vector with three Hermitian space-like components and one antiHermitian time-like component, i.e. we take A_μ to be of the form

$$A_\mu = N_\mu^{(1)}\Lambda^{(1)} + N_\mu^{(2)}\Lambda^{(2)} + N_\mu^{(3)}\Lambda^{(3)} + N_\mu^{(0)}\Lambda^{(0)}, \quad \dots\dots(1)$$

where $\Lambda^{(1)}, \Lambda^{(2)}, \Lambda^{(3)}, \Lambda^{(0)}$ are scalars, $\Lambda^{(1)}, \Lambda^{(2)}, \Lambda^{(3)}$ being Hermitian and $\Lambda^{(0)}$ anti-Hermitian, and $N_\mu^{(1)}, N_\mu^{(2)}, N_\mu^{(3)}, N_\mu^{(0)}$ are orthogonal unit 4-vectors, $N_\mu^{(1)}, N_\mu^{(2)}, N_\mu^{(3)}$ being space-like and $N_\mu^{(0)}$ time-like. It should be noted that we can choose a privileged frame of reference such that $A_i = \Lambda^{(i)}$, $A_0 = \Lambda^{(0)}$, and $N_\mu^{(0)} = (0, 0, 0, i)$. In general the components of $N_\mu^{(i)}$ and $N_\mu^{(0)}$ satisfy the relations

$$N_\mu^{(1)}N_\nu^{(1)} + N_\mu^{(2)}N_\nu^{(2)} + N_\mu^{(3)}N_\nu^{(3)} - N_\mu^{(0)}N_\nu^{(0)} = \delta_{\mu\nu}. \quad \dots\dots(2)$$

(2) We use an indefinite metric (Dirac 1942, 1943, Pauli 1943), i.e. we take the expectation value of an operator $f(A_\mu)$ for a state Φ of the radiation field to be given by

$$\langle f(A_\mu) \rangle = \Phi^\dagger f(A_\mu) \Phi, \quad \Phi^\dagger \equiv \Phi^* \eta, \quad \dots\dots(3)$$

where η is a Hermitian operator to be chosen later on in such a way that A_μ is self-adjoint in the sense:

$$A_\mu = \eta^{-1} A_\mu^* \eta = A_\mu^\dagger. \quad \dots\dots(4)$$

It follows from (4) that ηA_μ is Hermitian, and therefore the expectation values of A_μ are real.

The commutation relations for A_μ are given by

$$[A_\mu(x), A_\nu(x')] = (i/2)\delta_{\mu\nu}\Delta(x-x'), \quad \dots\dots(5)$$

where $\Delta(x-x')$ is the four-dimensional delta-function, and x denotes a space-time 4-vector. From (1) and (5) we obtain for the commutation relations of the Λ 's

$$\left. \begin{aligned} [\Lambda^{(1)}(x), \Lambda^{(1)}(x')] &= [\Lambda^{(2)}(x), \Lambda^{(2)}(x')] = [\Lambda^{(3)}(x), \Lambda^{(3)}(x')] = (i/2)\Delta(x-x') \\ [\Lambda^{(0)}(x), \Lambda^{(0)}(x')] &= -(i/2)\Delta(x-x'). \end{aligned} \right\} \quad \dots\dots(6)$$

We assume in the usual way that the radiation field is enclosed in a box of unit volume with periodic boundary conditions, and expand the Λ 's as follows:

$$\left. \begin{aligned} \Lambda^{(i)} &= \sum_{\mathbf{k}} \sqrt{\left(\frac{2\pi}{k}\right)} \{C_i(\mathbf{k}) \exp[i(\mathbf{k} \cdot \mathbf{r} - kt)] + C_i^\dagger(\mathbf{k}) \exp[-i(\mathbf{k} \cdot \mathbf{r} - kt)]\} \\ \Lambda^{(0)} &= \sum_{\mathbf{k}} \sqrt{\left(\frac{2\pi}{k}\right)} \{C_0(\mathbf{k}) \exp[i(\mathbf{k} \cdot \mathbf{r} - kt)] + C_0^\dagger(\mathbf{k}) \exp[-i(\mathbf{k} \cdot \mathbf{r} - kt)]\}, \end{aligned} \right\} \dots\dots(7)$$

$$\text{where} \quad C_i^\dagger(\mathbf{k}) = C_i^*(\mathbf{k}), \quad C_0^\dagger(\mathbf{k}) = -C_0^*(\mathbf{k}). \quad \dots\dots(8)$$

We then obtain from (6)

$$\left. \begin{aligned} [C_1(\mathbf{k}), C_1^\dagger(\mathbf{k})] &= [C_2(\mathbf{k}), C_2^\dagger(\mathbf{k})] = [C_3(\mathbf{k}), C_3^\dagger(\mathbf{k})] = 1 \\ [C_0(\mathbf{k}), C_0^\dagger(\mathbf{k})] &= -1, \end{aligned} \right\} \dots\dots(9)$$

all other commutators being zero. Thus, we have

$$C_i(\mathbf{k}) = \frac{\partial}{\partial C_i^\dagger(\mathbf{k})}, \quad C_0(\mathbf{k}) = -\frac{\partial}{\partial C_0^\dagger(\mathbf{k})}. \quad \dots\dots(10)$$

The Lagrangian density for the radiation field may be taken to be

$$\mathcal{L} = -\frac{1}{8\pi} \left\{ \left(\frac{\partial A_\mu}{\partial x_\mu} \right)^2 + \frac{1}{2} \left(\frac{\partial A_\mu}{\partial x_\nu} - \frac{\partial A_\nu}{\partial x_\mu} \right)^2 \right\}. \quad \dots\dots(11)$$

This gives in the usual way for the equation of motion and the Hamiltonian density respectively

$$\square^2 A_\mu = 0 \quad \dots\dots(12a)$$

and

$$\mathcal{H} = \frac{1}{8\pi} \left\{ \left(\frac{\partial \mathbf{A}}{\partial t} \right)^2 + (\text{curl } \mathbf{A})^2 + (\text{div } \mathbf{A})^2 - \left(\frac{\partial A_0}{\partial t} \right)^2 - (\text{grad } A_0)^2 \right\}. \quad \dots\dots(12b)$$

Substituting the Fourier expansions for A_μ from (1) and (7), using the commutation relations (9), and omitting the zero-point energy, we get for the Hamiltonian

$$\int \mathcal{H} dv = \sum_{\mathbf{k}} \{ C_1^\dagger(\mathbf{k}) C_1(\mathbf{k}) + C_2^\dagger(\mathbf{k}) C_2(\mathbf{k}) + C_3^\dagger(\mathbf{k}) C_3(\mathbf{k}) - C_0^\dagger(\mathbf{k}) C_0(\mathbf{k}) \}. \quad \dots\dots(13)$$

Corresponding to each value of \mathbf{k} , the Hamiltonian describes four 'radiation oscillators', which may be treated in the usual way.

We shall now confine our attention to a particular value of \mathbf{k} , and drop the suffix \mathbf{k} . We first consider the component $N_\mu^{(1)} \Lambda^{(1)}$ of the radiation field. The quantity $C_1^\dagger C_1$, which gives the number of photons associated with this component, has the eigenvalues 0, 1, 2, ... For a state containing n_1 such photons the eigenfunction $\phi_1(n_1)$ and its adjoint $\phi_1^\dagger(n_1)$ are given by

$$\phi_1(n_1) = (n_1!)^{-1/2} C_1^{n_1}, \quad \phi_1^\dagger(n_1) = (n_1!)^{-1/2} C_1^{n_1}, \quad \dots\dots(14)$$

$$\text{with} \quad \phi_1^\dagger(m_1) \phi_1(n_1) = \delta_{m_1 n_1}. \quad \dots\dots(15)$$

The operators C_1 and C_1^\dagger have the simple meaning of the absorption and the emission operators respectively, for

$$C_1 \phi_1(n_1) = n_1^{1/2} \phi_1(n_1 - 1), \quad C_1^\dagger \phi_1(n_1) = (n_1 + 1)^{1/2} \phi_1(n_1 + 1). \quad \dots\dots(16)$$

The matrix elements of C_1 and C_1^\dagger , as defined below, are given by

$$\left. \begin{aligned} [C_1]_{m_1 n_1} &= \phi_1^\dagger(m_1) C_1 \phi_1(n_1) = n_1^{1/2} \delta_{m_1, n_1-1} \\ [C_1^\dagger]_{n_1 m_1} &= \phi_1^\dagger(n_1) C_1^\dagger \phi_1(m_1) = n_1^{1/2} \delta_{m_1, n_1-1} \end{aligned} \right\} \dots\dots (17)$$

For the components $N_\mu^{(2)}\Lambda^{(2)}$ and $N_\mu^{(3)}\Lambda^{(3)}$, we have only to replace the suffix 1 by 2 and 3 respectively in the above results.

The treatment for the component $N_\mu^{(0)}\Lambda^{(0)}$ is somewhat different due to the difference of sign in (9), which makes the use of an indefinite metric necessary. In this case the quantity $C_0^\dagger C_0$ has the eigenvalues 0, -1, -2, ..., and therefore the number of photons is given by $-C_0^\dagger C_0$. In spite of this difference, according to (13) the eigenvalues of the energy of these photons are also positive. For a state containing n_0 such photons the eigenfunction $\phi_0(n_0)$ and its adjoint $\phi_0^\dagger(n_0)$ are again given by

$$\phi_0(n_0) = (n_0!)^{-1/2} C_0^\dagger n_0, \quad \phi_0^\dagger(n_0) = (n_0!)^{-1/2} C_0 n_0, \quad \dots\dots (18)$$

with a different normalization rule

$$\phi_0^\dagger(m_0) \phi_0(n_0) = (-1)^{n_0} \delta_{m_0 n_0}. \quad \dots\dots (19)$$

Again, C_0 and C_0^\dagger are the absorption and the emission operators respectively, for

$$C_0 \phi_0(n_0) = -n_0^{1/2} \phi_0(n_0-1), \quad C_0^\dagger \phi_0(n_0) = (n_0+1)^{1/2} \phi_0(n_0+1). \quad \dots\dots (20)$$

The matrix elements of C_0 and C_0^\dagger , as defined below, are given by

$$\left. \begin{aligned} [C_0]_{m_0 n_0} &= \phi_0^\dagger(m_0) C_0 \phi_0(n_0) = (-1)^{n_0} n_0^{1/2} \delta_{m_0, n_0-1} \\ [C_0^\dagger]_{n_0 m_0} &= \phi_0^\dagger(n_0) C_0^\dagger \phi_0(m_0) = (-1)^{n_0} n_0^{1/2} \delta_{m_0, n_0-1} \end{aligned} \right\} \dots\dots (21)$$

Since, according to (3), we have

$$\begin{aligned} \Phi^* \eta \Phi &= \phi_1^*(n_1) \phi_2^*(n_2) \phi_3^*(n_3) \phi_0^*(n_0) \eta \phi_1(m_1) \phi_2(m_2) \phi_3(m_3) \phi_0(m_0) \\ &= \phi_1^\dagger(n_1) \phi_2^\dagger(n_2) \phi_3^\dagger(n_3) \phi_0^\dagger(n_0) \phi_1(m_1) \phi_2(m_2) \phi_3(m_3) \phi_0(m_0), \end{aligned}$$

it follows from (15) and (19) that the operator η is given by

$$\langle n_1 n_2 n_3 n_0 | \eta | m_1 m_2 m_3 m_0 \rangle = (-1)^{n_0} \delta_{n_1 m_1} \delta_{n_2 m_2} \delta_{n_3 m_3} \delta_{n_0 m_0}. \quad \dots\dots (22)$$

This shows that states corresponding to odd values of n_0 occur with a negative normalization $\Phi^* \eta \Phi$. But this does not raise any difficulty of physical interpretation, as we shall see below.

§ 3. THE SUPPLEMENTARY CONDITION

We can choose the space-like unit 4-vectors $N_\mu^{(1)}$, $N_\mu^{(2)}$, $N_\mu^{(3)}$ in an infinite number of ways such that they are orthogonal to each other as well as to a given $N_\mu^{(0)}$. In particular, we can choose them in such a way that for the k_μ -component of the field

$$k_\mu N_\mu^{(1)} = k_\mu N_\mu^{(2)} = 0, \quad k_\mu N_\mu^{(3)} = -k_\mu N_\mu^{(0)}. \quad \dots\dots (23)$$

In this case, the photons corresponding to the k_μ -components of $N_\mu^{(1)}\Lambda^{(1)}$ and $N_\mu^{(2)}\Lambda^{(2)}$ may be called the transverse photons, and those corresponding to the k_μ -components of $N_\mu^{(3)}\Lambda^{(3)}$ and $N_\mu^{(0)}\Lambda^{(0)}$ may be called the longitudinal and the scalar photons respectively. Thus, corresponding to each value of k_μ , we have two transverse one longitudinal, and one scalar photon. We note that the

k_μ -components of $N_\mu^{(1)}\Lambda^{(1)} + N_\mu^{(2)}\Lambda^{(2)}$, $N_\mu^{(3)}\Lambda^{(3)}$, and $N_\mu^{(0)}\Lambda^{(0)}$ are not transverse, longitudinal and scalar in the ordinary sense. They may be called generalized transverse, longitudinal, and scalar components respectively, and they reduce to the ordinary meaning in the special frame of reference in which $N_\mu^{(0)} = (0, 0, 0, i)$.

In order to account for the experimental fact that only transverse photons are observed, we have to impose some supplementary condition which will make longitudinal and scalar photons unobservable. We choose the supplementary condition to be

$$\left[\frac{\partial A_\mu}{\partial x_\mu} \right]^+ \Phi = 0, \quad \Phi^\dagger \left[\frac{\partial A_\mu}{\partial x_\mu} \right]^- = 0, \quad \dots\dots(24)$$

where $\left[\frac{\partial A_\mu}{\partial x_\mu} \right]^+$ and $\left[\frac{\partial A_\mu}{\partial x_\mu} \right]^-$ are respectively the positive and the negative frequency parts of $\partial A_\mu / \partial x_\mu$. This condition is weaker than the usual supplementary condition $(\partial A_\mu / \partial x_\mu) \Phi = 0$, which is too restrictive to allow any state of the radiation field to satisfy it.

Using (1), (7) and (23), we obtain from (24) for a pure radiation field

$$(C_3 - C_0) \Phi = 0. \quad \dots\dots(25)$$

Now, a general state of the radiation field will be of the form

$$\Phi = \sum_{n_1, n_2, n_3, n_0} A_{n_1, n_2, n_3, n_0} \Phi(n_1, n_2, n_3, n_0), \quad \dots\dots(26)$$

where the A 's are numerical coefficients, and $\Phi(n_1, n_2, n_3, n_0)$ is a normalized eigenstate containing n_1 and n_2 transverse, n_3 longitudinal, and n_0 scalar photons. Applying the condition (25) to (26), we get

$$n_3^{1/2} A_{n_1, n_2, n_3, n_0-1} + n_0^{1/2} A_{n_1, n_2, n_3-1, n_0} = 0,$$

where $n_3, n_0 = 0, 1, 2, \dots$, and the coefficient A with a negative suffix is to be taken as zero. It follows that the states of the pure radiation field allowed by the supplementary condition are

$$\begin{aligned} \Phi_0 &= \Phi(n_1, n_2, 0, 0) \\ \Phi_1 &= \Phi(n_1, n_2, 1, 0) - \Phi(n_1, n_2, 0, 1) \\ \Phi_2 &= \Phi(n_1, n_2, 2, 0) - \sqrt{2} \Phi(n_1, n_2, 1, 1) + \Phi(n_1, n_2, 0, 2) \quad \text{etc.} \end{aligned} \quad \dots\dots(27)$$

These states can be added with arbitrary coefficients, and the resultant state normalized. But, for all of these states, except Φ_0 , the normalization $\Phi^\dagger \Phi$ vanishes on account of (15) and (19). Therefore, a state of the radiation field satisfying (24) will be of the form

$$\Phi = \Phi_0 + a_1 \Phi_1 + a_2 \Phi_2 + \dots, \quad \dots\dots(28)$$

where the a 's are arbitrary coefficients, and

$$\Phi^\dagger \Phi = \Phi_0^\dagger \Phi_0.$$

The terms with arbitrary coefficients in (28) do not contribute to the expectation value of the Hamiltonian of the radiation field. We call them the redundant terms, because they do not give rise to any observable effect. Thus, in a pure radiation field only transverse photons are present, and we may take

$$n_3 = n_0 = 0. \quad \dots\dots(29)$$

It should be noted that our supplementary condition (24) may still be regarded as the quantum analogue of the classical Lorentz condition $\partial A_\mu / \partial x_\mu = 0$, because according to (24) the expectation value of $\partial A_\mu / \partial x_\mu$ vanishes, i.e.

$$\Phi^\dagger \frac{\partial A_\mu}{\partial x_\mu} \Phi = 0. \quad \dots\dots (30 a)$$

We may also obtain the quantum analogues of the Maxwell's equations according to the present theory. The electric and the magnetic fields \mathbf{E} and \mathbf{H} are given by

$$\mathbf{E} = -\frac{\partial \mathbf{A}}{\partial t} - \text{grad } A_0, \quad \mathbf{H} = \text{curl } \mathbf{A}. \quad \dots\dots (30 b)$$

From (12 a), (30 a) and (30 b), we obtain

$$\left. \begin{aligned} \text{div } \mathbf{H} &= 0, \\ \frac{\partial \mathbf{H}}{\partial t} + \text{curl } \mathbf{E} &= 0, \\ \Phi^\dagger (\text{div } \mathbf{E}) \Phi &= 0, \\ \Phi^\dagger \left(\frac{\partial \mathbf{E}}{\partial t} - \text{curl } \mathbf{H} \right) \Phi &= 0. \end{aligned} \right\} \quad \dots\dots (30 c)$$

§ 4. INTERACTION OF ELECTRONS WITH RADIATION

So far we have considered a pure radiation field. The interaction of electrons with radiation may be treated in the usual way. However, to understand the meaning of our supplementary condition, the following remarks should first be noted:

(1) The supplementary condition (24), being weaker than the usual one, is evidently compatible with the equation of motion of the system. Therefore, if (24) holds for the initial state, it will also hold for all the subsequent states. A formal proof of its consistency may be given in the usual way.

(2) As shown in the last section, in the absence of interaction our supplementary condition implies the absence of longitudinal or scalar photons.

(3) In the presence of interaction the supplementary condition still holds, but (25) does not follow from it because now the field equation takes the form $\square^2 A_\mu = -j_\mu$ and we cannot use the expansions (7) with their time factors. Therefore, in the presence of interaction the supplementary condition does not imply the absence of longitudinal or scalar photons.

In most cases of practical interest, the initial and the final states may be taken to be interaction-free, while the interaction may be treated as a perturbation, which is switched on adiabatically in the initial state and switched off in the final state. In such cases, it follows from the above remarks that longitudinal or scalar photons do not exist in the initial state, and though they may occur in intermediate states, they will again disappear in the final state. We have also verified this situation by direct calculations in a number of cases. In fact, it is found that the effect of the emission of real longitudinal or scalar photons is merely to change the coefficients of the redundant terms in the final state. But since the redundant terms have zero normalization, the transition probability for the real emission of longitudinal or scalar photons vanishes. In other words, the probability of the emission of a real longitudinal photon is cancelled by the 'negative probability' of the emission of a corresponding scalar photon.

The Hamiltonian \tilde{H} for a system of electrons and the radiation field is given by

$$\tilde{H} = H_0 + H, \quad \dots\dots(31)$$

where H_0 is the sum of the Hamiltonians of the electron and the radiation field, and H is their mutual interaction given by

$$H = - \int A_\mu j_\mu dv, \quad j_\mu = e\psi^* \alpha_\mu \psi. \quad \dots\dots(32)$$

The expectation value of \tilde{H} is

$$\langle \tilde{H} \rangle = \Phi^* \eta \tilde{H} \Phi. \quad \dots\dots(33)$$

Using the ordinary perturbation theory or the method of canonical transformation, it may be easily seen that

$$H_1 = H_{ba}, \quad H_2 = \frac{H_{bc} \eta_{cc} H_{ca}}{E_a - E_c}, \quad \text{etc.}, \quad \dots\dots(34)$$

where H_1 and H_2 are the expectation values of the first and the second order interaction energies respectively for the transition from a state a to a state b , and

$$H_{ba} = \Phi_b^* \eta H \Phi_a, \quad \eta_{aa} = \Phi_a^* \eta \Phi_a, \quad E_a = \Phi_a^* H_0 \Phi_a. \quad \dots\dots(35)$$

Now, we have

$$H_{ba} = \eta_{bb} H'_{ba}, \quad \text{where} \quad H'_{ba} = \Phi_b^* H \Phi_a. \quad \dots\dots(36)$$

Since, according to (22) and (29), $\eta_{aa} = 1$ for a final state, and $\eta_{aa}^2 = 1$ for any state, (34) reduces to

$$H_1 = H'_{ba}, \quad H_2 = \frac{H'_{bc} H'_{ca}}{E_a - E_c}, \quad \text{etc.} \quad \dots\dots(37)$$

Thus, in spite of the use of the indefinite metric, η does not occur in the perturbation formulae.

Using Fourier expansions similar to (7), but without their time factors, we obtain from (32) in the usual way

$$\begin{aligned} H'_{ba} = -e \sqrt{\left(\frac{2\pi}{k}\right)} & \left[\{ [C_i(\mathbf{k})]'_{ba} \delta_{\mathbf{p}_a + \mathbf{k}, \mathbf{p}_b} + [C_i^\dagger(\mathbf{k})]'_{ba} \delta_{\mathbf{p}_a, \mathbf{p}_b + \mathbf{k}} \} N_\mu^{(i)} (u_b^* \alpha_\mu u_a) \right. \\ & \left. + \{ [C_0(\mathbf{k})]'_{ba} \delta_{\mathbf{p}_a + \mathbf{k}, \mathbf{p}_b} + [C_0^\dagger(\mathbf{k})]'_{ba} \delta_{\mathbf{p}_a, \mathbf{p}_b + \mathbf{k}} \} N_\mu^{(0)} (u_b^* \alpha_\mu u_a) \right], \end{aligned} \quad \dots\dots(38)$$

where \mathbf{p}_a and \mathbf{p}_b are the momenta of the electron, and u_a and u_b are its Dirac amplitudes, while $[C_\mu(\mathbf{k})]'_{ba}$ and $[C_\mu^\dagger(\mathbf{k})]'_{ba}$ are given by

$$\left. \begin{aligned} [C_i(\mathbf{k})]'_{ba} &= \Phi_b^* C_i(\mathbf{k}) \Phi_a = n_a^{1/2} \delta_{n_b, n_a-1}, \\ [C_i^\dagger(\mathbf{k})]'_{ba} &= \Phi_b^* C_i^\dagger(\mathbf{k}) \Phi_a = n_b^{1/2} \delta_{n_b, n_a+1}, \\ [C_0(\mathbf{k})]'_{ba} &= \Phi_b^* C_0(\mathbf{k}) \Phi_a = -n_a^{1/2} \delta_{n_b, n_a-1}, \\ [C_0^\dagger(\mathbf{k})]'_{ba} &= \Phi_b^* C_0^\dagger(\mathbf{k}) \Phi_a = n_b^{1/2} \delta_{n_b, n_a+1}. \end{aligned} \right\} \quad \dots\dots(39)$$

The occurrence of a minus sign in the matrix elements of $[C_0(\mathbf{k})]'_{ba}$ is very important, and is due to the fact that $\Lambda^{(0)}$ is antiHermitian.

As already mentioned, according to (2), there exists a special frame of reference in which $A_i = \Lambda^{(i)}$ and $A_0 = \Lambda^{(0)}$. Since there is no physical reason to choose this special frame of reference in any particular way, we may choose it arbitrarily

according to convenience. The most convenient choice, of course, will be to take this special frame of reference to be the same as that in which the calculations are to be carried out. In that case (38) reduces to

$$H'_{ba} = -e \sqrt{\left(\frac{2\pi}{k}\right)} \left[\{ [C_i(\mathbf{k})]_{ba} \delta_{\mathbf{p}_a + \mathbf{k}, \mathbf{p}_b} + [C_i^\dagger(\mathbf{k})]_{ba} \delta_{\mathbf{p}_a, \mathbf{p}_b + \mathbf{k}} \} (u_b^* \alpha_i u_a) \right. \\ \left. - \{ [C_0(\mathbf{k})]_{ba} \delta_{\mathbf{p}_a + \mathbf{k}, \mathbf{p}_b} + [C_0^\dagger(\mathbf{k})]_{ba} \delta_{\mathbf{p}_a, \mathbf{p}_b + \mathbf{k}} \} (u_b^* \alpha_0 u_a) \right]. \quad \dots\dots (40)$$

Using these matrix elements, we shall now consider some applications.

§ 5. INTERACTION OF TWO ELECTRONS

We consider the interaction between two electrons whose initial momenta are \mathbf{p}_1 and \mathbf{p}_2 and final momenta \mathbf{p}'_1 and \mathbf{p}'_2 . Let the Dirac amplitudes of the electrons be u_1 and u_2 in the initial state, and u'_1 and u'_2 in the final one. Neglecting the exchange effect, the following two transitions are possible:

(1) The electron \mathbf{p}_1 emits a photon $\mathbf{k} = \mathbf{p}_1 - \mathbf{p}'_1$ going to the state \mathbf{p}'_1 ; the electron \mathbf{p}_2 absorbs the photon \mathbf{k} going to the state \mathbf{p}'_2 .

(2) The electron \mathbf{p}_2 emits a photon $-\mathbf{k} = \mathbf{p}_2 - \mathbf{p}'_2$ going to the state \mathbf{p}'_2 ; the electron \mathbf{p}_1 absorbs the photon $-\mathbf{k}$ going to the state \mathbf{p}'_1 .

The total interaction energy is given by

$$I = \sum_n \frac{H'_{fn} H'_{ni}}{E_i - E_n}, \quad \dots\dots (41)$$

where i , n and f refer to the initial, intermediate and final states respectively. We add the contributions of the four types of photons, bearing in mind, according to (39), the minus sign in the matrix elements of the absorption operator for a scalar photon. We thus obtain

$$I = \frac{2\pi e^2}{k} \left(\frac{1}{E_1 - E'_1 - k} + \frac{1}{E_2 - E'_2 - k} \right) \left\{ \sum_{i=1,2,3} (u_1^* \alpha_i u_1) (u_2^* \alpha_i u_2) - (u_1^* \alpha_0 u_1) (u_2^* \alpha_0 u_2) \right\}.$$

Since the energy in the initial and the final states must be the same, we have

$$E_1 - E'_1 = -(E_2 - E'_2) = \epsilon, \quad \text{say.}$$

Hence

$$I = \frac{4\pi e^2}{\epsilon^2 - k^2} (u_1^* \alpha_\mu u_1) (u_2^* \alpha_\mu u_2), \quad \dots\dots (42)$$

which is Møller's well-known result (cf. Heitler 1944).

We further see that the contribution of the longitudinal and the scalar photons alone is

$$I = \frac{4\pi e^2}{\epsilon^2 - k^2} [(u_1^* \boldsymbol{\alpha} \cdot \mathbf{n} u_1) (u_2^* \boldsymbol{\alpha} \cdot \mathbf{n} u_2) - (u_1^* u_1) (u_2^* u_2)], \quad \mathbf{n} = \frac{\mathbf{k}}{k}, \\ = \frac{4\pi e^2}{k^2} (u_1^* u_1) (u_2^* u_2) \\ = \frac{4\pi e^2}{k^2} \exp \{i(\mathbf{k}, \mathbf{r}_2 - \mathbf{r}_1)\} \cdot (\psi_1^* \psi_1) (\psi_2^* \psi_2).$$

Therefore, the above exchange of the longitudinal and the scalar photons is equivalent to an interaction

$$V_k = \frac{4\pi e^2}{k^2} \exp \{i(\mathbf{k}, \mathbf{r}_2 - \mathbf{r}_1)\}.$$

Summing over all values of \mathbf{k} , we get

$$\begin{aligned} V &= \int \frac{e^2}{2\pi^2 k^2} \exp \{i(\mathbf{k}, \mathbf{r}_2 - \mathbf{r}_1)\} d\mathbf{k} \\ &= \frac{e^2}{|\mathbf{r}_2 - \mathbf{r}_1|}, \end{aligned} \quad \dots\dots(43)$$

which is the Coulomb interaction.

It should be noted that if we use the more general matrix elements (38), we obtain for the Møller interaction

$$I = \frac{4\pi e^2}{\epsilon^2 - k^2} (N_{\mu}^{(1)} N_{\nu}^{(1)} + N_{\mu}^{(2)} N_{\nu}^{(2)} + N_{\mu}^{(3)} N_{\nu}^{(3)} - N_{\mu}^{(0)} N_{\nu}^{(0)}) (u_1^* \alpha_{\mu} u_1) (u_2^* \alpha_{\nu} u_2)$$

which, on account of (2), is the same as (42).

§ 6. SELF-ENERGY OF THE ELECTRON

We shall now discuss the self-energy of the electron, which is defined as the interaction energy when the electron is present minus the interaction energy in vacuum. To calculate the self-energy of an electron with momentum \mathbf{p} , consider the following transitions:

(1) The electron \mathbf{p} emits a photon $-\mathbf{k}$ going to the state $(\mathbf{p} + \mathbf{k})$; the electron $(\mathbf{p} + \mathbf{k})$ re-absorbs the photon $-\mathbf{k}$ going to the original state \mathbf{p} .

(2) An electron \mathbf{p} and a positron $-(\mathbf{p} + \mathbf{k})$ are created with the emission of a photon \mathbf{k} ; the pair is annihilated with the re-absorption of the photon \mathbf{k} .

We notice that the first transition can occur only when the electron is present, while the second transition can occur only in its absence. Therefore, the self-energy is equal to the difference of the contributions of the above two transitions, and is given by

$$W = \sum_{\mathbf{k}} \frac{2\pi e^2}{k} \left[S^+ \frac{(u_0^* \alpha_{\mu} u)(u^* \alpha_{\mu} u_0)}{E_0 - E - k} - S^- \frac{(u_0^* \alpha_{\mu} u)(u^* \alpha_{\mu} u_0)}{-E_0 - E - k} \right],$$

where u_0 is the Dirac amplitude of the positive energy electron \mathbf{p} , and u and \underline{u} are the Dirac amplitudes of the electron $(\mathbf{p} + \mathbf{k})$ in positive and negative energy states respectively; S^+ and S^- denote summations over the spin directions of u and \underline{u} ; k is the energy of the virtual photon, $E = \{\mu^2 + (\mathbf{p} + \mathbf{k})^2\}^{1/2}$, and $E_0 = \{\mu^2 + \mathbf{p}^2\}^{1/2}$. After the usual simplifications we get

$$W = \frac{e^2}{4\pi^2 E_0} \int \frac{d\mathbf{k}}{Ek} \left[\frac{p^2 + 2\mu^2 - EE_0 + (\mathbf{k} \cdot \mathbf{p})}{E + k - E_0} + \frac{p^2 + 2\mu^2 + EE_0 + (\mathbf{k} \cdot \mathbf{p})}{E + k + E_0} \right]. \quad \dots\dots(44)$$

For the special case $\mathbf{p} = 0$, (44) gives the well-known results of Weisskopf (1939):

$$W = \frac{e^2 \mu}{\pi} \int dk \left(\frac{1}{E} + \frac{k}{E(E+k)} \right). \quad \dots\dots(45)$$

For the general case, in order to obtain the result in a covariant form, we evaluate (44) by a method similar to that used by Pauli and Rose (1936). We first carry out the transformation from the variables \mathbf{k} to the variables ϕ , v and w , where ϕ is the azimuthal angle around the axis parallel to \mathbf{p} , and

$$v = E - k, \quad w = E + k. \quad \dots\dots(46)$$

Computing the functional determinant, we obtain for the elements of volume the relation

$$\frac{d\mathbf{k}}{Ek} = \frac{1}{2p} dv dw d\phi. \quad \dots\dots(47)$$

The limits of integration of the new variables are

$$\left. \begin{aligned} 0 \leq \phi \leq 2\pi, \\ \frac{\mu^2 w - p(w^2 - p^2 - \mu^2)}{w^2 - p^2} \leq v \leq \frac{\mu^2 w + p(w^2 - p^2 - \mu^2)}{w^2 - p^2}, \\ (\mu^2 + p^2)^{1/2} \leq w \leq \infty. \end{aligned} \right\} \quad \dots\dots(48)$$

The above limits of integration of v are obtained from the inequality

$$(vw - \mu^2 - p^2)^2 = \frac{1}{k^2} (\mathbf{k} \cdot \mathbf{p})^2 (v - w)^2 \leq p^2 (v - w)^2$$

$$\text{or,} \quad (w^2 - p^2)v^2 - 2wp\mu^2 v + (\mu^4 + p^4 + 2p^2\mu^2 - p^2w^2) \leq 0. \quad \dots\dots(49)$$

Transforming (44) to the new coordinates, we obtain the simple expression

$$\begin{aligned} W &= \frac{e^2}{8\pi^2 E_0 p} \int dv dw d\phi \left(v + \frac{2\mu^2 w}{w^2 - E_0^2} \right) \\ &= \frac{\mu}{E_0} \frac{e^2 \mu}{2\pi} \int_1^\infty d\epsilon \left(\frac{3}{\epsilon} - \frac{1}{\epsilon^3} \right), \quad \dots\dots(50) \end{aligned}$$

where

$$\epsilon = [(w^2 - p^2)/\mu^2]^{1/2}. \quad \dots\dots(51)$$

It should be noted that the calculation of the self-energy involves a summation over states containing a virtual pair of electron and photon with momenta $(\mathbf{k} + \mathbf{p})$ and $-\mathbf{k}$ and energies E and k respectively. Since $(\mathbf{k} + \mathbf{p}, E)$ and $(-\mathbf{k}, k)$ are 4-vectors, their sum $(\mathbf{p}, E + k)$ is also a 4-vector, and hence ϵ is a Lorentz-invariant quantity. The self-energy (50) may, therefore, be expressed as

$$W = \frac{\mu}{[\mu^2 + p^2]^{1/2}} \delta\mu = \delta\mu \int \psi^* \beta \psi dv, \quad \dots\dots(52)$$

where $\delta\mu$, though divergent, is Lorentz-invariant. This shows that the effect of self-energy is equivalent to a change in the rest-mass of the electron. The same conclusion has also been arrived at by Schwinger and Tomonaga.

§ 7. CONCLUSION

For the purpose of applications, the main results of the present theory may be stated as follows:

(1) The electromagnetic 4-potential A_μ may be quantized as

$$\left. \begin{aligned} A_i &= \sum_{\mathbf{k}} \sqrt{\left(\frac{2\pi}{k}\right)} \{C_i(\mathbf{k}) \exp[i(\mathbf{k} \cdot \mathbf{r})] + C_i^\dagger(\mathbf{k}) \exp[-i(\mathbf{k} \cdot \mathbf{r})]\}, \\ A_0 &= \sum_{\mathbf{k}} \sqrt{\left(\frac{2\pi}{k}\right)} \{C_0(\mathbf{k}) \exp[i(\mathbf{k} \cdot \mathbf{r})] + C_0^\dagger(\mathbf{k}) \exp[-i(\mathbf{k} \cdot \mathbf{r})]\}, \end{aligned} \right\} \quad \dots\dots(53)$$

where C_i and C_0 are the absorption operators, and C_i^\dagger and C_0^\dagger the emission operators for four types of photons of positive energy.

(2) Ordinary perturbation formulae may be applied, taking the above absorption and emission operators to be the matrices

$$\left. \begin{aligned} [C_i]_{mn}' &= -[C_0]_{mn}' = n^{1/2} \delta_{m, n-1}, \\ [C_i^\dagger]_{nm}' &= [C_0^\dagger]_{nm}' = n^{1/2} \delta_{m, n-1}. \end{aligned} \right\} \dots\dots (54)$$

(3) All the four types of photons may be present in virtual states, but longitudinal photons (corresponding to the component of $C_i(\mathbf{k})$ along \mathbf{k}) and scalar photons do not exist in a pure radiation field.

Using the above results, we can easily treat the interaction of the radiation field with particles of any spin.

Note added in proof. In the present paper we have used the ordinary representation for the treatment of interaction. The extension of the present theory to 'interaction representation', which requires the generalization of our supplementary condition, has been given by K. Bleuler in a forthcoming note in the *Physical Review*.

ACKNOWLEDGMENTS

I wish to express my sincerest thanks to Professor W. Heitler for many useful comments, and for much help in the choice of the supplementary condition. I am also greatly indebted to Dr. S. T. Ma for many valuable discussions, and for pointing out to me the non-dependence of the results of physical interest on the choice of the time-like unit vector $N_\mu^{(0)}$.

REFERENCES

- DIRAC, P. A. M., 1942, *Proc. Roy. Soc. A*, **180**, 1; 1943, *Comm. Dublin Institute for Advanced Studies*, A, No. 1; 1947, *Principles of Quantum Mechanics* (Oxford: University Press), Chap. XII.
- FEYNMAN, R. P., 1948, *Phys. Rev.*, **74**, 1430.
- HEITLER, W., 1944, *Quantum Theory of Radiation* (Oxford: University Press), p. 101.
- MA, S. T., 1949, *Phys. Rev.*, **75**, 535.
- MAJUMDAR, R. C., and GUPTA, S. N., 1947, *Proc. Nat. Inst. Sci. Ind.*, **13**, 187.
- PAULI, W., 1943, *Rev. Mod. Phys.*, **15**, 175.
- PAULI, W., and ROSE, M. E., 1936, *Phys. Rev.*, **49**, 462.
- SCHWINGER, J., 1949, *Phys. Rev.*, **75**, 651.
- TATI, T., and TOMONAGA, S., 1948, *Prog. Theor. Phys.*, **3**, 391.
- WEISSKOPF, V., 1939, *Phys. Rev.*, **56**, 72.

On the Energy of the Alpha-Particles from Radioactive Nuclei

By M. H. L. PRYCE

Clarendon Laboratory, Oxford

MS. received 2nd January 1950

ABSTRACT. When the energy of α -particles emitted by radioactive nuclei is compared with the energy calculated from the usual semi-empirical formula for nuclear binding energies, systematic variations ranging from 4.5 mev. to -1.0 mev. are found, which exhibit in a very clear way the special importance of configurations containing 82 protons and/or 126 neutrons. The general features are readily explained in terms of the shell model. The analysis can be used to predict unknown α -energies. Calculated α -energies are tabulated for the heavy nuclei ($Z \geq 78$) and for nuclei in the rare-earth region.

§ 1. INTRODUCTION

It is well known that the general trend of the mass-defects of nuclei can be satisfactorily represented by a formula of the type

$$M(A, Z) = ZM_p + NM_n - \alpha A + \beta(N - Z)^2/A + \gamma A^{2/3} + \delta Z^2 A^{-1/3}, \quad \dots\dots(1)$$

where Z is the number of protons, N of neutrons, in the nucleus, $A = Z + N$ is the mass-number, $M(A, Z)$ is the mass of the nucleus, M_p , M_n are the masses of the proton and neutron, and α , β , γ , δ are constants. Such a formula represents an average variation of nuclear masses, and does not take into account the individual characteristics which arise from special groupings in the nuclear structure. In particular, it does not, as it stands, represent the fact that there are systematic variations with the parity of A , Z and N , nor the special importance of 'magic numbers'. On the other hand, it is sufficiently accurate to give a very good account of the beta-stability of nuclei. The difference between the actual mass of a nucleus and the mass calculated from the formula is in fact rather small, and shows systematic variations reflecting the individual characteristics of the nuclei, which presumably depend on combinatorial properties of A , Z and N , such as the completion of closed shells. Unfortunately only the masses of the lighter nuclei are known with sufficient accuracy to make a significant comparison directly, for the deviations are of the order of a few m.m.u., and the precision with which the masses are known decreases below this limit with increasing mass-number.

The energies of the alpha-particles emitted by radioactive nuclei, on the other hand, are known with very high precision and furnish a sensitive comparison with the calculated values of the difference $M(A, Z) - M(A - 4, Z - 2)$. The energy of disintegration (i.e. energy of the α -particle plus energy of recoil) in the reaction $(A, Z) \rightarrow (A - 4, Z - 2) + \alpha$ -particle is given by

$$E_\alpha(A, Z) = [M(A, Z) - M(A - 4, Z - 2) - M(4, 2)]c^2. \quad \dots\dots(2)$$

78	79	80	81	82	83	84	85	86	87	88	89	90	91	92	93	94	95	96
148																		
147																		
146																		
145																		
144																		
143																		
142																		
141																		
140																		
139																		
138																		
137																		
136																		
135																		
134																		
133																		
132																		
131																		
130																		
129																		
128																		
127																		
126																		
125																		
124																		
123																		
122																		
121																		
120																		
119																		
118																		
117																		
116																		
115																		
114																		
113																		
112																		
111																		
110																		
109																		
108																		
107																		
106																		
105																		
104																		

The difference between the observed value of E_α and the value calculated from (1) we shall call the *excess* and denote by $\Delta(A, Z)$:

$$\Delta(A, Z) = E_{\alpha\text{obs}} - E_{\alpha\text{calc}}. \quad \dots\dots(3)$$

It reflects the characteristics of the two nuclei involved in the disintegration.

For the purpose of the present calculation we shall take (1) in the numerical form

$$[M(A, Z) - \frac{1}{4}AM(4, 2)]c^2 = -7.0A + 0.39(N - Z) + 19.6(N - Z)^2/A \\ + 14.0A^{2/3} + 0.61Z^2A^{-1/3} \text{ Mev.} \quad \dots\dots(4)$$

These coefficients differ slightly from those given in the literature. They were chosen because tabulated values of $M(A, Z) - \frac{1}{4}AM(4, 2)$ were available for them, having been computed in 1945 for use in the Montreal Laboratory of the Canadian National Research Council, they then being the best values available; and it did not seem worth while recalculating them with newer values. The conclusions from the present analysis are essentially unaffected by the particular choice of constants.

§ 2. HEAVY NUCLEI

The results of the comparison for the heavy radioactive nuclei ($Z \geq 78$) are shown in Table 1. The nuclei are tabulated according to Z and N . For each nucleus there is listed:

- (a) Its chemical symbol (or classical radioactive symbol where appropriate) and mass-number: e.g. $\text{U}1238$.
- (b) The disintegration energy $E_{\alpha\text{obs}}$, where known (in roman type): e.g. 4.251.
- (c) The calculated value, $E_{\alpha\text{calc}}$ (in italic type): e.g. 5.249.
- (d) The excess $\Delta = E_{\alpha\text{obs}} - E_{\alpha\text{calc}}$ (in Clarendon type): e.g. -0.998.

Energies are in mev. Calculated values are believed accurate to two or three kev., and better in the middle part of the table. They are quoted to this accuracy so that they may be used for extrapolation, should occasion demand it. Experimental values are from Seaborg and Perlman (1948), Feather (1949) and Perlman, Ghiorso and Seaborg (1950), and are corrected for recoil; except for the α -emitting isotopes of gold and (?) mercury, which come from Thompson, Ghiorso, Rasmussen and Seaborg (1949). The energies for $\text{RaE} 210$, $\text{Pu} 241$ and $\text{Am} 242$ have been inferred from closed decay cycles, and that of $\text{At} 212$ from the life-time, following Broda and Feather (1947) and Perlman, Ghiorso and Seaborg (1948, 1950). The gold and mercury isotopes have been assigned, arbitrarily, the mass-number 186.

The table shows some remarkable regularities:

1. For the seventy-two nuclei with $Z \geq 84$, $N \geq 128$ (those in region A of Figure 1), Δ decreases reasonably smoothly with increasing mass-number, starting at 4.525 mev. for ThC' ($Z = 84$, $N = 128$), decreasing at first by 0.33 mev. per unit of mass-number, and then levelling off at approximately -1.0 mev. for the heaviest α -emitters. The excess appears to be closely correlated with the mass-number, as may be seen from Figure 2, in which it is plotted against A for the nuclei in the range from $A = 202$ to $A = 244$. The points for region A all lie reasonably close to one curve. There is no such close correlation with Z , N or $N - Z$. Nor are the departures from the curve correlated in any obvious way with Z , N or $N - Z$.

2. There is a sharp break between $Z=84$ and $Z=83$, and a similar break between $N=128$ and $N=127$. In the 'tram-line' regions B_1 and B_2 , corresponding to $Z=83$ and $N=127$ respectively, six experimental points are available. The excess starts at about 2.8 mev. and decreases with increasing mass-number with a slope somewhat smaller than in region A.

3. There is another break between $N=127$ and $N=126$, and, although no experimental points are available in region D_1 to prove it directly, there is probably

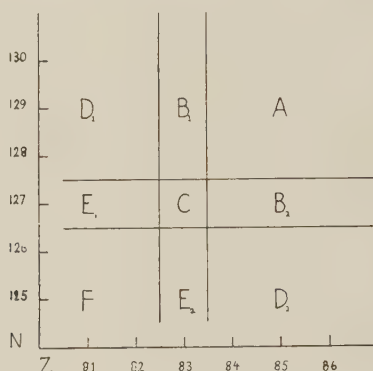


Figure 1. The classification of nuclei according to regions.

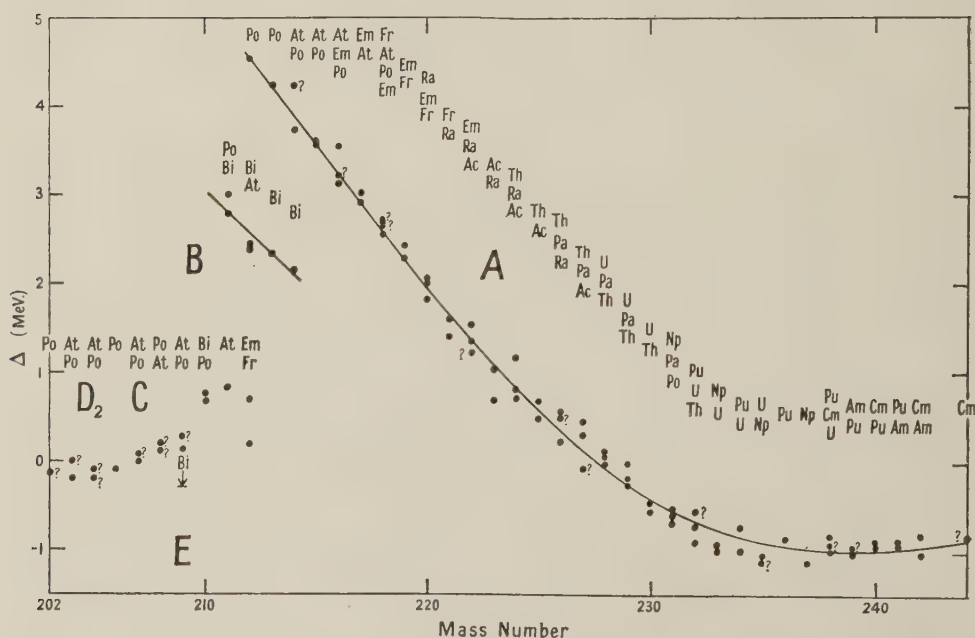


Figure 2. Plot of the excess of observed over calculated alpha-energy against mass-number.

a similar break between $Z=83$ and $Z=82$. There are sixteen points, some of which are still doubtful, in region D_2 ($Z \geq 84$, $N \leq 126$), which furnish the evidence for the former break.

The various regions have a definite significance in relation to a closed shell of 82 protons and a closed shell of 126 neutrons. In region A, both parent and

daughter nucleus have at least 82 protons and at least 126 neutrons. In region B_1 the parent has more, and the daughter less, than 82 protons, while both have at least 126 neutrons. In B_2 both have at least 82 protons, but the parent has more, and the daughter less, than 126 neutrons. And so on in a way which is clearly seen in Figure 1, if one remembers that the daughter is the nucleus with two protons and two neutrons less than the parent nucleus, which is the one indicated.

It will be seen from Figure 2 that the points belonging to region A clearly fall into one group, those in regions B_1 and B_2 into a second group lying close to a single curve, and those of regions C and D_2 fall into a third group, also lying close to a single curve. The data for the neutron-deficient bismuth isotopes, which lie in region E_2 , have not been plotted, their mass-number assignment being uncertain, but it is probable that they belong to a fourth group, particularly as Bi 209 (also in E_2) is apparently stable, from which it can be inferred that its excess is less than -0.3 Mev.

It is proper at this point to say something of what can be inferred concerning the apparently stable nuclei. On the basis of the relation between energy and lifetime it has been assumed in the table that if the α -particles had an energy greater than 4.0 Mev. they would have been detected. This estimate is open to question, for it depends on a specific assumption concerning the radius of the daughter nucleus, which is rather uncertain for the nuclei in question, probably being considerably smaller than for the classical radio-elements. And for rare isotopes of an element, α -emission would only be observed if the specific activity were higher than is necessary for detection in an abundant isotope. It has not been thought worth while to make a detailed estimate for each isotope, however, on account of the vagueness of the conclusions to be drawn in this way. An upper limit of 4.0 Mev. has therefore been assumed throughout for the elements from platinum to bismuth. This gives a few upper limits to Δ in the region F. Positive information comes from the newly discovered α -radioactive isotopes of gold and (?) mercury, whose mass-numbers are not yet certain. The gold isotope is quoted (Thompson *et al.* 1949) as lying in the mass-range 185–188, and for the purpose of tabulation it has been listed under 186.

§ 3. THEORETICAL DISCUSSION

The general features described above find a ready explanation in terms of the nuclear shell model (Mayer 1949, Nordheim 1949, Feenberg and Hammack 1949). If we assume that 82 protons form a closed proton shell, and 126 neutrons a closed neutron shell, and that the binding energy of a nucleon inside a closed shell is greater than of a nucleon outside a shell, by about 2 Mev., we can understand the breaks between the regions A, B, C, D etc. The decrease in Δ with increasing mass-number in regions A and B is also easily explained (cf. Glueckauf 1948) if we suppose that, as more and more nucleons are added outside a closed shell, their mutual binding energy increases, until the irregularity arising from the proximity of the closed shell is smoothed out, apart from minor fluctuations.

We may try to derive quantitative results from a quite naive application of the shell idea. Let us suppose that outside a closed shell the energy of a nucleus differs from the smoothed value (1) by a term proportional to the number of 'loose' nucleons, representing the lower binding outside the shell, together with a term which is quadratic in the number of loose nucleons, representing their mutual

binding; and that inside the closed shell it differs by a term proportional to the number of vacancies, representing the tighter binding inside the shell. The quadratic term will, of course, only be a good representation near a complete shell. We then get the following:

$$\begin{aligned}
 (M - M_{\text{calc}})c^2 &= \epsilon(A - 208) - \frac{1}{2}a(A - 208)(A - 209), & Z \geq 83, N \geq 127; \\
 &= \epsilon(N - 126) - \epsilon'(82 - Z) - \frac{1}{2}a(N - 126)(N - 127), & Z \leq 82, N \geq 127; \\
 &= \epsilon(Z - 82) - \epsilon'(126 - N) - \frac{1}{2}a(Z - 82)(Z - 83), & Z \geq 83, N \leq 126; \\
 &= -\epsilon'(208 - A), & Z \leq 82, N \leq 126. \\
 &\dots\dots(5)
 \end{aligned}$$

A constant term representing the discrepancy for the nucleus $Z = 82, N = 126$ (Pb 208) has been omitted, as it contributes nothing to the energy differences. The terms $\frac{1}{2}a(A - 208)(A - 209)$ etc. are proportional to the number of pairs of loose nucleons. It is assumed that in the interaction between loose nucleons it is immaterial whether they are protons or neutrons.

This gives the following results for the excess:

Region	Excess
A	$4\epsilon - 4a(A - 210.5)$
B ₁ , B ₂	$3\epsilon + \epsilon' - 3a(A - 210)$
C (RaE 210)	$2\epsilon + 2\epsilon' - a$
D ₁	$2\epsilon + 2\epsilon' - 2a(N - 127.5)$
D ₂	$2\epsilon + 2\epsilon' - 2a(Z - 83.5)$
E ₁ , E ₂	$\epsilon + 3\epsilon'$
F	$4\epsilon'$.
	$\dots\dots(6)$

If we take the slope of the smooth curve drawn through the points of region A in Figure 2 to determine a , we find the value $a = 0.083$ mev. The line through the points of the regions B has been drawn with slope $3a$, according to (6), and it will be seen that the fit is reasonable. The values of ϵ and ϵ' from these data are $\epsilon = 1.26$ mev., and $\epsilon' = -0.68$ mev.

This predicts the value $\Delta = 1.08$ mev. for RaE and the polonium isotopes of region D₂, and 0.92 mev. for the astatine isotopes. The agreement at this point is poor, but this is not surprising in view of the crudity of the assumptions. As will be seen later the discrepancy is readily accounted for when one makes more realistic assumptions.

We might refine our assumptions in several ways. In the first place, we could introduce different coefficients ϵ_p, ϵ_n and ϵ'_p, ϵ'_n for protons and neutrons. The good correlation between Δ and A in region A indicates, however, that ϵ_p and ϵ_n cannot in fact be very different. And the similar behaviour of regions B₁ and B₂ indicates further that ϵ'_p and ϵ'_n are nearly equal. We could also introduce different coefficients a_{pp}, a_{pn}, a_{nn} for the mutual interaction of loose nucleons. Again, the correlation of Δ and A indicates that a_{pp} and a_{nn} are not very different; and the relative slopes of the curves through the points of regions A and B indicate that a_{pn} is approximately equal to a_{pp} and a_{nn} , though this last datum is not very

significant. We should also introduce a term depending on the parity of Z and N ; this is particularly important in connection with regions B and E and the discrepancy just noted. Finally we might introduce quadratic terms inside the closed shell to represent the variation of the true smoothed mass from the calculated smooth mass, and bilinear terms for nuclei having loose protons and an incomplete neutron shell, and vice versa. With so many parameters, remembering that there must also be minor fluctuations of a combinatorial character, it is not worth while to pursue the matter very much further until more reliable data are available for regions D, E and F.

There are a few points, however, which may profitably be noted. It will be seen that region D_2 is represented in Figure 2 by points which fall clearly into two groups—those nuclei with 126 neutrons have a value of Δ around 0.7 mev., and those with 125 neutrons or less around 0 (± 0.2 mev.). This is readily explained if one assumes that the last neutron completing the shell is less tightly bound (by 0.7–0.8 mev) than the previous ones, though still much more tightly than neutrons outside the shell. This is in line with the recent observation that the γ -n threshold of Bi 209 is abnormally low (Collie and Parsons 1950).*

It is commonplace that nuclei with unpaired nucleons systematically have higher energies than nuclei with all nucleons paired. If we assume that this effect is more marked with nucleons outside a closed shell than inside we can understand why it is that the points of region B (extrapolated to $A=210$) lie higher than predicted on the simple theory, namely, halfway between A and D. Further, the assumption that this is particularly marked when there is only one loose nucleon, as in the regions E, would explain the apparent fact that the excess for the neutron-deficient bismuth isotopes of region E_2 is not so low as would have been expected on the simple theory.

We have said that there is no other obvious correlation of Δ than with mass-number. This is not altogether true, for it can be seen that the actinium points tend to lie below the curve, and the plutonium points to lie above it. And if one looks carefully, one can detect other indications of regularities, but it is doubtful whether they are very significant. It may be remarked that the low value for U 233 may be due to an error in the experimental value, for there is a γ -ray associated with the disintegration, whose energy ought perhaps to be added to the α -energy. The standard deviation of the points from the smooth curve is 0.15 mev., but there is a tendency for greater scatter in the region around $A=234$. This may be connected with the incidence of isomerism in this region.

That the general behaviour of the excess is very little sensitive to the choice of numerical constants in (1) may be seen from the following argument. If we consider the change in $E_{\alpha \text{ calc}}$ caused by a change $\delta\alpha$ etc. in the constants, we can estimate it sufficiently accurately by writing $4c^2(\partial M/\partial A)_{N,Z}$ for E_α . This gives

$$\delta E_{\alpha \text{ calc}} = -4\delta\alpha - 4\left(\frac{N-Z}{A}\right)^2 \delta\beta + \frac{4}{3}A^{-1/3}\delta\gamma + 4ZA^{-1/3}\left(1 - \frac{Z}{3A}\right)\delta\delta. \quad \dots\dots(7)$$

The constants given by Rosenfeld (1948) differ the most of any published from (4), namely $\alpha=14.66$ mev., $\beta=20.54$ mev., $\gamma=15.4$ mev., $\delta=0.602$ mev. The constants in (4) are, taking 28.2 mev. as the binding energy of the α -particle, $\alpha=14.05$ mev., $\beta=19.6$ mev., $\gamma=14.0$ mev., $\delta=0.61$ mev. This means that, had

* Note added in proof. The γ -n thresholds of Pb 206, Pb 207, Pb 208 recently measured by Hanson and Palevsky (private communication from G. T. Seaborg) confirm this further.

we adopted Rosenfeld's values, we should have obtained an α -energy lower, and so an excess higher, by

$$2.44 + 3.76 \left(\frac{N-Z}{A} \right)^2 - \left[3.73 - 0.032Z \left(1 - \frac{Z}{3A} \right) \right] A^{-1/3} \text{Mev.} \dots\dots(8)$$

The values of this, for three widely spaced nuclei, are, Sm 144: 2.11 mev., Pb 208: 2.38 mev., Cm 242: 2.43 mev. Although the discrepancies are considerable, they are nearly the same in all three cases. The major discrepancy comes from the value of α , which gives a constant difference of 2.44 mev. We may therefore regard the variation of $\Delta(A, Z)$ which we have evaluated to be a correct representation of the facts, but place no reliance on the zero with respect to which it is referred, as this is too sensitive to the choice of α , the mean binding energy per nucleon, which is not known sufficiently accurately for the purpose.

§ 4. RARE EARTH ISOTOPES

The existence of a natural α -emitting isotope of samarium, and the recent discovery (Thompson *et al.* 1949) of artificially produced α -emitting rare-earth isotopes, makes it desirable to extend the calculation to this region. The incidence of α -radioactivity in this region is presumably closely connected with the closing of a shell of 82 neutrons. This is done in Table 2, which lists $E_{\alpha\text{calc}}$.

Table 2. $E_{\alpha\text{calc}}$ in the Rare-earth Region

Element	Nd	Pm	Sm	Eu	Gd	Tb	Dy	Ho	Er	Tm	Yb
<i>Z</i>	60	61	62	63	64	65	66	67	68	69	70
<i>N</i>											
98									2.00	2.48	2.95
97									2.18	2.66	3.12
96									2.36	2.83	3.29
95								2.06	2.54	3.01	3.46
94							1.76	2.24	2.72	3.18	3.63
93						1.45	1.94	2.42	2.89	3.35	3.79
92					1.14	1.64	2.13	2.60	3.06	3.51	3.95
91				0.83	1.34	1.83	2.31	2.77	3.23	3.67	4.10
90			0.51	1.03	1.53	2.01	2.49	2.95	3.40	3.83	4.26
89		0.19	0.71	1.22	1.71	2.19	2.66	3.12	3.56	3.99	4.41
88	0.14	0.39	0.91	1.41	1.90	2.37	2.84	3.28	3.72	4.14	4.56
87	0.07	0.60	1.11	1.60	2.08	2.55	3.00	3.45	3.88	4.29	4.70
86	0.28	0.80	1.30	1.79	2.26	2.72	3.17	3.61	4.03	4.44	4.84
85	0.49	1.00	1.49	1.97	2.44	2.89	3.33	3.76	4.18	4.58	4.98
84	0.69	1.19	1.68	2.15	2.61	3.06	3.49	3.91	4.32	4.72	5.11
83	0.89	1.38	1.86	2.33	2.78	3.22	3.65	4.06	4.46	4.86	
82	1.08	1.57	2.05	2.51	2.95	3.38	3.80	4.21	4.61	4.99	
81	1.28	1.76	2.22	2.68	3.11	3.54					
80	1.46	1.94	2.40	2.84	3.27						
79	1.65	2.12	2.56	3.00							
78	1.83	2.29	2.73								
77	2.01	2.46	2.89								
76	2.18	2.62	3.05								

Beta-stable isotopes are indicated in heavy type. Sm 152 is naturally radioactive, with a disintegration energy of 2.4 mev., corresponding to an excess of 1.9 mev. The study of the artificial radioactivities will no doubt give more data in the near future.

§ 5. CONCLUSION

The advantage of subtracting the calculated from the observed energy of α -particles is that one then obtains a quantity which varies fairly smoothly with mass-number, independently of the element. The sharp breaks between proton-numbers 84 and 83, and between neutron-numbers 128 and 127, and between 127 and 126, are some ten times larger than the deviations from smooth behaviour, and are clearly real. There can in fact be no doubt concerning the special importance of a configuration of 82 protons, or of 126 neutrons. The reasonable success of the analysis of § 3, based on a very simple application of the shell model cannot, however, be taken as evidence for any very simple theory of the nature of the closed shells, though it may give one some confidence in the predictions concerning the regions where little or no experimental data are available.

The fact that the deviations from the smooth curve for the nuclei with $Z \geq 84$, $N \geq 128$ are of order 0.15 mev. indicates that one is able to predict the energies of unknown α -decays in this region to about this accuracy. This, of course, is no improvement on the plots of Glueckauf (1948) and Perlman *et al.* (1948).

The isotopes of lead ($Z=82$) present a case of some interest. So far, no α -active lead isotopes are known. The position of RaD (Pb 210), occupying in region D₁ the position corresponding to Po 210 in D₂, suggests that its excess is probably about the same (compare the similarity of regions B₁ and B₂), namely about 0.7 mev., and hence that it emits α -particles of energy about 4.1 mev. (disintegration energy 4.2 mev.). The partial lifetime for α -decay is obviously very long, but it may nevertheless be possible to detect α -decay competing with the 22-year β -decay if a careful search is made. The neutron-deficient lead isotopes lie in region F, and on the theory of § 3 would be expected to have an excess of about -3 mev., though the data for the gold isotope suggests that further away from the closed shells it may be considerably higher. If the former were the case, Pb 180 would emit α -particles of about 5 mev., and Pb 170 of 8 mev., and in view of the gold data, probably higher. It is therefore possible that α -emitters will be found among the very neutron-deficient lead isotopes.

The present method of comparing observed with calculated disintegration energies can obviously also be applied to beta-decay. The evidence there is not so clear-cut; for the β -energies are not known with such certainty as α -energies, particularly where there are γ -rays also; where electron capture is taking place there is so far no means of determining the disintegration energy directly; and for even nuclei there is the alternation of even-even and odd-odd nuclei. A preliminary analysis along these lines has been made by Dr T. R. Kaiser, who found certain sharp discontinuities for the heavier elements. In particular there is a sharp increase in the β -excess as one passes through the neutron-number 82. (This is clearly shown by the decay sequence for $A=137$, the β -energy of Cs 137 ($N=82$) being 1.4 mev., and of Xe 137 ($N=83$) being much higher, namely 4 mev.) What one expects on the shell model is a sharp increase in going through a neutron shell, and a similar sharp decrease in going through a proton shell. This comparison does not give any useful evidence at present for the heavy nuclei we have been discussing, for the line of stable nuclei goes simultaneously through a proton and a neutron shell at Pb 208, and the effects cancel out. The only reported β -emitter which should show an anomaly is Tl 209, but it does not. This may well be due to the presence of a so far unreported γ -ray.

ACKNOWLEDGMENTS

I would like to acknowledge my debt to Dr. A. N. May, who in 1945 first called my attention to the interesting results of the present type of analysis, and to the members of the Computing Division of the Canadian National Research Council's Montreal Laboratory, without whose tabulation of formula (4) the present work would not have been undertaken.

REFERENCES

- BRODA, E., and FEATHER, N., 1947, *Proc. Roy. Soc. A*, **190**, 20.
 COLLIE, C. H., and PARSONS, R. W., 1950, *Proc. Phys. Soc. A*, **63** (in the press).
 FEATHER, N., 1949, *Nucleonics*, **5**, 22.
 FEENBERG, E., and HAMMACK, K. C., 1949, *Phys. Rev.*, **74**, 1877.
 GLUECKAUF, E., 1948, *Proc. Phys. Soc.*, **61**, 25.
 MAYER, M. G., 1949, *Phys. Rev.*, **74**, 1969.
 NORDHEIM, L. W., 1949, *Phys. Rev.*, **74**, 1894.
 PERLMAN, I., GHIORSO, A., and SEABORG, G. T., 1948, *Phys. Rev.*, **75**, 1730; 1950, *Ibid.*, **77**, 26.
 ROSENFELD, L., 1948, *Nuclear Forces* (Amsterdam: North Holland Publ. Co.).
 SEABORG, G. T., and PERLMAN, I., 1948, *Rev. Mod. Phys.*, **20**, 585.
 THOMPSON, S. G., GHIORSO, A., RASMUSSEN, J. O., and SEABORG, G. T., 1949, *Phys. Rev.*, **76**, 1406.

Excited Electronic Levels in Conjugated Molecules— IV: Symmetrical Cyanine Dyes*

BY W. E. MOFFITT†

New College, Oxford

Communicated by C. A. Coulson; MS. received 27th July 1949

ABSTRACT. Topics in the electronic theory of the colour of symmetrical cyanine dyes have been discussed by means of resonance formalism. Our conclusions for the formamidinium ion have been confirmed by use of the molecular orbital method. As a result of this analysis, certain modifications in the qualitative symbolism of colour theory have been put forward in the hope that the factors governing absorption may be more clearly understood.

§ 1. INTRODUCTION

THIS note is concerned with the theory of the colour of symmetrical cationic dyes of the cyanine type. Maccoll (1947) has recently reviewed the present status of this theory and has distinguished, very pertinently, between two different approaches to this subject. The dye chemist, on the one hand, is primarily concerned with a qualitative interpretation of colour on the basis of resonance theory, which may enable him to understand the relationship between colour and chemical constitution. The molecules with which he is dealing are large and complicated, so that he requires a symbolism of wide generality. On the other hand, the quantum theorist is still perfecting his methods for dealing with the simplest of molecules, and may find himself embarrassed, if only temporarily, by the increasing demands of the dye chemist for such an all-

* Paper number III in this series is concerned with naphthalene, by Miss J. Jacobs, *Proc. Phys. Soc. A*, 1949, **62**, 710.

† Now at British Rubber Producers' Research Association, 48 Tewin Road, Welwyn Garden City, Herts.

encompassing theory. Nevertheless a synthesis of these different approaches has been attempted (Brooker 1942, 1945, Herzfeld and Sklar 1942) and proved to be quite successful.

It seems, however, that the ready acceptance with which Brooker's views have been greeted is liable to propagate an undesirable misunderstanding. For, as we shall show, the qualitative resonance symbolism which has been evolved is not entirely sound and, if the dye chemist is to rely on the results of qualitative considerations, it is surely desirable that the concepts from which these arise should be fundamentally well established. We shall endeavour to throw a clearer light on some of the factors governing the colour of symmetrical cationic dyes. It is not our intention to make any new calculations, but rather to develop a more reliable picture of the absorption process.

§ 2. THE FORMAMIDINIUM ION

Let us first consider the current theory of the colour of the simple formamidine ion:



This molecule has two 'extreme' structures, a and a', which do not 'interact' directly in the quantum-mechanical sense—that is, the matrix element

$$H_{aa'} = \int \Psi_a \mathcal{H} \Psi_{a'} dv$$

vanishes in the usual approximation. Both structures have the same energy, $E_a = E_{a'}$, so that the system is said to be degenerate. Another structure of higher energy E_r , namely



may be drawn, and this structure interacts with both a and a'. Brooker (1945) now envisages a resonance splitting of the degenerate energy levels of the extreme structures a, a', in which the intervention of this 'excited' structure is treated as a perturbation. Graphically such splitting is represented by Figure 1. The

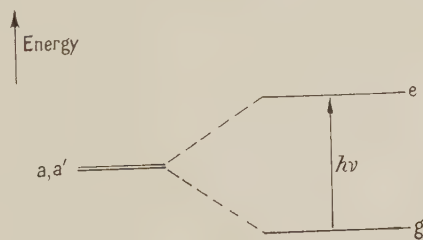


Figure 1. Erroneous splitting of levels of the formamidine ion.

resultant states e, g—of which g has the lower energy and is therefore identified with the ground state—are together considered as responsible for the first absorption maximum of the formamidine ion. (Since $(E_r - E_e) < (E_r - E_g)$, it is also deduced that the structure r is more important in the excited state than it is in the ground state.) The analogy between such symmetrical 'splitting' of the extreme energy levels, brought about by the contributions of r to the resonance hybrids, and the splitting of doubly degenerate $^1\Pi$ states of diatomic

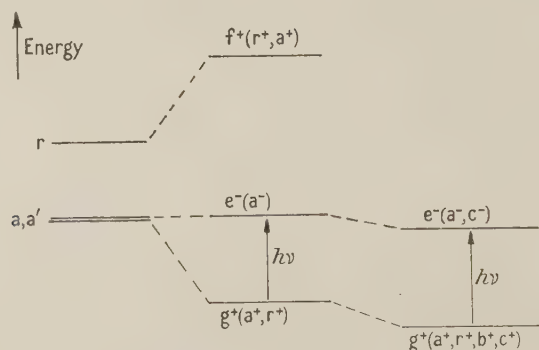
molecules in the presence of magnetic fields, seems inescapable—nevertheless it is quite incorrect.

Structures such as a , a' do not, of course, represent actual states any more than the excited structure r . Spectroscopic states, represented in atomic orbital approximation by linear combinations of structures, may contain more of a , a' than of r . And, in perturbation theory, it is legitimate to use simplified functions, such as the structures a , a' , which may be considered as 'splitting' under the influence of the perturbing Hamiltonian. But such a picture is apt to be misleading, especially when this 'splitting' is attributed to the intervention of the excited structures, such as r , and not to the Hamiltonian.

In the first place neither of the structures a , a' reflect the two-fold symmetry (C_{2v}) of the molecule, and are therefore unsatisfactory zeroth-order functions, mathematically. We use σ to denote the plane of the molecule; the plane of symmetry which contains the central carbon atom and is perpendicular to σ we shall denote by ν . It is better to construct linear combinations

$$\Psi_a^+ = \frac{1}{\sqrt{2}} \{\Psi_a + \Psi_{a'}\}, \quad \Psi_a^- = \frac{1}{\sqrt{2}} \{\Psi_a - \Psi_{a'}\},$$

which are symmetrical (A_1) and antisymmetrical (B_2) respectively with respect to reflections in ν . This process of constructing functions which fully participate in the molecular symmetry from functions which do not do this is called group-theoretical 'reduction'; we shall use the notation a , $a' \rightarrow a^+$, a^- to denote it. Since a , a' do not interact with each other, the energies associated with a^+ , a^- are the same as those of a , a' ; that is, $E_a = E_{a'} = E_a^+ = E_a^-$. We see that r remains invariant to reflection in ν and is therefore of the $+$ species (A_1). It thus interacts only with functions which are also of the $+$ species. This interaction of r^+ and a^+ will give rise to a state g^+ whose energy E_g^+ is less than $E_a^+ = E_a^-$, and also to another state f^+ , for which $E_f^+ > E_r$. The energy diagram representing this analysis is given in Figure 2(a).



(a) 1st approximation. (b) 2nd approximation.

Figure 2. Correct splitting of levels of the formamidinium ion.

We see that, if other structures are neglected, the first excited state e must be identified with a^- , and has the same energy as that of the extreme structures; e^- therefore contains no contribution from r , and the formal charge on the central carbon atom Q_C vanishes. The ground state, on the other hand, is only more stable than e^- by virtue of its component from r ; Q_C for the ground state is

therefore positive. It is easily shown that the intensity of the transition $g^+ \leftrightarrow e^-$ is greater than that of $g^+ \leftrightarrow f^+$, though the latter is not forbidden.

The contribution of the other possible structures may also be analysed. These are enumerated below:



b is essentially of the $+$ species, and $c, c' \rightarrow c^+, c^-$. On energetic grounds b^+, c^+ will be less important than r^+ in the ground state, but will serve to diminish Q_C there. Similarly the contribution of c^- to e^- will be small, but will make $Q_C < 0$ and bring E_c^- below E_a^- . The more complete energy diagram now follows Figure 2(b).

In this simple case, therefore, we can arrive at a complete description of the qualitative factors governing absorption. The ground state has $+$ symmetry A_1 ; the first excited state has $-$ symmetry B_2 . The dipole strength of transitions between these levels is relatively high. It is only because of structures such as r^+ and b^+ , which belong essentially to the $+$ species and have no analogues in the $-$ species, that the ground state lies below the first excited state. Structures giving rise to both $+$ and $-$ components, such as a, a' and c, c' , could not alone be responsible for this separation. Excited structures are therefore more important in the ground state than in the first excited state. Both g^+ and e^- states are associated with a positive resonance energy—that is, E_c^- and E_g^+ are both less than E_a or $E_{a'}$. Q_C is positive in g^+ and negative in e^- with $|Q_C(g^+)| > |Q_C(e^-)|$.

Next, let us see how the replacement of the central $-\text{CH}=\text{}$ group by a nitrogen atom $-\text{N}=\text{}$ will affect the absorption. To a good approximation we need only consider the structures analogous to a, a' and r. The problem is exactly the same as was the case formerly. If, therefore, we assume that the analogue of the matrix element

$$H_{ra} = \int \Psi_r \mathcal{H} \Psi_a dv$$

is not very different from that encountered earlier, it is easily shown that $(E_c^- - E_g^+)$ is smaller here than for the formamidinium ion. For, *ceteris paribus*, the greater the energy separation $(E_r^+ - E_a^+)$, the smaller will be the contribution of r^+ to g^+ . Thus the replacement of $-\text{CH}=\text{}$ by $-\text{N}=\text{}$ results in a bathochromic shift of the first absorption maximum (to longer wavelengths). Further, the formal positive charge $Q_N^*(g^+)$ on the central nitrogen atom in the ground state will be less than $Q_C(g^+)$. These predictions are confirmed by a molecular orbital treatment (see below).

§ 3. GENERALIZATION

A similar picture may be obtained of the long wave absorption of higher vinologues of the simple system we have been considering. These vinologues, namely



where the R groups on any N atom may participate, together with N, in the same cyclic system, contain the symmetrical cyanine-type dyes. If we consider only nearest-neighbour interactions, the conjugation problem may again be associated with a plane of symmetry ν , which contains the central carbon atom and is

perpendicular to the molecular plane σ , even when ν is not a plane of symmetry for the actual nuclear skeleton. (To this approximation, the actual shape of the conjugating system will affect only the intensity, and not the frequency, of the absorption.) Accordingly we may once more speak of states as belonging to the + or - species. From the observed regularities which are associated with the ascent of such a vinologous series (e.g. Maccoll 1947) we may infer that, whatever the value of n may be, the ground and first excited states are of the + and - species respectively, just as for the formamidinium ion.

Let us confine ourselves to some fixed value n , and retain the symbols a, a' for the 'extreme' structures, which have a positively charged nitrogen atom and contain no formal bonds. Thus a' is obtained by reflecting a in ν . Each of the possible $m=m(n)$ structures may be assigned to one of the three exclusive groups A, A' and B: to each structure i of A there corresponds a structure i' of A', obtained by reflecting i in ν . Further, if j' is any member of A', the matrix element $H_{ij'} = \int \Psi_i \mathcal{H} \Psi_{j'} dv$ vanishes; also, a belongs to A. Structures belonging neither to A nor to A' belong to B and are called 'bridge' structures. We may obtain functions of the + and - species from the structures of A, A' by means of the various processes $i, i' \rightarrow i^+, i^-$. In general, structures of B will also yield functions both of the + and - species; only when $n=0$ or 1 do we obtain no - components from B; the number of linearly independent + functions which may be constructed from the members of B exceeds the number of functions of the - species for all values of n .

Now, suppose we neglect the contribution of all the (excited) bridge structures B. Then it is easily shown that the energies of the lowest 'states' of both + and - types are equal to $E_h(n)$, say. If $E_a(n)$ denotes the energy of an extreme structure, it may further be shown that, as n increases, so does $\{E_a(n) - E_h(n)\}$. (For, of the k_{n+1} structures of $A(n+1)$, we may select a set of k_n structures whose $\frac{1}{2}k_n(k_n+1)$ different energy-matrix elements are identical with those of the set of k_n structures which comprise $A(n)$; and this selection does not exhaust $A(n+1)$.) To this degree of approximation, in which the contribution of the bridge structures is neglected, the ground and first excited states have the same energy and, as we ascend a vinologous series, so the resonance energies associated with these 'states' increases.

Clearly, therefore, no adequate description of the long wave absorption of these molecules can be obtained without the consideration of the bridge structures. And it may be shown that these will stabilize the ground state g^+ to a greater extent than the first excited state e^- , although both E_g^+ and E_e^- will lie below E_h . Once more we find that it is the greater importance of the excited structures to g^+ than to e^- which is responsible for the separation of the two levels.

Let $A(n), B(n)$ contain k_n, l_n structures respectively. Then it is easily shown, by simple enumeration, that the ratio l_n/k_n decreases fairly rapidly with increasing values of n . (For example, if we consider only those structures with no negatively charged carbon atoms and at most one formal bond, then $l_n/k_n = 1/2(n+1)$. With a more representative selection of structures, the ratio l_n/k_n decreases more rapidly than this.) This suggests, straight away, that as n increases so the extra stabilization of $g^+(n)$ with respect to $e^-(n)$ decreases. That is, the sequence $\{E_g^+(n) - E_e^-(n)\}^{-1}$ diverges and the vinylene shift of the absorption maximum is 'non-convergent' (Maccoll 1947). Conclusions derived

by means of such purely qualitative arguments should, whenever possible, be supplemented by more rigorous proofs—such as that put forward by Herzfeld and Sklar (1942). But they illustrate the way in which our use of resonance symbolism may be applied.

An essential feature of Brooker's theory (1945) was that the resonance energy $\{E_a(n) - E_g^+(n)\}$ should decrease with increasing values of n . In general, however, the calculations of Herzfeld and Sklar (1942) belied this conclusion, and the experimental evidence adduced in its favour—that the acidity required to decolourize a series of symmetrical cyanines decreases with n —is capable of a different interpretation. At best it only shows that the difference in the resonance energies of two systems, both of which are conjugated, decreases with increasing values of n . (This behaviour is, of course, not surprising because we should expect the differences between such odd- and even-numbered chains to decrease with n .) The more detailed analysis, which we have adumbrated above, does not require a decreasing resonance energy. On the contrary, since $\{E_a(n) - E_h(n)\}$ increases with n , we may infer that, at least ultimately, $\{E_a(n) - E_g^+(n)\}$ also increases with n . For, in the limiting case of a long chain, the non-convergence of λ_{\max} gives $E_g^+(n) \rightarrow E_e^-(n) \rightarrow E_h(n)$.

We may draw another corollary from this form of treatment. Suppose we have two molecules of the cyanine type, of the same chain length and differing only in, say, a particular substituent. If the importance of this substituent may be localized, as affecting only the energy of a particular bridge structure, then its effect on colour may be predicted. For if the substituent stabilizes the bridge structure, it is easily shown that such substitution is accompanied by a hypsochromic shift of the absorption maximum, and conversely. This theorem is a particular case of a more general colour rule used by Brooker and recently extended in application by Knott (1950).

§ 4. THE MOLECULAR ORBITAL METHOD

In order to confirm our qualitative conclusions for the formamidinium ion, we shall apply the molecular orbital method to this system. We must then assign the four π -electrons to molecular orbitals ψ which have nodes in σ . The ψ are expressed as linear combinations of atomic orbitals and are determined using the 'self-consistent' method recently introduced by the author (Moffitt 1949).

The electronic structure of the ground state of the formamidinium ion may be described by means of the configuration

$$[\psi^+]^2[\psi^-]^2,$$

where the superscripts + and - refer to the transformation properties of the individual orbitals (one-electron functions) with respect to ν . ψ^+ is strongly bonding and ψ^- is non-bonding; $[\psi^-]^2$ therefore represents two non-bonding electrons, one on each nitrogen atom. ψ^+ has the form

$$\psi^+ = \gamma_C^+ \phi_C^+ + \frac{1}{\sqrt{2}} \gamma_N^+ (\phi_N + \phi_{N'}),$$

with $\gamma_C^+ = \sin \theta$, $\gamma_N^+ = \cos \theta$,

and θ so chosen as to minimize the zeroth-order energy of the configuration and therefore satisfying

$$(\xi_C^+ - \xi_N^+) + 2\sqrt{2}\beta_{CN} \cot 2\theta = 0;$$

ξ_C^+ and ξ_N^+ describe the nature of the Hartree field near the C and N atoms (see Moffitt 1949). In terms of valence state ionization potentials I and electron affinities E , this becomes

$$(3I_N - 2I_C - 2E_C + E_N) - \cos 2\theta \{2(I_C - E_C) + (I_N - E_N)\} + 8\sqrt{2}\beta_{CN} \cot 2\theta = 0.$$

The π bond order and the resultant charge distribution are

$$p_{CN}^\pi = \frac{1}{\sqrt{2}} \sin 2\theta, \quad Q_N = \frac{1}{2} (1 - \cos 2\theta), \quad Q_C = \cos 2\theta.$$

Numerical values of the I , E are given by Mulliken (1934): $I_C = 11.2$, $E_C = 0.7$; $I_N = 12.2$, $E_N \sim 1.5$ ev. β_{CN} , the carbon-nitrogen resonance integral, has a negative value in the neighbourhood of -3 ev., but its precise value is unfortunately not known. We have therefore solved for θ , and hence determined p_{CN}^π , Q_N and Q_C for $\beta_{CN} = -2$, -3 and -4 ev. respectively. Our results for the ground state are to be found in the first three columns of Table 1.

Table 1

Bond Orders and Charge Distribution in the Formamidinium Ion

β_{CN}	Ground state			First excited state		
	p_{CN}^π	Q_N	Q_C	p_{CN}^π	Q_N	Q_C
-2 ev.	0.683	0.370	0.260	0.073	0.506	-0.011
-3 ev.	0.690	0.392	0.216	0.108	0.512	-0.024
-4 ev.	0.695	0.408	0.184	0.141	0.521	-0.041

Table 2

The Effect of Replacing $-\text{CH}=-$ by $-\text{N}=-$ in the Formamidinium Ion

β_{NN}	Ground state			First excited state		
	p_{NN}^π	Q_N	Q_N^*	p_{NN}^π	Q_N	Q_N^*
-2 ev.	0.700	0.428	0.144	0.067	0.505	-0.010
-3 ev.	0.702	0.439	0.121	0.100	0.510	-0.020
-4 ev.	0.703	0.448	0.104	0.132	0.518	-0.036

The first excited (singlet) state e^- arises from the configuration

$$[\psi^+]^2[\psi^-][\bar{\psi}^+];$$

ψ^+ is again bonding, ψ^- is non-bonding and $\bar{\psi}^+$ is antibonding. Setting $\gamma_C^\pi = \sin \theta$, as before, we find that

$$2(I_N - E_C) + \cos 2\theta \{2(I_C - E_C) + (I_N - E_N)\} + 4\sqrt{2}\beta_{CN} \cot 2\theta = 0.$$

The π bond order and charge distribution,

$$p_{CN}^\pi = \frac{1}{2\sqrt{2}} \sin 2\theta, \quad Q_N = \frac{1}{4} (3 - \cos 2\theta), \quad Q_C = -\frac{1}{2} (1 - \cos 2\theta),$$

are given in the last three columns of Table 1, for the same three values of β_{CN} . The qualitative conclusions as to charge distribution, derived above by means of resonance theory, are completely substantiated by the molecular orbital method. By the method of antisymmetrized molecular orbitals, using such LCAO forms, it is also possible to calculate the energy separation ($E_e^- - E_g^+$), but this is not our immediate intention.

The effect of replacing the central —CH= group by —N= is easily seen. We simply replace $(I_{\text{C}}, E_{\text{C}}, \beta_{\text{CN}})$ by $(I_{\text{N}}^*, E_{\text{N}}^*, \beta_{\text{NN}})$ in the above formulae, where $I_{\text{N}}^*, E_{\text{N}}^*$ and $I_{\text{N}}, E_{\text{N}}$ refer to different valence states of the nitrogen atom. Mulliken gives the values $I_{\text{N}}^*=13.8$, $E_{\text{N}}^*=1.0$ ev. If we now take the same set of values, namely -2 , -3 and -4 ev. for β_{NN} as for β_{CN} , we obtain the results of Table 2; Q_{N}^* refers to the charge on the central nitrogen atom. The differences between Tables 1 and 2 are in complete agreement with the results of our previous qualitative considerations.

ACKNOWLEDGMENTS

The author would like to thank Dr. E. B. Knott for arousing his interest in these problems and the Board of the British Rubber Producers' Research Association for a research grant.

REFERENCES

- BROOKER, L. G. S., 1942, *Rev. Mod. Phys.*, **14**, 275; 1945, *Frontiers in Chemistry*, Vol. 3 (New York: Interscience Publishers Inc.).
 HERZFELD, K. E., and SKLAR, A. L., 1942, *Rev. Mod. Phys.*, **14**, 294.
 KNOTT, E. B., 1950, *J. Chem. Soc.*, in the press.
 MACCOLL, A., 1947, *Quarterly Reviews*, **1**, No. 1.
 MOFFITT, W., 1949, *Proc. Roy. Soc. A*, **196**, 510.
 MULLIKEN, R. S., 1934, *J. Chem. Phys.*, **2**, 782.

Resolution and Analysis of Low Temperature Luminescent Spectra of Bi and Pb Activated Solids of Simple Crystal Structure

BY J. EWLES AND C. CURRY

The University, Leeds

MS. received 25th October 1949

ABSTRACT. Experimental arrangements are described by which clearly resolved spectra have been obtained of the luminescence, at the temperature of liquid air, of seven different phosphors of simple crystal structure (cubic) and of mixed crystals. The main peaks in each case may be arranged in a band series. The vibration frequency in the lower state is nearly the same for the same host lattice with different activators. The energy of the electronic transition is determined both by the activator and the host crystal and there is a progression of decreasing energy in the series of simple crystals MgO, CaO, SrO, CaS, and in the order CaO, CaO-SrO with mixed crystals. The most probable transitions are from the lowest level of the upper state. There is evidence that self-excitation occurs and for the view that the luminescent centres are large.

§ 1. INTRODUCTION

AMONG the many inorganic solids showing luminescence under irradiation by light, x-rays, cathode rays or radioactive radiations, only a few give emission spectra which can be resolved, even at low temperatures, into lines or narrow bands. The rare earths, both as pure solids and in solution, sometimes give line-like spectra which seem to be attributable to transitions in a shielded shell of the metallic ion. The uranyl salts as pure solids or in solution give well resolved spectra which appear to arise from transitions in a shielded shell of the uranyl ion. The narrow bands obtained with alkali halides have been interpreted by von Hippel (1936) as arising from the transference of an electron from a halogen to an alkali ion. Deutschbein (1932) explains the sharply resolved luminescent spectra sometimes obtained with Cr activated solids as arising from transitions in the Cr^{+++} ion modified by vibrations of the host lattice. For the most part, however, the luminescent spectra of impurity activated solids are broad and featureless even at liquid air temperature and lower, and it is not possible to evaluate with any accuracy the energy of the electronic transitions or to interpret, with any confidence, the way in which they arise.

Randall (1938) has pointed out that the similarity of the luminescent spectra of some solids activated with Mn to the spectra of pure manganous salts suggests that transitions in a shielded shell of the Mn^{++} ion are responsible in such cases, and surmised that the fluorescence of pure tungstates and molybdates originates in the WO_4 and MO_4 ions. Kroger (1948) has offered evidence supporting this view. One of us (Ewles 1938) reported previously that parts of the luminescent spectra of CaO-‘Specpure’, of CaO activated with Bi and of SrO could be resolved at the temperature of liquid air into narrow bands susceptible of interpretation as electron transitions modified by vibrations of the host lattice. The present contribution reports that this work has been extended to other cases which may be regarded as typical of a large class of impurity activated solids and suggests that the results may be of some use in the interpretation of the luminescence of this class.

§ 2. EXPERIMENTAL ARRANGEMENTS

The procedures for the preparation and heat treatment of the substances studied are described later, along with the analyses of the spectra. The source of excitation was a Mazda 125 watt Mercra Mercury vapour arc with the outer glass envelope removed. A clear silica flask of about 10 cm. diameter filled with a solution in distilled water of 145 gm. $\text{NiSO}_4 \cdot 7\text{H}_2\text{O}$ and 41.5 gm. $\text{CoSO}_4 \cdot 7\text{H}_2\text{O}$ per litre (Bowen 1935) served to focus an image of the source on the specimen and to remove all light between 3341 Å. and 5771 Å. The strong yellow lines at 5771 Å. and 5779 Å. may be removed by the addition of a piece of B.T.H. 'black glass' or Corning 9863. This addition, while reducing the intensity considerably in the shorter ultra-violet, is very useful for preliminary visual examination for visible luminescence, providing a source virtually free from all visible light, extending well into the far ultra-violet, and so strong that under its illumination very few substances are entirely free from luminescence.

An image of the irradiated specimen is focused on the slit of the spectrograph (Hilger E 383—quartz prism with Littrow mounting) with a glass lens which serves also to reduce scattered far ultra-violet light. A simple method of mounting the specimens for obtaining the luminescent spectra at low temperatures is

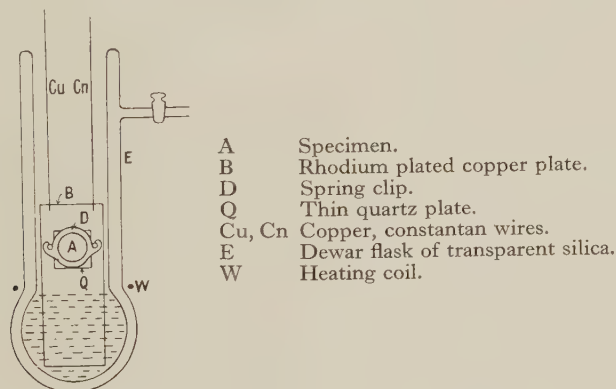


Figure 1.

shown in Figure 1. A very thin layer of the specimen about 1 cm^2 in area is deposited at A on a heavily rhodium plated copper plate B 4 in. long, $1\frac{1}{2}$ in. broad and $1/16$ in. thick. The specimen is covered by a thin quartz plate Q held firmly against the copper plate by a spring clip D. This arrangement is suspended by thin copper and constantan wires Cu and Cn, which also serve as a thermocouple, in a Dewar flask of transparent silica E containing the cooling liquid, so that the copper plate just touches the bottom of the Dewar and the specimen is above the level of the surface of the coolant. It is found with, for instance, liquid air as the coolant that the temperature as indicated by the copper-constantan couple remains at that of liquid air as long as any of this remains in the Dewar. To prevent condensation on the quartz plate covering the specimen it is necessary and effective first to fill the Dewar to the required depth with the coolant and to delay the immersion of the copper plate until the whole of the inside of the Dewar is well cooled—a matter of a few minutes only. Condensation on the outside of the Dewar in the neighbourhood of the specimen is prevented by an electrically heated wire W wound round the flask just below the level of the specimen.

§ 3. PREPARATION OF SPECIMENS AND ANALYSIS OF LOW TEMPERATURE LUMINESCENT SPECTRA

The preparation of the phosphors described below is indicated in each case. A Cambridge recording microphotometer was used to analyse the spectrograms. Wave-numbers were obtained from interpolation from superimposed Hg lines using the Hartmann dispersion formula where the resolution was sufficient to make it worth while, and in other cases a wave-number-distance calibration was obtained from a Hg spectrum. The probable error in the peaks is about 20 cm^{-1} . Reduced photometer curves are shown together for comparison in Figure 2.

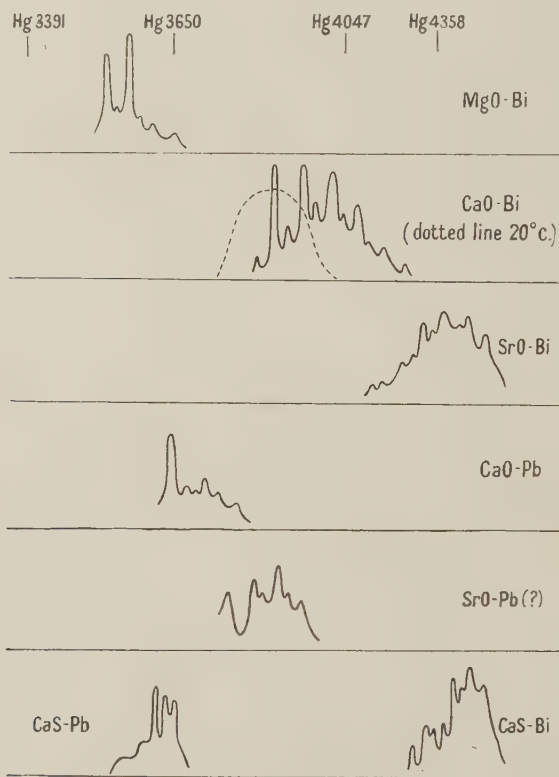


Figure 2. Photometer curves of luminescent spectra (all at temperature of liquid air except dotted curve CaO-Bi).

CaO-Pb and CaO-Bi

The resolved ultra-violet and violet spectra of CaO-Pb and CaO-Bi have already been reported (Ewles 1938) and the results are given again here for convenience of reference and discussion. In the earlier report the CaO-Pb spectrum, since it was obtained with a Hilger Specpure specimen, was attributed to the pure CaO but, as recently reported by us elsewhere (Ewles and Curry 1949), we have now reason to believe that Pb is the activator.

The CaO used in the present work was made from the oxalate prepared by fractional precipitation by recrystallized analar ammonium oxalate solution from recrystallized calcium nitrate solution. After adding activator and flux, mixing

and drying, the mixture was heated for about one hour at 750° c. The analysis of the photometer curves shows that the peaks follow electron band formulae:

CaO-Pb

$$\nu = 27526 + (v' + \frac{1}{2})264 - (v'' + \frac{1}{2})508 \text{ cm}^{-1}$$

Obsd.	Calcd.	v', v''	Obsd.	Calcd.	v', v''
27404	27404	0, 0	26385	26388	0, 2
27166	27160	1, 1	26142	26144	1, 3
26891	26896	0, 1	25886	25880	0, 3
26647	26652	1, 2			

CaO-Bi

$$\nu = 25815 + (v' + \frac{1}{2})298 - (v'' + \frac{1}{2})493 \text{ cm}^{-1}$$

Obsd.	Calcd.	v', v''	Obsd.	Calcd.	v', v''
26322	26314	2, 0	25017	25030	1, 2
26023	26016	1, 0	24732	24732	0, 2
25848	25821	2, 1	24521	24537	1, 3
25719	25718	0, 0	24245	24239	0, 3
25525	25523	1, 1	23758	23746	0, 4
25231	25225	0, 1			

SrO-(Pb?) and SrO-Bi

Strontium carbonate was fractionally precipitated by recrystallized analar ammonium carbonate solution from recrystallized strontium chloride solution. After washing and drying, one sample of the carbonate alone, and another after addition of $\text{Bi}(\text{NO}_3)_3$ solution, were heated in pure alumina crucibles for one hour at 1,100° c. to reduce to oxide. The sample containing no additional activator showed a weak resolved band in the near ultra-violet. The activator, if any, responsible for this is unknown. Although additions of Pb do not seem to intensify this band the recent findings with CaO-Pb referred to above suggest that here again some impurity such as Pb, which it is impossible to remove, may be responsible.

SrO (?)

$$\nu = 26538 + (v' + \frac{1}{2})230 - (v'' + \frac{1}{2})386 \text{ cm}^{-1}$$

Obsd.	Calcd.	v', v''	Obsd.	Calcd.	v', v''
26460	26460	0, 0	25690	25688	0, 2
26070	26074	0, 1	25510	25532	1, 3
25930	25918	1, 2	25300	25302	0, 3

SrO-Bi

$$\nu = 24180 + (v' + \frac{1}{2})190 - (v'' + \frac{1}{2})390 \text{ cm}^{-1}$$

Obsd.	Calcd.	v', v''	Obsd.	Calcd.	v', v''
24070	24080	0, 0	23100	23100	1, 3
23880	23880	1, 1	22910	22910	0, 3
23700	23690	0, 1	22730	22710	1, 4
23480	23490	1, 2	22450	22520	0, 4
23300	23300	0, 2			

MgO-Bi

Analar MgO, after mixture with the activator and 10% NaCl as flux, was heated for 5 hours at 700-800° c. This product gives a weak band in the ultra-violet with two well articulated peaks and a number of less defined peaks following the arrangement:

$$\nu = 28460 + (v' + \frac{1}{2})156 - (v'' + \frac{1}{2})346 \text{ cm}^{-1}$$

Obsd.	Calcd.	v', v''	Obsd.	Calcd.	v', v''
28350	28366	0, 0	27670	27674	0, 2
28180	28176	1, 1	27480	27484	1, 3
28020	28020	0, 1	27320	27328	0, 3
27820	27830	1, 2			

CaS-Bi and CaS-Pb

Calcium sulphide was prepared by intimately mixing analar calcium sulphate with an amount of pure sucrose corresponding to the relation $\text{CaSO}_4 + 3\text{C}$. After addition of the activator and drying, the mixture was heated in an alumina crucible with a close fitting lid at 900° c. for about an hour.

CaS-Bi

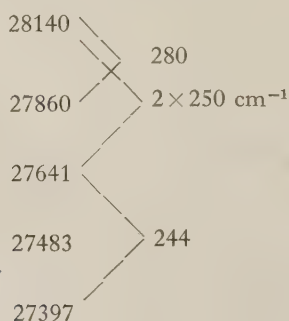
This gives a fairly well articulated band in the violet whose peaks follow the electron band formula:

$$\nu = 23397 + (v' + \frac{1}{2})130 - (v'' + \frac{1}{2})250 \text{ cm}^{-1}$$

Obsd.	Calcd.	v', v''	Obsd.	Calcd.	v', v''
23337	23337	0, 0	22588	22587	0, 3
23220	23217	1, 1	22322	22337	0, 4
23093	23087	0, 1	22086	22087	0, 5
22980	22967	1, 2	21950	21967	1, 6
22820	22837	0, 2			

CaS-Pb

This gives a weak band in the ultra-violet showing two very broad 'lines' on a rising background and three fairly well articulated peaks. The analysis of the photometer curve gives a frequency difference for the lower state similar to that obtained with CaS-Bi but there is not enough detail to make a reliable detailed analysis. The peaks and frequency differences are:



Mixed Crystals: CaO–SrO–Bi

Mixed crystals of the oxides were attempted by co-precipitation of the carbonates and, after addition of the activator and in some cases of up to 20% NaCl as flux, drying and heating for several hours at 1,100°C. The analysis of the photometer curves of the low temperature spectra show that, as the SrO content is increased,

(a) there results a progressive loss of resolution results up to a Sr/Ca ratio of 1/4, where resolution is completely lost and not recovered until the SrO–Bi spectrum appears at about 95% SrO;

(b) there is a slight progressive shift of the peaks to longer wavelengths.

The measurements given below and the photometer curves in Figure 3 for

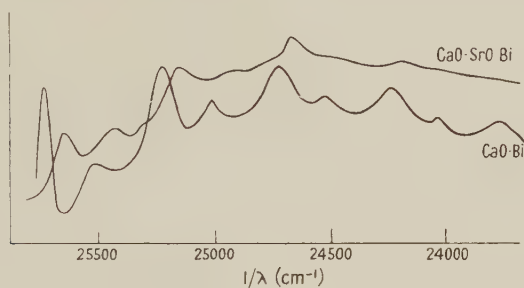


Figure 3. Comparison of resolved violet bands of CaO–(Bi) and the mixed crystals CaO–SrO–(Bi).

a Sr/Ca ratio of 1/5 show that there is also a slight change of vibrational frequency in this mixed crystal as compared with CaO.

CaO–Bi		CaO–SrO–(Bi)	
25719		25660	
	488		480
25231		25180	
	499		480
24732		24700	
	487		480
24245		24220	

§ 4. FACTORS INFLUENCING INTENSITY OF EMISSION AND RESOLUTION

Samples prepared with the addition of 10% NaCl as flux gave more intense emission in all cases than those without flux, generally by a factor of some 3 or 4 times. Resolution was also improved by a flux and, in the case of SrO and the mixed oxides, only obtained with the use of a flux. The spectra are, however, completely unaffected in electronic energy and vibrational frequency by flux—even up to 20% of this. The requirements regarding purity varied; in some cases, as with CaO, CaS and MgO–Bi analar materials were sufficiently pure to give well resolved spectra, while with SrO and the mixed oxides resolution was only obtained after careful further purification from analar materials. In general too, prolonged heating at a lower temperature than that normally required to initiate luminescent power improves both intensity and resolution. Grinding and rolling in an agate mortar decreases intensity.

§ 5. SURVEY AND DISCUSSION OF THE OBSERVATIONS

The resolution of the luminescent spectra of a number of different solids of simple crystal structure activated by different impurities makes it possible to draw conclusions which may be of general application to the interpretation of the luminescence of solids.

(a) The spacing of the vibrational levels in the lower state involved in emission is nearly the same for the same host lattice activated with different impurities.

Host	Activator	
	Bi	Pb
CaO	493 cm ⁻¹	508 cm ⁻¹
SrO	390	386
CaS	250	244
MgO	346	—

This seems to indicate that the vibrational frequency of the luminescent centre is to be identified with a vibration of the host lattice.

(b) The energy of the electronic transition is determined both by the activator and by the host lattice, e.g.

Phosphor	Electronic energy in wave-numbers (cm ⁻¹)	Phosphor	Electronic energy in wave-numbers (cm ⁻¹)
CaO-Pb	27525	CaS-Bi	23397
CaO-Bi	25816	CaS-Pb	about 28000
SrO-Pb ?	26538	MgO-Bi	28460
SrO-Bi	24180		

(c) There is a progression of decreasing electronic energy of transition in the order MgO, CaO, SrO, CaS with these simple crystals and in the order CaO, CaO-SrO with mixed crystals.

(d) If the proposed analyses of the resolved bands be accepted, the strongest components all represent transitions from the lowest level of the upper state.

(e) The relative weakening of some of the early members of the series (seen by comparison of the numerical analyses with the photometer curves) is due, it is suggested, to self-excitation by the overlapping of the long-wave tail of the excitation region with the short-wave tail of the emission region. Excitation curves obtained by Ewles and Curry (1949) indicate that such overlapping does indeed occur in these cases.

(f) Both the levels involved in a transition giving rise to emission of a member of a band series must be very narrow. In CaO-Bi for example the half-width of a member is about 30 cm⁻¹ corresponding to a width of level of about 0.008 e.v.

(g) It is suggested that the observations are in accord with the view that the luminescent centre consists of an impurity (a term which may include a lattice defect) associated with a large but not too large number of lattice ions. This view, originally put forward in some sort by Lenard in 1904 and developed quantitatively by one of us in 1930 (Ewles 1930) now appears to be receiving new support from various sources (Ewles and Curry 1949, Gibson 1948, Garlick 1948). It has been shown (Ewles and Curry 1949) that in doubly activated calcium oxide, Pb centres interfere with Bi centres when the concentration of the lead is between 10⁻⁴ and 10⁻⁵. If the 'size of the centre' is *n* lattice spacings each way from the impurity then interference would occur when the chance of one lead atom occurring

in a volume occupied by $(2n)^3$ calcium atoms is appreciable. If the chance for a detectable quenching is put at 10% then $Pb/Ca = 5 \times 10^{-5} = 1/10(2n)^3$ giving $n=6$ lattice spacings each way for the effective size of the centre in this case. It does not appear that there is any evidence from the observations reported here as to whether the association of the Bi or Pb with the crystal is by replacement of a lattice ion or by interstitial entry into the lattice.

(h) Seitz (1938) and Williams (1948) have estimated the peak absorption and emission energies in the luminescent spectra of some impurity activated solids in terms of transitions in the activator atom in association with the host lattice. Attempts are being made to apply such methods to the spectra reported here. The precise experimental evaluation of electronic and vibrational energies, made possible by the resolution and analyses given in this paper, should afford a more definite test of such methods than the broad bands of $ZnS(Zn)$, $ZnS(Cu)$, $ZnO(Zn)$ and $KCl(Tl)$ to which they have been applied so far.

ACKNOWLEDGMENTS

We are grateful to Professor R. Whiddington, Cavendish Professor of Physics, The University of Leeds, for facilities for carrying out the work and for his continual interest in it. One of us (J.E.) is indebted to the Leverhulme Research Fellowship Fund for a personal grant, to the Department of Scientific and Industrial Research for a grant enabling us to make use of the assistance of Mr. C. N. Heap in the preparation of some materials and to the Government Grants Committee of the Royal Society for an Apparatus Grant.

REFERENCES

- BOWEN, E. J., 1935, *J. Chem. Soc.*, p. 36.
 DEUTSCHBEIN, O., 1932, *Ann. Phys., Lpz.*, **14**, 7.
 EWLES, J., 1930, *Proc. Roy. Soc. A*, **129**, 509; 1938, *Ibid.*, **167**, 34.
 EWLES, J., and CURRY, C., 1949, *Proc. Leeds Phil. Soc.*, **5**, Part III, p. 240.
 GARLICK, G. F. J., 1948, *Solid Luminescent Materials* (Cornell Symposium of American Physical Society).
 GIBSON, A. F., 1948, *Thesis* (University of Birmingham).
 VON HIPPEL, A., 1936, *Z. Phys.*, **101**, 680.
 KROGER, F. A., 1948, *Some Aspects of the Luminescence of Solids* (Amsterdam : Elsevier Publishing Co.).
 RANDALL, J. T., 1938, *Discussion on Luminescence* (London : Faraday Society).
 SEITZ, F., 1938, *J. Chem. Phys.*, **6**, 454.
 WILLIAMS, F. E., 1948, *Phys. Rev.*, **73**, 1257.

Influence of Dipole-Dipole Coupling on the Dielectric Constant of Dipolar Substances

By A. A. SABRY

Department of Applied Mathematics, Faculty of Science, Cairo

Communicated by H. Fröhlich; MS. received 24th October 1949

ABSTRACT. Kirkwood's formula for dielectric constant, ϵ , gives it in terms of a correlation coefficient which depends on the probability that any two dipolar molecules have a certain configuration.

The main object of this paper is to calculate the configurational probability of the dipole orientations; this is dealt with in the first part of the paper by considering two dipoles and replacing the rest by a homogeneous dielectric. The dipolar molecules are regarded as point dipoles and the effect of other forces on the orientation of the molecules is neglected.

In the second part of the paper the calculation of the correlation coefficient appearing in Kirkwood's dielectric constant formula is carried out. This correlation coefficient is evaluated for water, and the value of ϵ then obtained from Kirkwood's formula is in fair agreement with the observed value.

INTRODUCTION

IN early relations of the dielectric constant, the interaction between dipolar molecules has not been taken into account. Kirkwood (1939) and then Fröhlich (1948) constructed formulae which depend on a knowledge of the configurational probability of dipolar molecules.

Kirkwood, in the application of his formula to water, considered that for any two first neighbours (owing to hydrogen bonds between them) the two dipole directions make a constant angle with the line joining them, and can rotate freely about that line. The value of the dielectric constant of water obtained on that assumption is fairly good.

These formulae are a useful means of checking the accuracy of the configurational probability calculated by other methods.

A knowledge of the configurational probability of the dipoles can also be used in calculating an additional average potential energy and an additional specific heat due to dipole-dipole coupling, the effect of dipole rotation on the x-ray scattering, the hydration of salts and many other things.

In the first part of the paper a method for the calculation of the configurational probability of dipole orientations is carried out on the assumption that the molecules are point dipoles. The two dipoles concerned are considered as in a cavity (or two cavities), the mutual potential energy is formed and the probability for such a configuration calculated by use of Boltzmann's law.

In the second part of the paper the calculation of the correlation coefficient is given in terms of double integrals which can only be evaluated by numerical methods. The numerical evaluation of this correlation coefficient for water leads to a value of the dielectric constant in fair agreement with the observed value. It may be noted, in the application to water, that the effect of hydrogen bonds has not been taken into account, since we have used a model in which all molecules were substituted by point dipoles.

PART I

THE CONFIGURATIONAL PROBABILITY

The rigorous method of evaluating the probability $\rho_0^j(\mathbf{p}_{i0}\mathbf{p}_j)$ that two dipoles i, j have simultaneously a certain configuration is to write down the probability for the whole set of dipoles in the form

$$\rho Z = \exp(-W/kT)$$

where

$$Z = \sum_{\mathbf{p}_1 \dots \mathbf{p}_n} \exp(-W/kT), \quad \dots\dots\dots (1.1)$$

and then sum ρ over all orientations of the dipoles except those for the two dipoles i, j in question. Since it is impracticable to evaluate such a sum, we have to use some approximate method to find the required probability.

We replace the rest of the molecules macroscopically by a homogeneous dielectric. The form of the internal boundary will be assumed to be simply two separate spheres with the two molecules concerned at their centres; the volume of each sphere is $1/N = 4\pi a^3/3$ where N is the number of molecules per unit volume. If the two molecules are first neighbours, the two spheres will overlap and thus form a single cavity of volume less than $2/N$; we might therefore consider the radius of each of the overlapping spheres to be xc where c is the distance between first neighbours. In this case the volume of the cavity would be $\pi c^3(2x+1)^2(4x-1)/12$. Equating this to $8\pi a^3/3$ we obtain

$$\frac{1}{x^3} - \frac{12}{1+32a^3/c^3} \frac{1}{x} - \frac{16}{1+32a^3/c^3} = 0, \quad \dots\dots\dots (1.2)$$

which is a cubic equation to determine $1/x$ and hence the radius xc of each of the overlapping spheres.

The evaluation of the field inside such a cavity is, however, found to be very difficult and therefore a cavity in the form of an ellipsoid of revolution will actually be considered. If the distance between the foci is $2b$ and the major axis is $2b \cosh t$, then equating the volume of the ellipsoid to $8\pi a^3/3$ one obtains

$$(\cosh t)^3 - (\cosh t) - 2 \frac{a^3}{b^3} = 0. \quad \dots\dots\dots (1.3)$$

This equation, although it has fixed the volume of the cavity, has not fixed the form of the ellipsoid of revolution. This will be chosen to coincide as far as possible with the cavity of the two overlapping spheres whose dimensions are given by (1.2).

In order to calculate the probability ρ_0^{ij} , we shall calculate the mutual potential energy between the two dipoles in a given configuration, taking into account the image field, or the average effect of the rest of the dipoles.

If we write the total field acting on one of the dipoles i in the form

$$-\alpha F^{(i)} = (A_0 - 1)\boldsymbol{\mu}^{(1)} + (B_0 - A_0)(\boldsymbol{\mu}^{(1)} \cdot \mathbf{k})\mathbf{k} + A\boldsymbol{\mu}^{(2)} + (B - A)(\boldsymbol{\mu}^{(2)} \cdot \mathbf{k})\mathbf{k}, \quad \dots\dots\dots (1.4)$$

then when the two molecules are first neighbours, the constants A_0 , B_0 , A , B will be shown in the first Appendix to be

$$\left. \begin{aligned} A_0 - 1 &= \frac{\alpha}{b^3} \sum_{n=0}^{\infty} (n + \tfrac{1}{2}) \left\{ P'_n \left(\frac{c}{2b} \right) \right\}^2 \frac{Q'_n(\cosh t)}{P'_n(\cosh t)} \frac{1}{1 - X_n^{(1)}}, \\ B_0 - 1 &= -\frac{2\alpha}{b^3} \sum_{n=0}^{\infty} (n + \tfrac{1}{2}) \left\{ P'_n \left(\frac{c}{2b} \right) \right\}^2 \frac{Q_n(\cosh t)}{P_n(\cosh t)} \frac{1}{1 - X_n}, \\ A &= \frac{\alpha}{c^3} - \frac{\alpha}{b^3} \sum_{n=0}^{\infty} (-)^n (n + \tfrac{1}{2}) \left\{ P'_n \left(\frac{c}{2b} \right) \right\}^2 \frac{Q'_n(\cosh t)}{P'_n(\cosh t)} \frac{1}{1 - X_n^{(1)}}, \\ B &= -\frac{2\alpha}{c^3} + \frac{2\alpha}{b^3} \sum_{n=0}^{\infty} (-)^n (n + \tfrac{1}{2}) \left\{ P'_n \left(\frac{c}{2b} \right) \right\}^2 \frac{Q_n(\cosh t)}{P_n(\cosh t)} \frac{1}{1 - X_n}, \end{aligned} \right\} \dots\dots\dots (1.5)$$

where

$$\left. \begin{aligned} (\epsilon - 1)X_n &= \frac{Q_n(\cosh t)P'_n(\cosh t) - Q'_n(\cosh t)P_n(\cosh t)}{P_n(\cosh t)Q'_n(\cosh t)}, \\ (\epsilon - 1)X_n^{(1)} &= \frac{\sinh^2 t}{P'_n(\cosh t)} \cdot \frac{Q'_n(\cosh t)P''_n(\cosh t) - Q''_n(\cosh t)P'_n(\cosh t)}{Q'_n(\cosh t)\cosh t + Q''_n(\cosh t)\sinh^2 t}. \end{aligned} \right\} \dots\dots\dots (1.6)$$

$2b$ is the distance between the foci, $2b \cosh t$ is the major axis and c is the distance between first neighbours.

It may be noted that for large ϵ , X_n , $X_n^{(1)} \rightarrow 0$ and so all A_0 , B_0 , A , B will be independent of ϵ .

The field acting on one of the two molecules given by equation (1.4) in vector form can be re-written in the tensor form

$$-\alpha F_s^{(i)} = \sum_{j's'} (\lambda - 1)_{ss'}^{ij} \mu_{s'}^j. \dots\dots\dots (1.7)$$

If the axes considered are orthogonal then λ will be given by

$$\begin{aligned} \lambda_{ss'}'' &= \lambda_{ss'}^{22} = A_0 \delta_{ss'} + (B_0 - A_0) k_s k_{s'} = \gamma_{ss'}^{(0)}, \text{ say,} \\ \lambda_{ss'}^{12} &= \lambda_{ss'}^{21} = A \delta_{ss'} + (B - A) k_s k_{s'} = \gamma_{ss'}, \text{ say,} \end{aligned}$$

where \mathbf{k} is a unit vector along the line joining the two molecules. Omitting the suffixes s , s' then

$$\lambda \equiv \begin{pmatrix} \gamma^{(0)} & \gamma \\ \gamma & \gamma^{(0)} \end{pmatrix} \dots\dots\dots (1.8)$$

where

$$\left. \begin{aligned} \gamma^{(0)} &= A_0 + (B_0 - A_0)(kk) \\ \gamma &= A + (B - A)(kk). \end{aligned} \right\} \dots\dots\dots (1.9)$$

Since

$$\mu_s^{(i)} = p_s^{(i)} + \alpha F_s^{(i)}, \dots\dots\dots (1.10)$$

then, eliminating $F_s^{(i)}$ between (1.7), (1.10) we obtain

$$\mu_j^{(i)} = \sum_{j's'} (\lambda^{-1})_{ss'}^{ij} p_{s'}^j, \dots\dots\dots (1.11)$$

where λ^{-1} is the reciprocal of the tensor λ .

The mutual potential energy W is given by

$$-\frac{\partial W}{\partial \mu_s^{(i)}} = F_s^{(i)} - \frac{1}{\alpha} (\mu_s^{(i)} - p_s^{(i)}). \quad \dots\dots (1.12)$$

By use of (1.7), (1.11) and (1.12) we obtain

$$W = \frac{-1}{2\alpha} \sum_{ij} \sum_{ss'} (\lambda^{-1})_{ss'}^{ij} p_s^{(i)} p_{s'}^{(j)} + \text{const.} \quad \dots\dots (1.13)$$

It is proved in the second Appendix that if λ is given by (1.8) and $f(\lambda)$ is any function of (λ) then

$$[f(\lambda)]^{11} = [f(\lambda)]^{22} = \frac{1}{2} f(\gamma^{(0)} + \gamma) + \frac{1}{2} f(\gamma^{(0)} - \gamma)$$

$$[f(\lambda)]^{12} = [f(\lambda)]^{21} = \frac{1}{2} f(\gamma^{(0)} + \gamma) - \frac{1}{2} f(\gamma^{(0)} - \gamma).$$

In particular taking $f(\lambda) = -\lambda^{-1}$, and omitting suffixes s, s'

$$-(\lambda^{-1})^{11} = \frac{-\gamma^{(0)}}{\gamma^{(0)^2} - \gamma^2} = F_0(\gamma^{(0)}\gamma), \quad \text{say},$$

$$-(\lambda^{-1})^{12} = \frac{\gamma}{\gamma^{(0)^2} - \gamma^2} = F(\gamma^{(0)}\gamma), \quad \text{say.} \quad \dots\dots (1.14)$$

The expression (1.13) can then be written, using (1.14), in the form

$$W = \frac{1}{2\alpha} \sum_{ss'} [F_0(\gamma^{(0)}\gamma)]_{ss'} [p_s^{(1)} p_{s'}^{(1)} + p_s^{(2)} p_{s'}^{(2)}] + \frac{1}{\alpha} \sum_{ss'} [F(\gamma^{(0)}\gamma)]_{ss'} p_s^{(1)} p_{s'}^{(2)} \quad \dots\dots (1.15)$$

where the tensors $\gamma^{(0)}, \gamma$ are given by (1.9).

It is proved in the third Appendix that if $F(\gamma^{(0)}\gamma)$ is a tensor function of the two tensors $\gamma^{(0)}$ and γ given by (1.9), then

$$F(\gamma^{(0)}\gamma) = F(A_0 A) + [F(B_0 B) - F(A_0 A)](kk). \quad \dots\dots (1.16)$$

A similar equation holds for $F_0(\gamma^{(0)}\gamma)$. Substituting in (1.15) the values of $F_0(\gamma^{(0)}\gamma)$ and $F(\gamma^{(0)}\gamma)$ given by (1.16) and remembering that

$$\sum_{ss'} p_s^{(1)} p_{s'}^{(2)} k_s k_{s'} = (\mathbf{p}^{(1)} \cdot \mathbf{k})(\mathbf{p}^{(2)} \cdot \mathbf{k}) \quad \text{and} \quad \sum_{ss'} p_s^{(1)} p_{s'}^{(2)} \delta_{ss'} = (\mathbf{p}^{(1)} \cdot \mathbf{p}^{(2)}),$$

we obtain the final formula for W

$$W = \frac{1}{2\alpha} [F_0(B_0 B) - F_0(A_0 A)] [(\mathbf{p}^{(1)} \cdot \mathbf{k})^2 + (\mathbf{p}^{(2)} \cdot \mathbf{k})^2]$$

$$+ \frac{1}{\alpha} \{F(A_0 A)(\mathbf{p}^{(1)} \cdot \mathbf{p}^{(2)}) + [F(B_0 B) - F(A_0 A)](\mathbf{p}^{(1)} \cdot \mathbf{k})(\mathbf{p}^{(2)} \cdot \mathbf{k})\}. \quad \dots\dots (1.17)$$

The functions F_0 and F are given by (1.14) on replacing $\gamma^{(0)}, \gamma$ by the constants A_0, A or B_0, B .

The probability for a given configuration can then be easily found by Boltzmann's law, using for W the expression given by (1.17).

APPENDIX 1

The internal boundary of the dielectric is an ellipsoid of revolution of major axis (along the axis of revolution) $2b \cosh t$ and the distance between the foci is $2b$. A dipole μ lies at distance $c/2 < b$ from the centre of the ellipsoid and on the line joining the two foci. It is required to find the field at the position of the dipole and at a point on the line joining the two foci at distance c from the dipole μ (on the other side of the centre).

Using orthogonal coordinates (t, θ, ϕ) given by

$$x_1 = b \cosh t \cos \theta \quad x_2 = b \sinh t \sin \theta \cos \phi \quad x_3 = b \sinh t \sin \theta \sin \phi$$

where (x_1, x_2, x_3) are orthogonal axes, the first along the axis of revolution, the second in the plane of the dipole μ and the first axis, the general potential V satisfying $\nabla^2 V = 0$ can be written in terms of (t, θ, ϕ)

$$V(t\theta\phi) = \sum_{n=0}^{\infty} \sum_{m=0}^n [A_n^m P_n^m(\cosh t) + B_n^m Q_n^m(\cosh t)] T_n^m(\cos \theta) \cos m\phi \quad \dots\dots\dots (1.18)$$

where
$$T_n^m(x) = (1 - x^2)^{m/2} (-)^m \frac{d^m P_n(x)}{dx^m},$$

$$P_n^m(x) = (x^2 - 1)^{m/2} \frac{d^m P_n(x)}{dx^m}, \quad Q_n^m(x) = (x^2 - 1)^{m/2} \frac{d^m Q_n(x)}{dx^m}.$$

The coordinates of the dipole are $(0, \theta_0, 0)$ and those of the other point at which we want to find the field are $(0, \pi - \theta_0, 0)$ where $\cos \theta_0 = c/2b$. If R is the distance between (t, θ, ϕ) , (t', θ', ϕ') then,

$$\begin{aligned} \frac{1}{R} = & \frac{1}{b} \sum_{n=0}^{\infty} (2n+1) \left[Q_n(\cosh t) P_n(\cosh t') P_n(\cos \theta) P_n(\cos \theta') \right. \\ & + 2 \sum_{m=1}^{\infty} (-)^m \left\{ \frac{(n-m)!}{(n+m)!} \right\}^2 Q_n^m(\cosh t) P_n^m(\cosh t') T_n^m(\cos \theta) T_n^m(\cos \theta') \\ & \left. \times \cos m(\phi - \phi') \right]. \quad \dots\dots\dots (1.19) \end{aligned}$$

Taking a charge $-e$ at $t=0, \theta=\theta_0$ and a charge $+e$ at $t=t', \theta=\theta'$, then if the dipole makes an angle α with the direction of the axis x_1 ,

$$\frac{\mu}{be} \cos \alpha = \cosh t' \cos \theta' - \cos \theta_0; \quad \frac{\mu}{be} \sin \alpha = \sinh t' \sin \theta'. \quad \dots\dots\dots (1.20)$$

The potential of the dipole μ at $(0, \theta_0, 0)$ is then, by use of equations (1.19) and (1.20), given by

$$\begin{aligned} V = & \frac{\mu}{b^2} \sum_{n=0}^{\infty} (2n+1) P_n'(\cos \theta_0) \left\{ \cos \alpha Q_n(\cosh t) P_n(\cos \theta) \right. \\ & \left. + \frac{\sin \alpha}{n(n+1)} Q_n^{(1)}(\cosh t) T_n^{(1)}(\cos \theta) \cos \phi \right\}. \quad \dots\dots\dots (1.21) \end{aligned}$$

To find the image field inside the cavity, let the potentials outside and inside the cavity be, following (1.18),

$$\begin{aligned} V_0 &= \sum_{n=0}^{\infty} \sum_{m=0}^n C_n^m Q_n^m(\cosh t) T_n^m(\cos \theta) \cos m\phi \\ V_1 &= \sum_{n=0}^{\infty} \sum_{m=0}^n [A_n^m P_n^m(\cosh t) + B_n^m Q_n^m(\cosh t)] T_n^m(\cos \theta) \cos m\phi. \end{aligned} \quad \dots\dots (1.22)$$

The second part in the expression for V_1 is the potential of the dipole μ and is given by (1.21); the first part is the additional or image potential inside the cavity. Applying the boundary conditions $V_0 = V_1$, $\epsilon(\partial V_0/\partial t) = \partial V_1/\partial t$ at the boundary $t = t_1$ one obtains

$$A_n^{(m)} = - \frac{Q_n^m(\cosh t_1)}{P_n^m(\cosh t_1)} \cdot \frac{1}{1 - X_n^{(m)}} B_n^{(m)} \quad \dots\dots (1.23)$$

where

$$(\epsilon - 1)X_n^{(m)} = \left[\frac{Q_n^{(m)} \frac{\partial P_n^m}{\partial t} - P_n^m \frac{\partial Q_n^m}{\partial t}}{P_n^m \frac{\partial Q_n^m}{\partial t}} \right]_{t=t_1} \quad \dots\dots (1.24)$$

Using the expression for $B_n^{(m)}$ from (1.21) we obtain

$$\left. \begin{aligned} A_n^{(0)} &= - \frac{Q_n(\cosh t_1)}{P_n(\cosh t_1)} \frac{1}{1 - X_n^{(0)}} \frac{\mu \cos \alpha}{b^2} (2n+1) P_n'(\cos \theta_0) \\ A_n^{(1)} &= - \frac{Q_n'(\cosh t_1)}{P_n'(\cosh t_1)} \cdot \frac{1}{1 - X_n^{(1)}} \cdot \frac{\mu \sin \alpha}{b^2} \frac{(2n+1)}{n(n+1)} P_n'(\cos \theta_0), \end{aligned} \right\} \quad \dots\dots (1.25)$$

where

$$\left. \begin{aligned} (\epsilon - 1)X_n^{(0)} &= \left(\frac{Q_n P_n' - Q_n' P_n}{P_n Q_n'} \right)_{t=t_1}, \\ (\epsilon - 1)X_n^{(1)} &= \frac{\sinh t_1}{P_n'(\cosh t_1)} \left(\frac{Q_n' P_n'' - Q_n'' P_n'}{Q_n' \cosh t + Q_n'' \sinh^2 t} \right)_{t=t_1}. \end{aligned} \right\} \quad \dots\dots (1.26)$$

The field components are given by

$$\frac{-1}{b\sqrt{(\cosh^2 t - \cos^2 \theta)}} \frac{\partial V}{\partial t}, \quad \frac{-1}{b\sqrt{(\cosh^2 t - \cos^2 \theta)}} \frac{\partial V}{\partial \theta},$$

and at $\theta = \theta_0$, $t = 0$ the image field inside is given by

$$\left. \begin{aligned} F_t^{(0)} &= \frac{1}{b} \sum_{n=0}^{\infty} A_n^{(1)} P_n'(\cos \theta_0) \frac{n(n+1)}{2} \cos \phi \\ F_{\theta}^{(0)} &= \frac{1}{b} \sum_{n=0}^{\infty} A_n^{(0)} P_n'(\cos \theta_0), \end{aligned} \right\} \quad \dots\dots (1.27)$$

and at $\theta = \pi - \theta_0$, $t = 0$

$$\left. \begin{aligned} F_t &= \frac{-1}{b} \sum_{n=0}^{\infty} (-)^n A_n^{(1)} P_n'(\cos \theta_0) \frac{n(n+1)}{2} \cos \phi \\ F_{\theta} &= \frac{-1}{b} \sum_{n=0}^{\infty} (-)^n A_n^{(0)} P_n'(\cos \theta_0). \end{aligned} \right\} \quad \dots\dots (1.28)$$

Putting the fields at $x_1 = c/2$, $x_1 = -c/2$ as

$$\mathbf{F}^{(0)} = C_0 \boldsymbol{\mu} + D_0 (\boldsymbol{\mu} \cdot \mathbf{k}) \mathbf{k} \quad \text{and} \quad \mathbf{F} = C \boldsymbol{\mu} + D (\boldsymbol{\mu} \cdot \mathbf{k}) \mathbf{k} \quad \dots\dots (1.29)$$

respectively, then

$$\left. \begin{aligned} F_t^{(0)} &= C_0 \mu \sin \alpha \cos \phi, & F_t &= C \mu \sin \alpha \cos \phi, \\ F_\theta^{(0)} &= -(C_0 + D_0) \mu \cos \alpha, & F_\theta &= -(C + D) \mu \cos \alpha. \end{aligned} \right\} \dots\dots (1.30)$$

Using equations (1.25), (1.27), (1.28) and (1.30) we finally obtain

$$\left. \begin{aligned} C_0 &= \frac{-1}{b^3} \sum_{n=0}^{\infty} \frac{Q'_n(\cosh t_1)}{P'_n(\cosh t_1)} \frac{1}{(1 - X_n^{(1)})} (n + \tfrac{1}{2}) \{P'_n(\cos \theta_0)\}^2 \\ C &= \frac{1}{b^3} \sum_{n=0}^{\infty} \frac{Q'_n(\cosh t_1)}{P'_n(\cosh t_1)} \frac{(-)^n}{(1 - X_n^{(1)})} (n + \tfrac{1}{2}) \{P'_n(\cos \theta_0)\}^2 \\ C_0 + D_0 &= \frac{2}{b^3} \sum_{n=0}^{\infty} \frac{Q_n(\cosh t_1)}{P_n(\cosh t_1)} \frac{1}{(1 - X_n^{(0)})} (n + \tfrac{1}{2}) \{P'_n(\cos \theta_0)\}^2 \\ C + D &= -\frac{2}{b^3} \sum_{n=0}^{\infty} \frac{Q_n(\cosh t_1)}{P_n(\cosh t_1)} \frac{(-)^n}{(1 - X_n^{(0)})} (n + \tfrac{1}{2}) \{P'_n(\cos \theta_0)\}^2. \end{aligned} \right\} \dots\dots (1.31)$$

APPENDIX 2

We wish to prove that if λ is a tensor given by

$$\lambda \equiv \begin{pmatrix} \gamma^{(0)} & \gamma \\ \gamma & \gamma^{(0)} \end{pmatrix}, \quad \dots\dots (1.32)$$

and if $f(\lambda)$ is any tensor function of λ , then

$$\begin{aligned} [f(\lambda)]^{11} &= [f(\lambda)]^{22} = \tfrac{1}{2} f(\gamma^{(0)} + \gamma) + \tfrac{1}{2} f(\gamma^{(0)} - \gamma) \\ [f(\lambda)]^{12} &= [f(\lambda)]^{21} = \tfrac{1}{2} f(\gamma^{(0)} + \gamma) - \tfrac{1}{2} f(\gamma^{(0)} - \gamma). \end{aligned}$$

Suppose that

$$\lambda^n \equiv \begin{pmatrix} \gamma^{(0)}(n) & \gamma(n) \\ \gamma(n) & \gamma^{(0)}(n) \end{pmatrix}. \quad \dots\dots (1.33)$$

Multiplying the tensor λ in (1.32) by the tensor λ^n given by (1.33) we obtain

$$\left. \begin{aligned} \gamma^{(0)}(n+1) &= \gamma^{(0)} \gamma^{(0)}(n) + \gamma \gamma(n) \\ \gamma(n+1) &= \gamma^{(0)} \gamma(n) + \gamma \gamma^{(0)}(n). \end{aligned} \right\} \dots\dots (1.34)$$

Eliminating $\gamma(n)$ from equations (1.34) we obtain

$$\gamma^{(0)}(n+2) - 2\gamma^{(0)}\gamma^{(0)}(n+1) + (\gamma^{(0)2} - \gamma^2)\gamma^{(0)}(n) = 0. \quad \dots\dots (1.35)$$

By eliminating $\gamma^{(0)}(n)$ we obtain a similar equation for $\gamma(n)$. Putting $\gamma^{(0)}(n) \propto x^n$ we obtain from (1.35)

$$x^2 - 2\gamma^{(0)}x + \gamma^{(0)2} - \gamma^2 = 0, \quad \dots\dots (1.36)$$

giving

$$x = \gamma^{(0)} \pm \gamma.$$

The general expression for $\gamma^{(0)}(n)$ is therefore

$$\gamma^{(0)}(n) = A_0(\gamma^{(0)} + \gamma)^n + B_0(\gamma^{(0)} - \gamma)^n;$$

similarly

$$\gamma(n) = A(\gamma^{(0)} + \gamma)^n + B(\gamma^{(0)} - \gamma)^n$$

where A_0 , B_0 , A and B are arbitrary constants, which can easily be found to be $A_0 = B_0 = A = -B = \frac{1}{2}$.

Therefore

$$\gamma^{(0)}(n) = \frac{1}{2}(\gamma^{(0)} + \gamma)^n + \frac{1}{2}(\gamma^{(0)} - \gamma)^n = (\lambda^n)^{11} = (\lambda^n)^{22}$$

$$\gamma(n) = \frac{1}{2}(\gamma^{(0)} + \gamma)^n - \frac{1}{2}(\gamma^{(0)} - \gamma)^n = (\lambda^n)^{12} = (\lambda^n)^{21}.$$

Hence the required formula follows.

APPENDIX 3

The tensors $\gamma^{(0)}$, γ are given by

$$\gamma_{ss'}^{(0)} = A_0 \delta_{ss'} + (B_0 - A_0) k_s k_{s'}; \quad \gamma_{ss'} = A \delta_{ss'} + (B - A) k_s k_{s'} \quad \dots \dots (1.37)$$

where A_0 , B_0 , A and B are constants, \mathbf{k} is a unit vector and k_s ($s=1, 2, 3$) are its components referred to an orthogonal triad. It is required to prove that if $F(\gamma^{(0)}, \gamma)$ is any tensor function of $\gamma^{(0)}, \gamma$ then

$$[F(\gamma^{(0)}, \gamma)]_{ss'} = F(A_0 A) \delta_{ss'} + [F(B_0 B) - F(A_0 A)] k_s k_{s'} \quad \dots \dots (1.38)$$

We first consider the tensor $(\gamma^n)_{ss'}$; omitting the suffixes s, s' we have

$$\left. \begin{aligned} \gamma &= A + (B - A)(kk) \\ \gamma^n &= \sum_{r=0}^n A^{n-r} (B - A)^r \binom{n}{r} (kk)^r. \end{aligned} \right\} \quad \dots \dots (1.39)$$

We also have

$$[(kk)^2]_{ss'} = \sum_{s''} k_s k_{s''} k_{s''} k_{s'} = k_s k_{s'} = (kk)_{ss'};$$

by successive pre-multiplication by (kk) we obtain

$$(kk)^r = (kk) \quad r \geq 1. \quad \dots \dots (1.40)$$

Substituting from (1.40) into (1.39) we obtain

$$\begin{aligned} \gamma^n &= A^n + (kk) \sum_{r=1}^n A^{n-r} (B - A)^r \binom{n}{r} \\ &= A^n + (B^n - A^n)(kk), \end{aligned} \quad \dots \dots (1.41)$$

similarly

$$\gamma^{(0)n} = A_0^n + (B_0^n - A_0^n)(kk). \quad \dots \dots (1.42)$$

From (1.40), (1.41), and (1.42)

$$\gamma^{(0)m} \gamma^n = A_0^m A^n + (B_0^m B^n - A_0^m A^n)(kk). \quad \dots \dots (1.43)$$

Hence the required formula (1.38) follows.

PART II

THE CORRELATION COEFFICIENT

The equation for the dielectric constant ϵ given by Kirkwood for isotropic media may be written (Kirkwood 1939)

$$\frac{\epsilon - 1}{3} = \frac{\epsilon + 2}{3} + \frac{3\epsilon}{2\epsilon + 1} \frac{p^2}{a^3 kT} \frac{Q}{(1 - \beta f)} \quad \dots\dots (2.1)$$

$$Q = \frac{1}{3}[1 + z \cos \gamma] \quad \dots\dots (2.2)$$

where $\beta = \alpha/a^3$, $f = 2(\epsilon - 1)/(2\epsilon + 1)$; α is the polarizability, p the permanent moment of a molecule, z the coordination number, i.e. the number of first neighbours, and γ is the angle between the two dipole directions of two first neighbours.

We shall calculate the average of $\cos \gamma$ by multiplying it by the probability, given in Part I, that two dipoles have a given configuration, and then integrating over the orientations of the two dipoles. Since this probability depends on ϵ (because in the calculation, the action of distant molecules on a given one is replaced by that of a continuous distribution) Q will also depend on ϵ , but for high values of ϵ the probability depends very little on ϵ and tends to a definite limiting value as ϵ tends to ∞ . In the application when the formula is of interest ϵ is very large indeed, therefore in the calculation of Q we can use an approximate large value of ϵ , say the experimental one. By substituting this value of Q in equation (2.1) it becomes quadratic in ϵ and its positive root represents the theoretical value.

The degree of coincidence of this value to the experimental value of the dielectric constant is a very useful means of checking the configurational probability and the simple model which have been used.

Let $(\theta, 0)$ and (θ', ϕ) be the polar coordinates of the two dipoles, assumed to be first neighbours, then

$$\cos \gamma = \cos \theta \cos \theta' + \sin \theta \sin \theta' \cos \phi. \quad \dots\dots (2.3)$$

The expression for W given by (1.17) can then be written in the form

$$-\frac{W}{kT} = G(\cos^2 \theta + \cos^2 \theta') + L \cos \theta \cos \theta' + M \sin \theta \sin \theta' \cos \phi \quad \dots\dots (2.4)$$

where

$$\left. \begin{aligned} -G &= \frac{p^2}{2\alpha kT} [F_0(B_0B) - F_0(A_0A)] \\ -L &= \frac{p^2}{\alpha kT} F(B_0B) \\ -M &= \frac{p^2}{\alpha kT} F(A_0A). \end{aligned} \right\} \quad \dots\dots (2.5)$$

The average of $\cos \gamma$ can be written

$$\overline{\cos \gamma} = \overline{\cos \theta \cos \theta'} + \overline{\sin \theta \sin \theta' \cos \phi} = \frac{K_1}{K_0} + \frac{K_2}{K_0}, \text{ say, } \dots\dots (2.6)$$

where

$$K_0 = \frac{1}{8\pi} \int \exp \{ -W/kT \} \sin \theta \sin \theta' d\theta d\theta' d\phi \quad \dots\dots (2.7)$$

$$K_1 = \frac{1}{8\pi} \int \cos \theta \cos \theta' \exp \{ -W/kT \} \sin \theta \sin \theta' d\theta d\theta' d\phi \quad \dots\dots (2.8)$$

$$K_2 = \frac{1}{8\pi} \int \sin \theta \sin \theta' \cos \phi \exp \{ -W/kT \} \sin \theta \sin \theta' d\theta d\theta' d\phi. \quad \dots\dots (2.9)$$

Performing the integration over ϕ by use of the formula

$$\int_0^{2\pi} \cos n\phi \exp \{ x \cos \phi \} d\phi = 2\pi (-i)^n J_n(ix) = 2\pi I_n(x),$$

where $J_n(x)$ is a Bessel function of order n . Afterwards for the integrals over θ, θ' we use the formula

$$\int_0^{\pi/2} \int_0^{\pi} F(\theta, \theta') d\theta d\theta' = \int_0^{\pi/2} \int_0^{\pi/2} [F(\theta, \theta') + F(\pi - \theta, \theta') + F(\theta, \pi - \theta') + F(\pi - \theta, \pi - \theta')] d\theta d\theta',$$

and obtain the following expressions for K_0, K_1 and K_2

$$K_0 = \int_0^{\pi/2} \int_0^{\pi/2} \cosh (L \cos \theta \cos \theta') \exp \{ G(\cos^2 \theta + \cos^2 \theta') \} \\ \times I_0 (M \sin \theta \sin \theta') \sin \theta \sin \theta' d\theta d\theta' \quad \dots\dots (2.10)$$

$$K_1 = \int_0^{\pi/2} \int_0^{\pi/2} \sinh (L \cos \theta \cos \theta') \exp \{ G(\cos^2 \theta + \cos^2 \theta') \} \\ \times I_0 (M \sin \theta \sin \theta') \sin \theta \sin \theta' \cos \theta \cos \theta' d\theta d\theta' \quad \dots\dots (2.11)$$

$$K_2 = \int_0^{\pi/2} \int_0^{\pi/2} \cosh (L \cos \theta \cos \theta') \exp \{ G(\cos^2 \theta + \cos^2 \theta') \} \\ \times I_1 (M \sin \theta \sin \theta') \sin^2 \theta \sin^2 \theta' d\theta d\theta'. \quad \dots\dots (2.12)$$

Application to Water

In this section we shall calculate Q for water, on the assumption that only dipolar forces are essential. This seems to be rather doubtful (Pauling 1935) as the hydrogen bonds may influence the orientational distribution; but it will be shown that at least the exceptional size of ϵ can be explained by taking into account only the dipolar interactions.

The Mutual Potential Energy

The field acting on one of the two first neighbours, included inside a cavity of the form of an ellipsoid of revolution is given by equations (1.4), (1.5) and (1.6), with the condition that the ellipsoid should coincide as nearly as possible with the cavity of two overlapping spheres whose dimensions are given by (1.2).

The average distance between first neighbours c will be taken to be

$$c = 3.27 \times 10^{-8}, \quad \dots\dots (2.13)$$

thus at $T = 273^\circ \text{K}$.

$$\frac{a^3}{c^3} = 0.2042, \quad \dots\dots (2.14)$$

where $4\pi a^3/3 = 1/N$, and N is the number of molecules per unit volume.

Substituting this value of a^3/c^3 in equation (1.2) we find

$$x = 0.5923, \quad \dots\dots (2.15)$$

which determines the radius xc of each of the overlapping spheres. Putting $\cosh t = \dots 1.2, 1.3, 1.4, \dots$ we find that for $\cosh t = 1.3$ the ellipsoid will coincide as nearly as possible with the cavity of the two overlapping spheres. For $\cosh t = 1.3$

$$c/2b = 0.6499, \quad c^3/b^3 = 2.19625. \quad \dots\dots (2.16)$$

Using these values of $c/2b$ and $\cosh t$, and taking for ϵ its experimental value 88.25 (Dorsey 1940) one obtains

$$A_0 = 0.7317; \quad A = 0.00946; \quad B_0 = 0.7802; \quad -B = 0.08161. \quad \dots\dots (2.17)$$

The mutual potential energy is expressed by (2.4) and (2.5). Using the values provided by (2.17) one obtains

$$-G = 1.998; \quad L = 7.628; \quad -M = 0.9945 \quad \dots\dots (2.18)$$

at $T = 273^\circ \text{K}$.

The Correlation Coefficient Q

The double integrals K_0, K_1, K_2 given by (2.10), (2.11) and (2.12) were evaluated numerically using the values of G, L, M given by (2.18). These were found to be

$$\left. \begin{aligned} K_0 &= (\pi/2)^2 6.8381/81 \\ K_1 &= (\pi/2)^2 3.3185/81 \\ -K_2 &= (\pi/2)^2 0.8578/81 \end{aligned} \right\} \quad \dots\dots (2.19)$$

$$\text{then from (2.6)} \quad \overline{\cos \gamma} = 0.36. \quad \dots\dots (2.20)$$

Taking $z = 4$ we obtain from (2.2)

$$Q = 0.8133. \quad \dots\dots (2.21)$$

$$\text{Putting} \quad \beta = 0.2248, \quad \frac{p^2}{a^3 k T} = 12.6493, \quad \dots\dots (2.22)$$

and substituting for Q from (2.21), equation (2.1) becomes

$$1.20187\epsilon^2 - 1.12373\epsilon - 2.10134 = 92.59288\epsilon, \quad \dots\dots (2.23)$$

$$\text{giving} \quad \epsilon = 78. \quad \dots\dots (2.24)$$

ACKNOWLEDGMENTS

The author wishes to thank Professor M. Born, in whose department this work was done, for his supervision and interest in the preparation of this work, and for many helpful criticisms. He also wishes to thank Dr. H. S. Green for assistance given from time to time and Professor Fröhlich for his help in the final formulation of the paper.

REFERENCES

- DORSEY, N. E., 1940, *Properties of Ordinary Water Substances* (New York: Reinhold Publishing Corpn.):
 FRÖHLICH, H., 1948, *Trans. Faraday Soc.*, **44**, 238; 1949, *Theory of Dielectrics* (Oxford: Clarendon Press).
 KIRKWOOD, J., 1939, *J. Chem. Soc. Phys.*, **7**, 911.
 PAULING, J., 1935, *J. Amer. Chem. Soc.*, **57**, 2681.

The Effect of Occluded Hydrogen on the Electrical Resistance of Palladium

By P. WRIGHT

University College of North Wales, Bangor

Communicated by E. A. Owen; MS. received 10th November 1949

ABSTRACT. Agreement between the results of theoretical and experimental investigations of the absorption of hydrogen by palladium indicates that, at least at higher temperatures, the hydrogen is contained in solid solution. Apparatus for observing the changes in electrical resistance of palladium during absorption and evolution of hydrogen is described, with which resistance-pressure isotherms from 75° to 150° c. were obtained for pressures increasing and decreasing between zero and atmospheric. Factors affecting the resistance of the Pd-H system are discussed and an explanation of the form of the isotherms is given; a decrease in resistance which is observed, when hydrogen is added to the alloy in the β phase, is attributed to completion of the d shells of palladium.

I. SOLUBILITY OF HYDROGEN IN PALLADIUM

§ 1. INTRODUCTION

FEW special problems have been so extensively investigated as that of the occlusion of hydrogen by palladium. McKeehan (1923) gives a bibliography of 66 titles of papers mostly published between 1900 and 1922, and many more are quoted by Ubbelohde in reviews of the subject in 1932 and 1937. The inconclusive nature of much of the earlier work appears to be due to a failure to recognize the solubility of gases in metals as simply a particular aspect of the general problem of pressure-temperature equilibrium of alloys. In his general review (1937) of the properties of metallic hydrogen and its alloys, Ubbelohde advanced explanations of various phenomena associated with the palladium-hydrogen system in terms of the then recently developed theories of the metallic state. The exceptional properties of transition metals generally, are due to the partly-filled d band. Palladium, for example, has approximately 0.6 unoccupied states per atom in the d band, and there is now adequate evidence that when hydrogen dissolves in palladium, it is almost completely ionized and its electrons enter the d band. In a statistical interpretation of the solubility, Lacher (1937) calculates, from measurements of equilibrium isotherms at various temperatures, that the number of potential 'holes' per Pd atom which are available for hydrogen is nearly constant and equal to 0.6 approximately. From this result, it is to be inferred that the process of hydrogen absorption reaches completion when the d band is filled, that is, when the ratio r of H to Pd atoms is approximately 0.6. When palladium is charged with hydrogen electrolytically, however, values of r greater than 0.6 are observed at temperatures below about 80° c. At 0° c., for example, the maximum concentration approaches unity. If the hydrogen is entirely located interstitially in solid solution, the additional absorption of hydrogen may occur with entry of electrons into the s band of palladium. Such a possibility is assumed by Wagner (1944) in calculating the solubility from thermodynamic principles. It is also possible that the formation

of simple solid solutions is not the only absorptive process operating. In a recent note (1948), D. P. Smith presents a formidable body of experimental evidence in support of his view that a large proportion of the occluded hydrogen is concentrated in rifts or widened spacings in the palladium lattice. Assuming at 0° c. a total concentration $r \simeq 1$, of which the concentration in solid solution is 0.6, we find that the metal occludes about 500 times its own volume of hydrogen (measured at normal pressure) by some additional absorptive process. If Smith's view is correct, we may suppose that when palladium is charged with hydrogen electrolytically, the gas (probably in a highly ionized state (Moore 1939)) is concentrated under enormous pressure in the intergranular fissures in the metal.

§ 2. THEORETICAL FORMULAE FOR THE SOLUBILITY

Lacher's formula is developed by assuming that a definite number of holes in the metal are available for hydrogen and that the heat of absorption increases with the number of holes filled. It gives a critical temperature above which only one solid phase can exist and below which two solid phases can be in equilibrium with one another. The equation for the concentration-pressure isotherm at any temperature T may be expressed in the form :

$$\log p^{1/2}(\text{atm.}) = \log \frac{r}{0.59 - r} - 2.3009 - (445.6 + 1672r)/T.$$

Over a certain range of pressure on any isotherm there are three roots to this equation, one of which, $r = 0.59/2$, corresponds to an unstable state at the critical pressure at which the phase transformation occurs. If r_α and r_β are, respectively, the concentrations in the α and β phase at this critical pressure, for equilibrium conditions these roots must satisfy $r_\alpha + r_\beta = 0.59$. The 100° c. isotherm, calculated from the above formula, is shown in Figure 1. The continuous line is the equilibrium isotherm, and by putting $r = 0.59/2$, the value 28.1 cm. Hg is obtained for the critical pressure at which the phase change takes place.

Over the greater part of the range of temperature investigated experimentally, Lacher's formula gives a satisfactory representation of the 'equilibrium' pressure-composition isotherms for the Pd-H system. It must be observed, however, that the term 'equilibrium isotherms' as used above applies to those isotherms which give the same value to the pressure for a given value of r no matter how that value of r is approached. At higher temperatures (200° to 313° c.), Gillespie and Galstoun (1936) obtained such reversible isotherms without using any special preliminary heat treatment. Wagner contends that because of the inadequate mobilities of the Pd atoms at the comparatively low temperatures at which some isotherms have been determined, it is not legitimate to assume that complete thermodynamic equilibrium is established. He points out that in the experiments of Gillespie and Hall (1926), for example, a preliminary heat treatment was used in order to obtain definite single values of the pressure when the α and β phases co-exist, and that the values thus determined approximate to those for complete equilibrium probably because they lie within a 'hysteresis' loop. In most experimental investigations it has been found that, over a certain range of pressure, absorption and evolution isotherms do not coincide. This hysteresis phenomenon indicates that thermodynamic equilibrium has not been completely established, and is ascribed by Wagner to restricted exchange of Pd atoms between the two phases at the comparatively low temperatures of

observation. In expressing the conditions of equilibrium by using Gibbs' equation, he observes, therefore, that whereas equality of chemical potentials is true for transitions of H atoms between the two phases, the analogous condition for transitions of Pd atoms is not applicable. From this new viewpoint, Wagner offers a qualitative explanation of the experimental results and shows that the above assumptions lead also quantitatively to good agreement as to the width of the hysteresis loop. The solubility isotherms are expressed by the formula

$$\sqrt{p} = \frac{r}{1-r} K \exp(\Delta\mu/RT)$$

in which K is the solubility constant for ideally dilute solutions, i.e. $K = \sqrt{p}/r$ for $r \ll 1$; and $\Delta\mu$ is a function of r calculable from experimental isotherms for

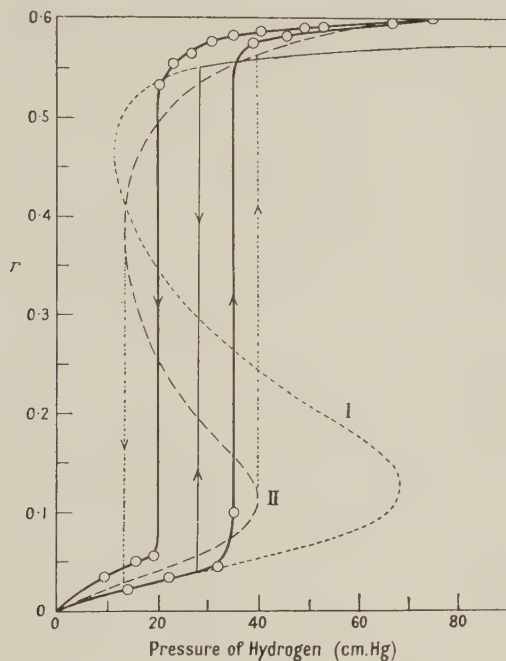


Figure 1. Concentration-pressure isotherms at 100° c.

Experimental: Sieverts and Danz, ————
 Theoretical: I Lacher - - - - - , equilibrium ————
 II Wagner — - - - - , path followed between upper
 and lower isotherms - · - · - ·

the single-phase region above the critical mixing temperature. For calculating the isotherms at lower temperatures, $\Delta\mu$ must be assumed independent of temperature and K must be known. In calculating the 100° c. isotherm (Figure 1) from the above expression, K was chosen by trial to give the best representation of the experimental results of Sieverts and Danz (1937). Bearing in mind the idealized assumptions necessarily involved in deducing the solubility (complications such as the effect on the equilibrium pressure of hydrogen of strains in the regions bordering the two phases are ignored), the correspondence with experiment is remarkably good.

§ 3. EXPERIMENTAL STUDIES OF THE HYSTERESIS EFFECT

An examination of experimental data reveals that reversible isotherms have been obtained only by using palladium in a finely divided state. With palladium in the form of filings, sponge, wire, etc., it has been found that the isotherms for increasing and decreasing hydrogen pressure do not coincide. Sieverts and his co-workers (1933, 1935, 1937, 1938) have also used palladium 'black' with similar results. This hysteresis effect has been observed in x-ray investigations of the expansion of the hydrogen-charged palladium lattice. Detailed studies by Owen and Jones (1937) and by Owen and Williams (1944) establish the presence of two co-existent expanded lattices occurring over different ranges of pressure, and at different mean pressures, on ascending and descending isothermals. In a later publication, Owen (1944) discusses the results of the x-ray work in the light of Lacher's hypothesis that there exist metastable states of supersaturated α and undersaturated β phase in the palladium-hydrogen system. The experimental evidence clearly indicates that the mixed-phase or $(\alpha + \beta)$ regions within the hysteresis loop are characteristic of a system in which thermodynamic equilibrium is not completely established. The x-ray studies also indicate that the new phase, α or β , exists finely dispersed throughout the old phase, the establishment of a new phase occurring, presumably, by the process of nucleation and growth.

The above conclusions support the assumptions on the basis of which Lacher explains the hysteresis in the pressure-concentration isotherms. Smith questions the validity of these assumptions and seeks to account for the behaviour of the Pd-H system in terms of occlusion in rifts as the principal absorptive process, rather than solid solution. Experimental evidence mentioned by Smith appears to show that the α and β phases do not exist interdispersed but are separated by a single-phase boundary which migrates inwards from the surface of the metal as the concentration of hydrogen either increases or diminishes. The present work (II, § 2) indicates that, at low temperatures, the $(\alpha + \beta)$ phase exists over an extremely small range of pressure and, further, that the transition from one pure phase to the other takes place very rapidly when the pressure change is sufficient to carry the system over the two-phase region. All the experiments referred to by Smith are conducted at room temperature, the palladium being charged by making it the cathode of an electrolytic cell. Under these conditions it is probable that the interdispersion of phases would escape observation.

Pressure-concentration isotherms obtained by Sieverts and his co-workers show that the width (pressure range) of the hysteresis loops increases with rise of temperature up to about 220°C., and then decreases, becoming zero at about 300°C. Lacher's formula predicts this feature of the isotherms, though it gives a greater width to the hysteresis loops than is observed experimentally. From Lacher's hypothesis of the persistence of metastable states, it follows that the range of metastability increases with temperature up to 220°C. This conclusion has been criticized, it being assumed on general grounds that the system should attain a state of equilibrium more readily at higher temperatures. It must be pointed out that the pressure at which the phase transformation occurs increases with rise of temperature, and that the persistence of the metastable state should be considered also in relation to this pressure variable. If P_1 and P_2 are, respectively, the upper and lower pressure limits of the hysteresis effect at any temperature T , we might expect the ratio $(P_1 - P_2)/\frac{1}{2}(P_1 + P_2)$, rather than the

value of $(P_1 - P_2)$, to diminish as T increases. Both Lacher's formula and the experimental results of Sieverts and others show that the ratio does, in fact, diminish rapidly as the temperature rises.

Lacher's calculation of the solubility, whilst using the value $r = 0.59$ as a limiting hydrogen concentration set by the completion of the palladium d band, does not exclude the possibility of higher concentrations due to the occupation of other regions of energy. Such a possibility is assumed in Wagner's thermodynamical theory which, as we have seen, gives a remarkably good estimate of the widths of the hysteresis loops. The substantial measure of agreement between theory and experiment may be taken as an indication that, at least at higher temperatures, solid solution is capable of accounting for the occlusion of hydrogen by palladium.

The primary object of the present investigation was to discover if the hysteresis effects in the electrical resistance of Pd-H could also be explained by assuming the hydrogen to be held in solid solution. In the experiments described below, the change in resistance of palladium charged from the gas phase was studied under carefully controlled conditions, and at temperatures lower than those covered by Brüning and Sieverts, particular attention being given to phenomena at 100°C. , for which temperature x-ray and solubility data were available.

II. ELECTRICAL RESISTANCE OF PALLADIUM-HYDROGEN

§ 1. EXPERIMENTAL

Resistance was measured by the potentiometer method, all the usual precautions being taken to avoid errors due to thermo-electric effects. A Cambridge vernier potentiometer and D'Arsonval galvanometer were used and the unknown resistance measured in terms of standards from a multi-range current shunt. A large capacity 2-volt accumulator maintained an extremely steady current of about 1 ampere through the two resistances and a series-connected ballast resistance of rolled manganin wire. Under the least favourable conditions, the resistances of the palladium wire specimens could be determined to within 0.1%. A 15 cm. length of thick palladium wire was clamped at both ends to small blocks of copper mounted on a slab of steatite. The current leads were thin copper rods screwed into the clamping blocks, and the potential contacts to the wire consisted of sharp steel knife-edges about 10 cm. apart. The latter were riveted to copper plates which were screwed down so that the wire was gripped between the knife-edges and the steatite base.

Temperature was measured with a platinum-rhodium thermocouple, the junction of which was flattened and clamped to the palladium wire at its mid-point. Alumel-chromel couples, also in contact with the wire, were located between each knife-edge and clamping block; these were used to measure the temperature gradient along the wire. The whole system, enclosed in a quartz tube, occupied a central position in a tubular furnace which had been specially wound to minimize temperature gradients. Gradients and fluctuations were further reduced by two copper cylinders separated by a layer of magnesium oxide. These filled the remaining annular space between the quartz tube and the wall of the furnace. By means of a small electric heater situated inside the quartz tube and fed from the furnace supply voltage through a transformer, the gradient along the palladium wire was finally reduced to less than $0.05^\circ\text{C. per cm.}$ The temperature of the wire,

as measured by the platinum-rhodium couple, was maintained constant to within 0.2°C . for periods of over a month by a continuous-control thermo-regulator (Wright 1947) operated by a platinum resistance thermometer. The platinum wire was wound between thin sheets of mica on the outer of the two copper cylinders mentioned above.

Before charging with hydrogen, the palladium wires were annealed *in vacuo* at 400°C . for about twelve hours, and their resistances measured at various temperatures between 400°C . and room temperature. Wires of pure palladium, of diameters 0.0805 and 0.210 cm., supplied by Johnson Matthey and Co. Ltd., were found to have an average temperature coefficient of 0.0036 per $^{\circ}\text{C}$., and a resistivity of 10.0 ohm.cm. at 0°C . In the case of wires which had been charged with hydrogen at 100° and 75°C ., it was found that a process of annealing and degassing at 300°C . for several hours was sufficient to restore the wires to their original state as regards electrical resistance.

Pure dry hydrogen was prepared in the manner described by Owen and Jones, and similar measures were taken to avoid contamination of the gas in the apparatus. Any pressure of hydrogen up to one atmosphere could be rapidly established in the observation tube by placing it in communication with a large reservoir containing hydrogen at the desired pressure. Normally, the reservoir was left in communication with the tube to reduce pressure changes due to absorption and evolution of gas by the palladium. After measurement of the resistance of the annealed specimen *in vacuo* at a known temperature, the standard procedure at the beginning of an experiment consisted in raising the temperature of the palladium to within about 5°C . of that finally required, and then admitting hydrogen to a pressure of about 3 cm. Hg. A slight re-adjustment of the thermo-regulator was then sufficient to hold the palladium at the required temperature. Subsequent changes of gas pressure could be made rapidly, since they produced only a small momentary fall in temperature. Pressures were measured to the nearest millimetre with a Bourdon type gauge.

§ 2. RESULTS

Resistance-pressure isotherms for pressures of hydrogen up to 73 cm. Hg are shown in Figure 2, and the observations at 75°C . and 100°C . are recorded in the Table in the order in which they were taken.

With the exception of those marked with an asterisk, the figures represent constant final values of resistance corresponding to each value of the hydrogen pressure. In the case of the 100°C . isotherm, for example, the final resistance was found by plotting a resistance-time graph after each alteration of pressure. For increments of pressure in the range of ascending pressure 0 to 31 cm. Hg the resistance attained its maximum value in less than 5 hours. This part of the isotherm is reversible, that is, it can be re-traversed by reducing the pressure of hydrogen. The second part of the 100°C . isotherm, extending from 31 to about 55 cm. Hg pressure, is irreversible. The observations in this range of ascending pressure are plotted against time in Figure 3, and the values quoted in the Table are the approximate maxima obtained from these resistance-time curves. After each pressure change, the resistance reaches an apparent maximum in a few days. This is followed, however, by a much slower increase. At some pressures, readings were taken daily for over a month; though a gradual diminution in the rate of increase of resistance was observed, the resistance was

Palladium Wire, diameter 0.0805 cm.

 $T=100^{\circ}$ $T=75^{\circ}$

Increasing pressure		Decreasing pressure		Increasing pressure		Decreasing pressure	
p	R/R_0	p	R/R_0	p	R/R_0	p	R/R_0
5.4	1.040	31.1	1.545	1.75	1.020	63.8	1.580
6.8	1.046	21.7	1.560	3.6	1.030	42.0	1.570
11.7	1.060	20.7	1.563	8.0	1.060	21.6	1.570
16.1	1.077	19.5	1.570	12.8	1.090	11.5	1.580
21.8	1.092	18.5	1.570	17.1	*1.460	5.5	1.593
24.2	1.107	17.5	1.570	22.0	*1.550	2.7	1.033
26.8	1.116	16.6	*1.210	27.8	1.570	1.3	1.023
30.7	1.127	15.7	*1.185	38.5	1.570	0.0	1.000
33.8	*1.342	13.8	*1.122	55.4	1.575		
36.5	*1.415	11.2	*1.070	73.0	1.580	11.6	1.083
40.0	*1.480	8.3	1.047			12.7	1.110
44.9	*1.513	4.2	1.030				
55.4	1.530	1.8	1.020				
72.5	1.530	0.0	1.000				
		7.2	1.042				
		17.7	1.082				

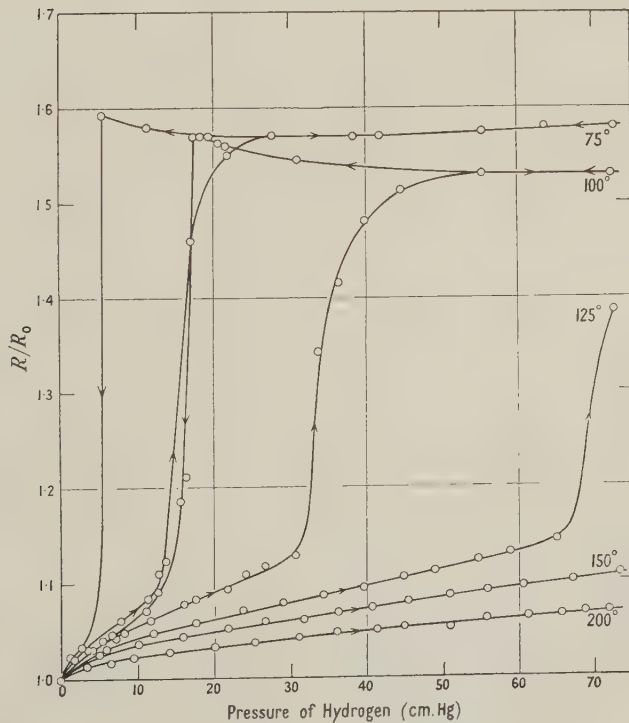
 R/R_0 =ratio of resistance of Pd-H to that of pure Pd, at T° C. p =pressure of hydrogen in cm. of mercury.* Resistance changing $\sim 0.1\%$ per day.

Figure 2. Resistance-pressure isotherms for the palladium-hydrogen system.

still increasing at the end of the month. The constant-pressure sections of the curve *a* in Figure 3 terminate at the stage when the resistance is increasing at a rate of less than 0.1% per day.

The third part of the isotherm, ascending pressures 55 to 73 cm. Hg and descending pressures 73 to 17 cm. Hg, is reversible, the maximum resistance values being attained in less than 2 hours after altering the pressure. The fourth part, descending pressures 17 to about 8 cm. Hg, is irreversible. Here the experimental procedure corresponded to that adopted in obtaining the second part of the isotherm, except that the pressure changes were smaller. The resistance-time curve, *c*, is shown in Figure 3, each section being plotted to the stage when the rate of decrease is less than 0.1% per day. The fourth part of the 100° C. isotherm re-joins the first part at about 8 cm. Hg pressure, follows it to zero pressure, and (without annealing *in vacuo*) re-traverses it with

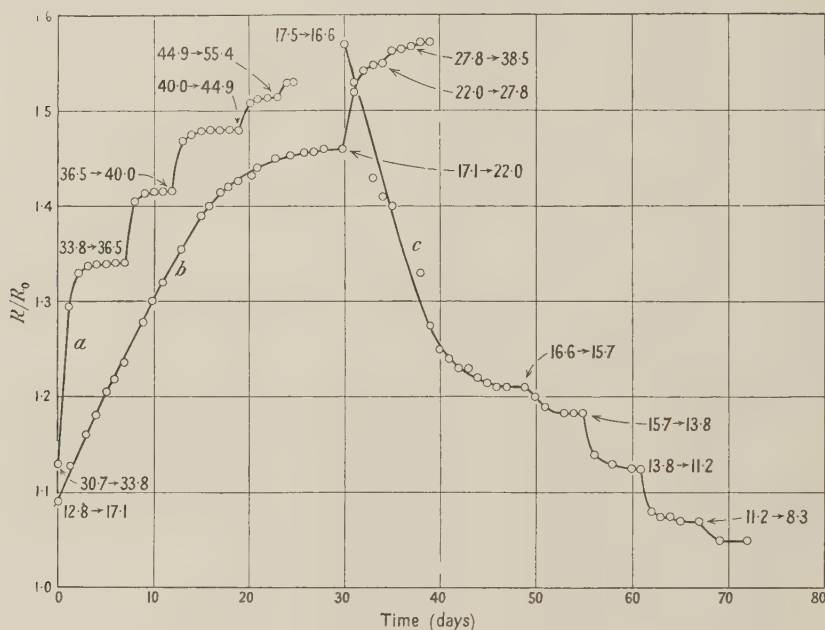


Figure 3. Curves showing change of resistance with time. Initial pressure changes (in cm. Hg) are indicated.

a. ($\alpha + \beta$) to β , 100° C. *b.* ($\alpha + \beta$) to β , 75° C. *c.* ($\alpha + \beta$) to α , 100° C.

ascending pressures. The resistance-pressure isotherm at 75° C. exhibits the same general characteristics as that at 100° C. In all parts of the cycle, however, the system was slower in attaining maxima (or minima) of resistance following a pressure change. At 125°, 150° and 200° C., the maxima were reached more rapidly than at 100° C.

The resistance-time curves at 100° C. shown in Figure 4 were obtained in traversing the hysteresis loop by making four pressure changes, each of which was just sufficient to carry the palladium-hydrogen system through one of the four well-defined stages previously considered. In the reversible ranges of pressure, curves showing growth and decay of resistance are given. The curves covering the irreversible pressure ranges were determined at pressures necessary

to take the system to the next reversible part of the isotherm, hence in each case the resistance acquires a constant final value. It will be seen that the irreversible parts of the isotherm are thus crossed in a few hours, a longer time being taken on the descending part than on the ascending part.

The $(R/R_0, p)$ isotherms at 75° and 100°C. are the same in general form as those determined at 180°C. and higher temperatures by Brüning and Sieverts. The lowest temperature isotherm, that at 160°C. , determined by these investigators, rises less steeply on the first irreversible part. From the experiments described above, it is now clear that the slope of this part of the isotherm is appreciably affected by the time of exposure to hydrogen. In all of these experiments, the same palladium specimen, a wire 0.0805 cm. in diameter, was used. A brief resumé will now be given of some additional results obtained

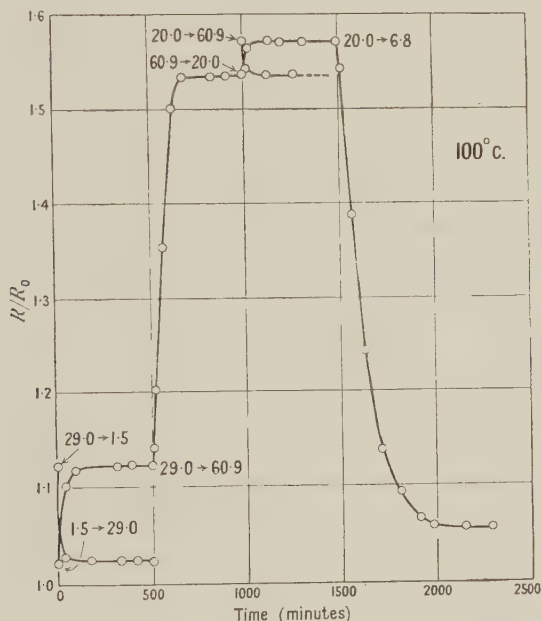


Figure 4. Curves showing change of resistance with time, at 100°C. Initial pressure changes (in cm. Hg) are indicated.

$$1.5 \rightleftharpoons 29.0, \alpha \rightleftharpoons (\alpha + \beta); \quad 29.0 \rightarrow 60.9, (\alpha + \beta) \rightarrow \beta; \\ 60.9 \rightleftharpoons 20.0, \beta \rightleftharpoons (\alpha + \beta); \quad 20.0 \rightarrow 6.8, (\alpha + \beta) \rightarrow \alpha.$$

by using a thin palladium rod, 0.210 cm. in diameter and 15 cm. long. From a knowledge of volumes of apparatus and palladium, and observation of pressures, a rough determination of the concentration-pressure isotherm at 100°C. was first made. The values of r were found to be higher than those obtained by Sieverts and Danz (1937) who used palladium black. The high values were probably due to absorption of hydrogen by various materials other than palladium inside the apparatus. In other respects the two isotherms were very similar, and are in agreement as to the pressure limits of the hysteresis loop. A careful re-determination of the resistance-pressure isotherm at 100°C. , using the palladium rod, was next carried out. This isotherm was found to be identical with that obtained with the wire, though a decidedly longer period of time was required to obtain the readings in the case of the rod. Comparing the (r, p)

and $(R/R_0, p)$ isotherms at 100°C. , it is found that the pressure limits of the hysteresis are the same for concentration and resistance, in agreement with the observations of Brüning and Sieverts at higher temperatures. Both the concentration and the resistance measurements just considered indicate that the pressure limits of the hysteresis are definite and independent of both the form and the bulk of the palladium.

No detailed analysis of the form of the resistance-time curves in Figures 3 and 4 has yet been made. Over the reversible stages of the cycle at least, these curves are of an exponential character. Some accurate observations at 100°C. with the palladium rod were made at constant hydrogen pressures of 8.7 and 23.3 cm. Hg, the initial pressure changes being, respectively, 23.3 to 8.7 cm. Hg and 8.7 to 23.3 cm. Hg. If δR_0 is the difference between equilibrium values of resistance of palladium-hydrogen at the two pressures, and δR the change of resistance in t minutes after making the initial alteration of pressure, it is found that $\delta R = \delta R_0(1 - e^{-\alpha t})$, approximately, where $\alpha = 0.004$ for decreasing resistance, and 0.006 for increasing resistance. Using Sievert's values for the concentration of hydrogen in palladium at 100°C. , we find in the single-phase region under consideration, the relation $(R/R_0 - 1) = ar$, which expresses a proportionality between increase of resistance and concentration in the α phase also observed previously by Brüning and Sieverts at higher temperatures. We may, therefore, re-write the resistance-time equation as

$$\ln q = A - Bt$$

where q now represents rate of change of either concentration or resistance, and A and B are constants. For a gas initially uniformly distributed in a homogeneous wire of circular section, a similar expression has been deduced, from Fick's linear diffusion law, for the rate of desorption (Smithells 1937).

§ 3. DISCUSSION OF RESULTS

(i) *Hysteresis Phenomena*

The experimental values for the pressure limits of the hysteresis at 100°C. are about 20 and 35 cm. Hg according to Sieverts and Danz, as compared with about 17 and 33 cm. Hg indicated by the present measurements of the electrical resistance of the system. Both sets of pressure values are read from the most steeply rising and falling parts of the isotherms. It is evident from preceding changes of curvature, however, that the new phase is in the process of formation before the pressure limits are reached. This is borne out by x-ray analysis (Owen and Williams 1944), which reveals co-existing α and β phases in the range of ascending pressures 27 to 41 cm. Hg, and in the range of descending pressures 19 to 13 cm. Hg. We must now form a picture of the hysteresis cycle which is consistent with all the experimental data. As the pressure is increased from zero, the α phase at first exists alone. The β phase begins to form probably before a pressure of 27 cm. is reached, and up to about 31 cm. Hg it disappears again if the pressure is reduced (the system is reversible in the range 0–31 cm. Hg). If the pressure is increased beyond 31 cm. Hg, the system transforms irreversibly into the β phase, and the rate of transformation increases very rapidly with the pressure. Analogously, with pressures descending from atmospheric, the β phase at first exists alone, and the α phase appears before the pressure falls to

19 cm. Hg. The system is reversible between atmospheric and about 17 cm. Hg, and if the pressure falls below 17 cm. Hg the α phase is established irreversibly. Assuming that nuclei of a new phase are formed dispersed throughout the old phase, it is possible, as Lacher has shown, to explain the hysteresis by considering the contribution to the free energy of the system made by the surface separating the two phases. The vapour pressure of the dispersed β -phase particles would be greater than the pressure they would exert in bulk, hence they could not form without some degree of supersaturation in the α phase. Similarly, during evolution of hydrogen, an undersaturated β phase would be necessary for the formation of α -phase nuclei. Over a certain range of pressure up to the point where the isotherms rise (or fall) sharply, it must be assumed that the two phases co-exist in a state of metastable equilibrium. Beyond this stage, the degree of supersaturation in the α phase (or undersaturation in the β phase) is such that the system becomes unstable and the new phase is rapidly formed in fairly large blocks out of the finely dispersed particles. This version of the behaviour of the Pd-H system is supported by the x-ray evidence and appears to be not inconsistent with the results of solubility measurements. We shall, therefore, proceed to use it as a working hypothesis in an attempt to account for certain characteristics of the resistance isotherms.

(ii) *Origin of Resistance Changes*

When hydrogen is alloyed with palladium by the process involved in determining the resistance-pressure isotherms, the palladium lattice retains its face-centred cubic structure throughout. In transforming from the α phase to the hydrogen-rich or β phase, and again during the transformation back from β phase to α phase, the new phase appears as a conglomeration of small crystals. Crystal size is not, however, an important factor as regards the electrical resistance since the present results (II, §2) show that the resistance-pressure isotherms can be repeated without any initial annealing of the palladium. Hydrogen in solid solution may influence the resistance of palladium by disturbing the periodicity of the lattice or by contributing electrons to fill the incomplete d band of palladium. From the close correspondence between concentration and resistance isotherms we may deduce that the scattering centres provided by the hydrogen atoms are mainly responsible for increasing the resistance. The observed increase of resistance brought about by extensive cold-working of pure metals is small compared with the effect of alloying, hence we should expect lattice distortion at phase boundaries to be a relatively unimportant factor. The increase in resistivity introduced by it during the formation of a new phase is likely to be a maximum when the particles are very small, since the scattering should be a maximum when the wavelength of the conduction electrons is comparable with the dimensions of the particles (Mott 1940). The high resistance of the transition metals is attributed to scattering processes in which the electrons make transitions into vacant states in the d band. The transition probability is high because of the high density of states in the partially filled d band of the transition metals. It has, in fact, been verified experimentally that the electrical resistance decreases when, as a result of alloying, the incomplete d shells are filled. Thus, Rosenhall (1935) has shown that the addition of hydrogen to palladium-silver alloys reduces the total resistance. Since the density of states in the d band is proportional to the cube root of the number of positive

holes, we should expect the reduction in resistance due to alloying with hydrogen to be apparent in the β phase of palladium-hydrogen when the hydrogen concentration r approaches the value 0.6.

Consider the resistance-pressure isotherm at 100°C. As the gas pressure increases from zero, the α phase at first exists alone and the total resistance, which is here proportional to r , consists principally of the scattering resistance due to hydrogen atoms. When the pressure approaches 27 cm. Hg, the β phase begins to form and the total resistance is slightly augmented as a result of strains at the phase boundaries. The magnitude of this contribution depends upon the number and size of the β -phase nuclei and would probably increase with pressure up to 31 cm. Hg. At about 31 cm. Hg the system becomes unstable and transforms completely into the β phase, the rate of evolution increasing rapidly with the pressure. As mentioned previously, the slope of the isotherm between 31 and about 55 cm. Hg depends upon the time of exposure of the palladium to hydrogen. If sufficient time were allowed, this part of the isotherm would be parallel to the resistance axis and would join the evolution curve at a pressure just exceeding 31 cm. Hg. A comparison of solubility and resistance isotherms in the pressure range between atmospheric and about 17 cm. Hg, reveals that a marked increase in resistance occurs as the hydrogen concentration diminishes. With descending pressures, the β phase does not form until the pressure approaches 19 cm. Hg, hence the increased resistance cannot be due to strains but must be attributed to the increase in the number of positive holes in the d band of palladium. If the isotherm is re-traversed with pressures ascending from 19 cm. Hg, to atmospheric, r increases from about 0.53 to 0.60, and R/R_0 diminishes from 1.57 to 1.53 as the positive holes in the d band become filled. If this explanation is correct, since the concentration of hydrogen in the β phase is less at higher temperatures, we should expect the effect to diminish with rise of temperature. The isotherms of Brüning and Sieverts show that the expected diminution does actually take place. Solubility data at 75°C. are not available; at 80°C. the saturation value r is greater than 0.6. The still greater value of r at 75°C. may account for the fact that the resistance isotherm at 75°C. shows a slight rise as the concentration in the β phase approaches its maximum value.

The upward trend of the resistance isotherm at 100°C. terminates abruptly as the pressure descends to about 17 cm. Hg. Here the system becomes unstable and transforms completely into the α phase. With the evolution of hydrogen, the total resistance drops when the rise due to removal of electrons from the d band is outweighed by the fall due to reduced hydrogen scattering. The experimental points on the descending curve between 17 cm. and 6 cm. Hg do not represent constant values of the resistance. As in the case of the transformation from α to β phase, the change should be represented by a line parallel to the resistance axis.

At the temperatures considered, we conclude that the general characteristics of the resistance isotherms in the system Pd-H can be satisfactorily explained on the basis of Lacher's suggestions, and by assuming that the occluded hydrogen is held entirely in solid solution. The incomplete d shells of the Pd atoms become filled when the ratio, r , of H to Pd atoms in solid solution is approximately 0.6. Thus, the form of the isotherms in the β phase may be accepted as evidence in support of the theory that the high resistance of a transition metal is due to its partly filled d band.

ACKNOWLEDGMENT

The author has pleasure in expressing his sincere thanks to Professor E. A. Owen for his continued interest and encouragement.

REFERENCES

- BRÜNING, H., and SIEVERTS, A., 1933, *Z. phys. Chem. A*, **163**, 409.
 GILLESPIE, L. J., and GALSTOUN, L. S., 1936, *J. Amer. Chem. Soc.*, **58**, 2565.
 GILLESPIE, L. J., and HALL, F. P., 1926, *J. Amer. Chem. Soc.*, **48**, 1207.
 LACHER, J. R., 1937, *Proc. Roy. Soc. A*, **161**, 525.
 MCKEEHAN, L. W., 1923, *Phys. Rev.*, **21**, 334.
 MOORE, G. A., 1935, *Trans. Electrochem. Soc.*, **75**, 237.
 MOTT, N. F., 1940, *Proc. Phys. Soc.*, **52**, 86.
 OWEN, E. A., 1944, *Phil. Mag.*, **35**, 50.
 OWEN, E. A., and JONES, J. I., 1937, *Proc. Phys. Soc.*, **49**, 587, 603.
 OWEN, E. A., and WILLIAMS, E. ST. J., 1944, *Proc. Phys. Soc.*, **56**, 52.
 ROSENHALL, G., 1935, *Ann. Phys., Lpz.*, **24**, 297.
 SIEVERTS, A., and DANZ, W., 1937, *Z. phys. Chem. A*, **38**, 46, 61.
 SIEVERTS, A., and ZAPF, G., 1935, *Z. phys. Chem. A*, **174**, 359.
 SIEVERTS, A., ZAPF, G., and MORITZ, H., 1938, *Z. phys. Chem. A*, **1**, 19.
 SMITH, D. P., 1948, *Phil. Mag.*, **39**, 477.
 SMITHELLS, C. J., 1937, *Gases and Metals* (London: Chapman and Hall).
 UBBELOHDE, A. R., 1932, *Trans. Faraday Soc.*, **28**, 275, 284; 1937, *Proc. Roy. Soc. A*, **159**, 295.
 WAGNER, C., 1944, *Z. phys. Chem. A*, **193**, 386.
 WRIGHT, P., 1947, *J. Sci. Instrum.*, **24**, 258.

The Barkhausen Effect

BY R. S. TEBBLE, I. C. SKIDMORE, AND W. D. CORNER

Physics Department, University of Leeds

Communicated by R. Whiddington; MS. received 24th October 1949 and in amended form 19th December 1949

ABSTRACT. An account is given of further experiments on the Barkhausen effect in cylindrical ferromagnetic specimens. The form of the decay of induction following a Barkhausen discontinuity has been investigated and there is reasonable agreement between the theory given and the experimental results. As a result of this investigation it has been possible to satisfy the different conditions which are necessary for the detection of the discontinuities so as to obtain (a) accurate reproduction of the form of the discontinuities and (b) maximum sensitivity in the counting experiments. The number and size of the discontinuities are measured, and an estimate is made of the contribution of the discontinuous processes to the total change in magnetization over the relevant part of the hysteresis curve. Discontinuous changes in magnetic moment greater than 0.3×10^{-6} E.M.U. (corresponding to a minimum volume of 0.9×10^{-10} cm³ for iron) account for from 47% to 86% of the total change in magnetization. This is considered in relation to associated work on reversible changes, and the nature of a Barkhausen discontinuity is briefly discussed with reference to other investigations on domain structure.

§ 1. INTRODUCTION

IN a paper by Bush and Tebble (1948) (which will be referred to as I), an account is given of measurements on the contribution of the discontinuous processes, known as the Barkhausen effect, to the total change in magnetization as a ferromagnetic is taken through a hysteresis cycle. It was possible to detect discontinuities corresponding to reversals of magnetization in volumes of the

order of 10^{-9} cm^3 and it was found that over the region of the magnetization curve considered, 10 to 30% of the total change in magnetization could be accounted for by the Barkhausen discontinuities detected. Since reversible changes, not detected by the apparatus, contribute only 10 to 15% of the change in magnetization, there was a considerable discrepancy. This could have arisen from the presence of discontinuous changes too small to be detected, and an improvement in sensitivity was, therefore, considered desirable.

The method used, both in the work described here and in the previous paper, is as follows. The magnetic field, applied in a direction parallel to the axis of a cylindrical specimen, is slowly changed and the resulting discontinuous changes in magnetization are detected as voltage pulses, induced in a search coil wound round the specimen. These voltage pulses are amplified and can be displayed on an oscilloscope or passed to a suitable recording device as indicated in Figure 1. From the amplitude and shape of a pulse, an estimate can be made of the corresponding change in magnetization in the ferromagnetic material. By means of an amplitude discriminator and counting unit connected to the output of the amplifier, the number and size of these discontinuities can be measured as the specimen is taken through part of a hysteresis loop. Hence an estimate can be made of the contribution of the Barkhausen effect to the total change in magnetization over that part of the hysteresis curve examined.

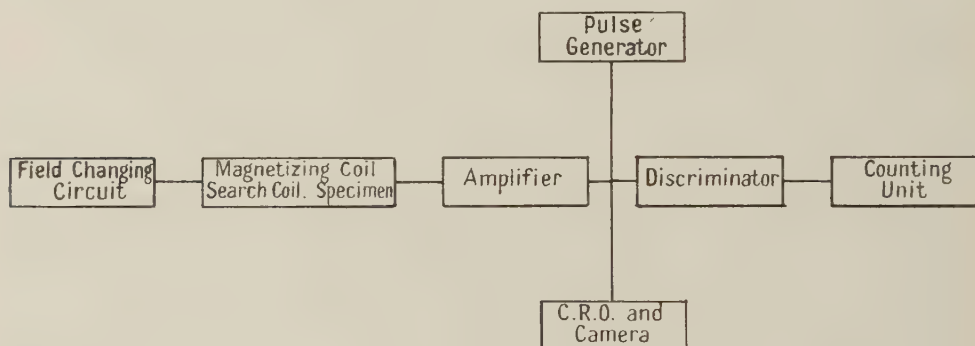


Figure 1. Block diagram of the apparatus.

The main problem in this method of approach is that the amplitude of the induced voltage pulses is small, of the order of a few microvolts. It is thus essential, if the smaller discontinuities are to be detected, that the search coil and amplifier should be designed to give the maximum possible signal-to-noise ratio; and it has been found necessary, in view of the lack of information on the subject, to carry out a thorough examination of the factors affecting the relation between the primary changes and the measured effects (§ 2). This involves a theoretical investigation into the rate of decay of induction in cylindrical specimens following a discontinuous change in magnetization (§ 2(ii)), and into the effect of the search coil on the form of the induced voltage pulse (§ 2(iii)). The effect of thermal agitation noise and stray capacities on the sensitivity of the apparatus is also considered (§§ 2(iv) and 2(v)). The conclusions which can be drawn from this examination have been applied to the problems arising in two distinct sets of experimental investigations. In the first (§ 3), which is subsidiary to the main purpose of this work, measurements have been made on the time constant of the discontinuities and the results are compared with those given by the

treatment in § 2. The improved apparatus has been used to carry out further experiments on the contribution of the Barkhausen discontinuities to the total change in magnetization, and the results are discussed with reference to present ideas on domain structure (§ 4). Although the contents of §§ 2 and 3 are necessary to justify the methods used, a detailed study of these sections is not necessary to an understanding of § 4, in which the main investigation is described.

§ 2. THEORY

§ 2 (i). *Introductory*

It is convenient to consider briefly the possible mechanism by which a Barkhausen discontinuity is produced. In a ferromagnetic in low fields the primary effect of any increase in the applied field is to cause a movement of the boundaries of the domains, such that those magnetized with components parallel to the field expand, absorbing those less favourably magnetized. As the field is changed a given boundary is displaced, at first reversibly, until at a critical field it moves spontaneously (i.e. without further increase of field) over a considerable fraction, or even the whole of the length, of a neighbouring domain.

It was for some time thought that such an irreversible boundary movement, from one energy minimum to another, corresponded to a Barkhausen discontinuity. The extent of these boundary movements must be limited to some degree by the presence of the usual irregularities in the structure of the material; the results of the work of Williams and Shockley (1949) on powder patterns on single crystals suggest that the Barkhausen effect may be related, at least in part, to the secondary domain structure round these imperfections. However, in polycrystalline specimens, particularly if the grain size is small, the distinction between primary and secondary domains may be less sharp, and the Barkhausen effect in such specimens might be a guide to the structure of the material.

The case will now be considered of a cylindrical ferromagnetic specimen in a field applied in a direction parallel to the cylinder axis. A Barkhausen discontinuity in such a specimen, resulting from a small change in the applied field, can be considered as a change in magnetic moment ΔM , resolved in a direction parallel to the applied field, over a small volume v . This results in a change in the flux of induction over the cross section of the specimen given by

$$\phi_0 = \frac{4\pi\Delta M}{d}, \quad \dots\dots(1 a)$$

where d is the length of the region of the discontinuity.

The volume v is given by

$$v = \frac{\Delta M}{2I_s \cos \theta}, \quad \dots\dots(1 b)$$

where I_s is the saturation intensity of magnetization, θ is the angle between the direction of I_s and the applied field, and the volume is a minimum, v_m , when $\cos \theta = 1$.

The total flux through the search coil, and the time-varying voltage $E(t)$ induced in the coil, are related by

$$\phi_c = \int E(t) dt, \quad \dots\dots(2)$$

with appropriate limits of integration. The amplitude and form of the voltage pulse will, therefore, depend, *inter alia*, on the rate of change of induction in the specimen. This, together with the original boundary movement, is controlled by the eddy currents set up in the specimen, and it is necessary, therefore, to consider first the factors controlling the decay of induction in a cylinder.

§ 2 (ii). *Decay of Induction accompanying a Barkhausen Discontinuity in a Cylindrical Specimen*

Bozorth and Dillinger (1930), in their work on the Barkhausen effect, assumed for the change in flux of induction over the cross section of the specimen an expression given by Wwedensky

$$\phi = 4\phi_0 \sum \frac{\exp(-\lambda_n^2 \xi)}{\lambda_n^2}, \quad \dots\dots(3)$$

where λ_n is the n th root of $J_n(\lambda) = 0$, and $\xi = t/4\pi\mu a^2\sigma$, σ being the conductivity of the specimen, μ the reversible permeability, and a the radius of the specimen. This gives a 'time-constant', τ_w , in which the flux falls to $1/e$ of its total change at $\xi = 0.103$, i.e. when

$$t = \tau_w = 0.43\pi\mu a^2\sigma. \quad \dots\dots(4)$$

For a specimen of radius 0.2 mm., $\mu = 100$, resistivity $1/\sigma = 10^{-5}$ ohm cm., this gives $\tau_w = 5.4$ microseconds.

This expression, however, was originally derived by Wwedensky (1921) for the decay of induction following a sudden change in applied field, i.e. the initial change in induction takes place over the whole cross section of the specimen. This is not quite the same problem as in the Barkhausen effect, where there is an initial localized discontinuity that can take place at any position in the specimen.

In the treatment given below, the following assumptions are made:

(a) The area of cross section over which the initial boundary movement takes place is small compared with that of the specimen. This holds, in the conditions of the present experiments whatever the precise process involved.

(b) The movement of the boundary takes place in a time which is short compared with the time taken for the decay of the resulting change in induction throughout the specimen. This is justified later.

(c) The permeability is constant. (Since a single isolated boundary movement is being considered, the resulting changes in induction in the specimen are reversible i.e. it is reversible permeability which is involved. If this were not so, it would imply the occurrence of further discontinuities during the incident under consideration. This reversible permeability is taken as constant during the whole process associated with a given single discontinuity, but it will, of course, depend on the magnetic state of the specimen, i.e. on its position on the magnetization curve.)

(d) The applied field is changing so slowly that it remains sensibly constant during what may be called the single discontinuity process.

Consider a discontinuous change in magnetic moment taking place over a small area ΔS about the point P, ($r = b$, $\theta = 0$, $z = z_0$), see Figure 2, in the cross section of the specimen $z = z_0$. This corresponds to a discontinuous change in induction ΔB_0 over an area ΔS , and the change in flux over the whole of the specimen is given by

$$\phi_0 = \Delta B_0 \Delta S \quad \dots\dots(5)$$

which will be retarded by the eddy currents set up about P.

The equation for the propagation of this change in induction B is in cylindrical coordinates,

$$\frac{\partial^2 B}{\partial r^2} + \frac{1}{r} \frac{\partial B}{\partial r} + \frac{1}{r^2} \frac{\partial^2 B}{\partial \theta^2} = \gamma \frac{\partial B}{\partial t}, \quad \dots\dots(6)$$

where $\gamma = 4\pi\mu\sigma$, μ and σ are as defined above, and μ is assumed constant.

The solution of this equation is

$$B = \sum_k \sum_{m=0}^{m=\infty} A_{km} J_m(kr) \cos m\theta \cdot \exp \{-(k^2/\gamma)t\}, \quad \dots\dots(7)$$

where k , A_{km} are constants and $m=0, 1, 2, 3 \dots$

The boundary conditions are: (i) for all values of θ and for $t>0$, $B=0$ for $r=a$; (ii) at $t=0$, $B=0$ except over ΔS at $(b, 0)$ where $B=\Delta B_0$. With these conditions, the solution (7) takes the form

$$B = \frac{2\phi_0}{\pi a^2} \sum_{n=1}^{\infty} \sum_{m=0}^{\infty} \frac{J_m(\lambda_n b/a)}{\delta J_{m+1}^2(\lambda_n)} J_m(\lambda_n r/a) \cos m\theta \cdot \exp(-\lambda_n^2 \xi), \quad \dots\dots(8)$$

where $\xi = t/4\pi\mu a^2\sigma$ and $\delta=1$ for $m>0$, $\delta=2$ for $m=0$.

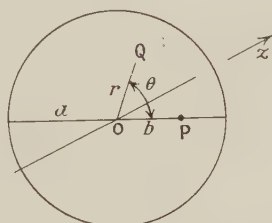


Figure 2.

The flux of induction over the cross section of the cylinder is

$$\phi = \int_0^{2\pi} \int_0^a B r dr d\theta = 2\phi_0 \sum_1^{\infty} \frac{J_0(\lambda_n b/a) \exp(-\lambda_n^2 \xi)}{\lambda_n J_1(\lambda_n)}. \quad \dots\dots(9)$$

Thus the flux changes in a manner dependent on the distance of the initial discontinuity from the axis of the cylinder b . This is shown in Figure 3, where ϕ/ϕ_0 is plotted against ξ for different values of b/a , together with the curve obtained from Wwedensky's equation (3). In the case of a discontinuity on the cylinder axis, ϕ falls to ϕ_0/e when $\xi=0.253$, i.e. the 'time constant' is

$$\tau_0 = 1.01\pi\mu a^2\sigma, \quad \dots\dots(10)$$

giving, for the specimen quoted above, $\tau_0=12.7$ microseconds. The time constant, τ_1 , decreases from τ_0 to 0 as b/a increases from 0 to 1; τ_0 , given by equation (10), will be referred to as the 'time constant' of the discontinuity.

The rate of change of flux is given by

$$e = -\frac{d\phi}{dt} = \frac{\phi_0}{2\pi\mu\sigma a^2} \sum_{n=1}^{n=\infty} \frac{\lambda_n J_0(\lambda_n b/a)}{J_0(\lambda_n)} \exp(-\lambda_n^2 \xi); \quad \dots\dots(11)$$

$$\text{with } b/a=0, \quad e_{\max} = \phi_0/\tau \quad \dots\dots(11a)$$

where $\tau=1.04\pi\mu a^2\sigma$. (This can be compared with an exponential decay curve which would give $\tau=\tau_0$.)

The form of equation (11) is shown in Figure 4 for different values of b/a , with $E = 2\pi\mu a^2\sigma e/\phi_0$. The curve of $d\phi/dt$, obtained from Wwedensky's expression is also shown. These curves give the shape of the voltage pulses that would be induced in a search coil, wound closely round the specimen and introducing no distortion itself. It can be seen that the shape and amplitude of the pulse

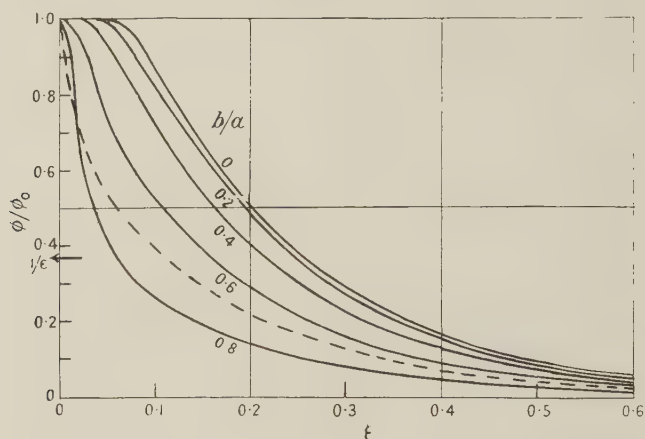


Figure 3. Decay of induction following a discontinuity.

Full line : equation (9) for various values of b/a .

Broken line : equation (3) (Wwedensky).

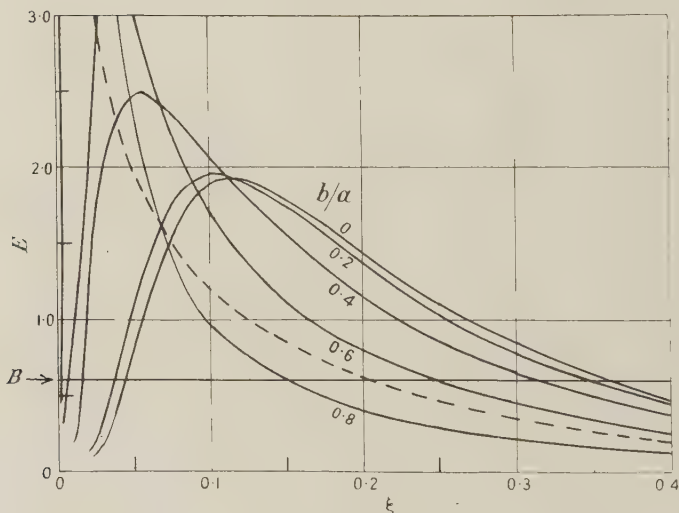


Figure 4. E - ξ curves.

Full line : equation (11) for various values of b/a .

Broken line : equation (3) (Wwedensky).

varies considerably with b/a , i.e. with the distance of the discontinuity from the axis of the specimen. Since μ varies with the magnetic state of the material, the form of the voltage pulse will also change as a specimen is taken round a hysteresis cycle.

The assumption (a) of §2(ii) concerning the rapidity of the original boundary movement can now be justified. Becker (1938) shows that for a small cubical

domain, at the centre of a specimen, the discontinuous boundary movement takes place in a time which can be written

$$\tau_B = \frac{0.3\pi I_s h^2 \sigma}{H}, \quad \dots\dots (12)$$

where h is the length of the cube edge, and I_s is the saturation intensity of magnetization.

In the case under consideration, the 'domain' is the region of the local discontinuous boundary movement. Comparing the above expression with equation (10), it can be seen that with $I_s \simeq 100 \mu$, provided $h < a/10$, the condition (b) will be satisfied. Although equation (12) does not hold for boundary movements taking place at a distance from the axis of the specimen, τ_B would then be reduced in a somewhat similar manner to τ_1 , and the condition $\tau_1 \gg \tau_B$ would still hold.

§ 2 (iii). Form of the Voltage Pulses induced in a Search Coil

The change in flux through a search coil following a change in magnetic moment at the centre of the coil is given by

$$\phi_c = \int E(t) dt = \frac{2\pi \Delta M N_2}{(r^2 + l_2^2)^{1/2}}, \quad \dots\dots (13)$$

where ΔM is the change in magnetic moment resolved in a direction parallel to the axis of the coil, N_2 is the total number of turns in the coil, r is the radius of the coil, and $2l_2$ the length of the coil.

If this is compared with equation (1) it can be seen that since the induced voltage is a function of ϕ_c , the sensitivity of the system is determined in the first place by the dimensions of the search coil, which are controlled by the experimental requirements. Ideally the shape and amplitude of the pulses would be given by equation (11), but in practice modifications are introduced by the search coil circuit, and it is necessary to consider this effect in some detail.

In examining the effect of the search coil circuit on the form of the voltage pulses, it is convenient to consider the decay of the flux through the specimen as exponential, with a time constant given by equation (10) with the numerical factor appropriate to the position of the discontinuity in the specimen. The specimen can then be replaced by a single-turn coil of similar dimensions, inductance L_1 , cross section area A_1 , and circuit resistance R_1 , giving $\tau_1 = L_1/R_1$. A change in current i_0 through the coil is equivalent to a change in magnetic moment given by

$$\Delta M = i_0 A_1, \quad \dots\dots (14)$$

The specimen and search coil can now be replaced by two coupled circuits of mutual inductance M , with the 'equivalent coil' as the primary and the search coil circuit as the secondary ($\tau_2 = L_2/R_2$). From the theory of coupled circuits (Jeans 1946), the current induced in the secondary circuit by a change in current i_0 in the primary is

$$i_2 = \frac{M i_0 (\alpha^2 - \beta^2)}{R_2} e^{-\alpha t} [e^{+\beta t} - e^{-\beta t}], \quad \dots\dots (15)$$

where
$$\alpha = \frac{\tau_1 + \tau_2}{2\tau_1\tau_2(1 - k^2)}, \quad \beta = \frac{\{(\tau_1 - \tau_2)^2 + 4k^2\tau_1\tau_2\}^{1/2}}{2\tau_1\tau_2(1 - k^2)},$$

and $k = M/\sqrt{(L_1 L_2)}$, is the coefficient of coupling.

It is sufficient to examine the form of the induced voltage pulse for two special cases which are of practical significance:

(a) When the time constant of the search coil circuit is much smaller than that of the discontinuity, i.e. $\tau_1 \gg \tau_2$, the solution becomes

$$i_2 = \frac{Mi_0}{R_2} \cdot \frac{1}{\tau_2} \{ \exp(-t/\tau_1) - \exp(-t/\tau_2') \}, \quad \dots\dots(16)$$

where $\tau_2' = \tau_2(1 - k^2)$.

The effect of the search coil circuit on the shape of the pulse is then confined to the leading edge as indicated in Figure 5. With $k=1$, i.e. the coefficient of coupling a maximum, $\tau_2' = 0$ and the search coil has no effect on the shape of the pulse, provided $\tau_1 \gg \tau_2$.

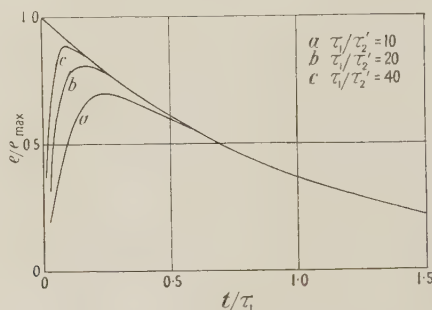


Figure 5. Effect of search coil circuit on form of induced voltage pulse. The numbers on the curves give the values of τ_1/τ_2' , where τ_1 is the time constant of the discontinuity, and τ_2' the modified time constant of the search coil circuit (see equation (16)).

If the search coil is solenoidal, then the amplitude of the pulse is

$$e_{\max} = i_{2, \max} R_2 = \frac{Mi_0}{\tau_1} = \frac{4\pi N_2 A_1}{\tau_1 (2l_2)} \cdot \frac{\Delta M}{A_1} = \frac{2\pi N_2 \Delta M}{\tau_1 l_2}, \quad \dots\dots(17)$$

which can be compared with equation (13) with $r=0$. Obviously if the coil is not solenoidal equation (17) becomes

$$e_{\max} = \frac{2\pi N_2 \Delta M}{\tau_1 (l_2^2 + r^2)^{1/2}}. \quad \dots\dots(17a)$$

(b) When the time constant of the search coil circuit is much longer than that of the discontinuity, i.e. $\tau_1 \ll \tau_2$, the shape of the pulse is largely determined by the constants of the search coil circuit, and is practically independent of the rate of decay of the induction in the specimen. The case of practical interest is that for a solenoidal coil when (cf. equation (17))

$$e_{\max} = \frac{2\pi N_2 \Delta M}{\tau_2 l_2}, \quad \dots\dots(18)$$

and for a non-solenoidal coil

$$e_{\max} = \frac{2\pi N_2 \Delta M}{\tau_2 (l_2^2 + r^2)^{1/2}}. \quad \dots\dots(18a)$$

When $k=1$ the specimen has no effect on the shape of the pulse.

The above two cases are of particular interest in experimental work. The first, (a), gives the condition which must be fulfilled if the voltage pulse induced

in the search coils is to be that given by equation (11). The shape of the pulse is then a guide to the manner in which the induction changes in the specimen take place. The second case, (b), is that in which the conversion factor from pulse amplitude e_{\max} to flux change in the specimen is independent of the magnetic state of the material and of the position of the discontinuity relative to the axis of the specimen. The fact that the decay of induction is not a simple exponential but is in the form of a sum of exponentials will obviously have little effect on the conclusions drawn, provided the conditions given are fulfilled (cf. equation (10) and (11 a)).

§ 2 (iv). Signal-to-Noise Ratio

The voltage generated in the search coil circuit by the thermal agitation of the electrons in the conductors sets a lower limit to the size of discontinuities which can be detected. If a valve amplifier is used in connection with the search coil, there is also the effect of shot noise in the first valve. If the impedance is mainly resistive the total noise voltage produced in the first stage can be written

$$e_n^2 = 4kT(R + R_v)\nu = 4kT(R + R_v)(\nu_1 - \nu_2), \quad \dots\dots(19)$$

where k is Boltzmann's constant, T is the absolute temperature, ν_1 and ν_2 the upper and lower frequency limits of the apparatus, R the effective resistance of the search coil circuit between grid and cathode, and R_v the 'equivalent noise resistance' of the valve. If the inductance is appreciable the effect is to increase the noise as the frequency increases. The term R_v , which may be written $R_v = 2.5/g_m$ for a triode, where g_m is the mutual conductance of the valve, allows for shot effect (Terman 1943). It is thus desirable that a valve with a high value of g_m should be used, at least in the first stage of amplification. The noise generated in the later stages can usually be neglected.

It is generally assumed that the lower the effective resistance of the conductors in a circuit, the lower the thermal noise, but it can be seen from the above that little useful purpose is served by reducing the resistance of the search coil circuit much below the 'shot resistance' of the first valve. A further important point is that if the impedance of the circuit is mainly resistive, and if, as is usually the case, $\nu_1 \gg \nu_2$, it is the upper frequency limit of the apparatus which is of importance in controlling the noise, which can then be written

$$e_n^2 = 4kT(R + R_v)\nu_1. \quad \dots\dots(19 a)$$

If a search coil of length $2l$, and inner radius r , is wound with wire, n turns per cm. (i.e. diameter $1/n$), to a winding depth of t , the total number of turns is $N = 2ltn^2$, and, if t is not too large, $R \propto ltn^4(2r + t)$. The signal-to-noise ratio is then, from equations (13) and (19 a), (for a given time constant and frequency range):

$$\frac{e_{\max}}{e_n} \propto \left[\frac{lt}{(2r + t)(\bar{r}^2 + l^2)} \right]^{1/2}, \quad \dots\dots(20)$$

where \bar{r} is a mean radius. It can be seen therefore that the thickness of the winding should be as great as possible up to the point where the effect of an increase in t is nullified by corresponding increases in radius and inductance. The dimensions of the coil, r and l , should be as small as possible.

§ 2 (v). *Effect of Distributed Capacity in the Search Coil Circuit*

In practice it is impossible to wind a search coil without introducing stray capacity into the circuit, represented by C_c in Figure 6. The input capacity of the following amplifier is represented by C_a . Because of the presence of these capacities, unless the resistance of the search coil R_c is sufficiently high, a voltage pulse induced in the coil, inductance L , will produce damped oscillations with a frequency

$$\nu = \left[\frac{1}{LC} - \frac{R^2}{4L^2} \right]^{1/2} / 2\pi, \quad \text{or, if } C \text{ is small, } \nu = \frac{1}{2\pi\sqrt{LC}},$$

where $C = C_c + C_a$. The condition for critical damping is

$$R_c^2 = \frac{4L}{C_c + C_a}. \quad \dots\dots (21)$$

If the capacities are small enough the frequency may lie outside the range of the apparatus and the effect may then be small. Should this not be so, and if

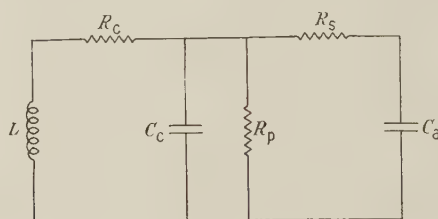


Figure 6. Search coil circuit.

R_c is not large enough, further damping must be provided. This can be done either by means of a resistance R_p in parallel with the stray capacities or by means of a series resistance such as R_s . The required values of R_p and R_s for a capacity C are

$$R_s \geq 2\sqrt{(L_2/C)}$$

$$R_p \leq \frac{L/C}{R_c + 2\sqrt{(L/C)}}, \quad \text{or, if } C \text{ is small, } R_p \leq \frac{1}{2}\sqrt{(L/C)}. \quad \dots\dots (22)$$

However since the search coil capacity C_c cannot be physically separated from the coil, only a parallel resistance can be used in that case. Whether a series or parallel resistance is used with C_a depends on its effect on the sensitivity of the system.

§ 3. MEASUREMENTS ON THE TIME CONSTANTS OF THE DISCONTINUITIES

§ 3 (i). *Introductory*

The investigation of the accuracy of equations (9)–(11) is based on an examination of the ‘width’ of the voltage pulses induced in a search coil by the discontinuities, which, if no distortion is produced by the apparatus, will be of the form shown in Figure 4. The ‘reduced width’ ξ_p can be measured on any convenient reference line and that shown as B (corresponding to $\phi \sim 0.2\phi_0$) in Figure 4 is suitable. The ‘wider’ voltage pulses are produced on the average by those discontinuities lying nearer the axis of the specimen. Now the number of

discontinuities, N , with a given mean cross-sectional area, lying within a cylinder radius b (the radius of the specimen being a), is given by

$$\frac{N}{N_0} = \frac{b^2}{a^2} \quad \dots\dots(23)$$

where N_0 is the total number of discontinuities in the specimen. These discontinuities, N , will produce voltage pulses whose reduced width ξ_p is greater than that given by the (E, ξ_p) curve, for the given value of b/a . In Figure 7, the variation of N/N_0 with the corresponding value of ξ_p is shown.

Unfortunately the detection and reproduction of the form of these voltage pulses results in practice in a low sensitivity (low signal-to-noise ratio) which severely limits the accuracy of the investigation. The low sensitivity is a result of the requirements (1) that the search coil time constant shall be short (see § 2 (iii), assumption (a), and (2) that the pass band of the amplifier shall be wide enough to permit the recording of pulses over a frequency range at least as wide

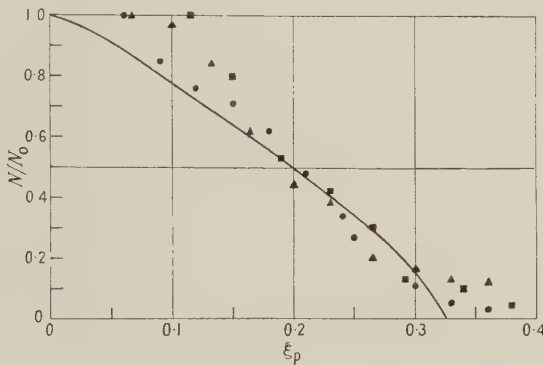


Figure 7. $(N/N_0, \xi_p)$ curve.

- 16 s.w.g. hard drawn iron $\times 2.6$.
- 16 s.w.g. annealed iron $\times 3.0$.
- ▲ 26 s.w.g. large grained iron $\times 3.3$.

as that indicated by Figure 7. Under such conditions the self capacity of the coil must be kept very small thus limiting the number of turns with which the coil can be wound. Since the self capacity of the coil cannot be estimated with any accuracy, the most satisfactory method is to examine the effects of various search coils on induced voltage pulses of known form; the required damping resistances and resultant resolving times can then be found by systematic trial, and the optimum number of turns estimated.

§ 3 (ii). Method

A block diagram of the apparatus is shown in Figure 1. The search coil, surrounding the wire specimen, was wound with 5,000 turns of 44 s.w.g. copper wire, and was 0.6 cm. mean diameter and 2 cm. long. The magnetic field was applied to the specimen by a magnetizing coil, surrounding both search coil and specimen, and could be slowly changed by means of a circuit which slowly altered the current through the coil. The circuit is an improved version of that referred to in I, p. 371.

The resistance-capacity coupled amplifier used in this and in the counting experiments, was constructed from a design of A.E.R.E. (Gillespie 1947). The main features are its high stability, low noise and wide frequency band. The first is obtained by the use of negative feedback in all three circuits, each of the three stages of which the amplifier is made up, and by the use of high stability components. The first valve is a miniature triode CV138 ($g_m = 8.5$ ma/v.) giving a low shot resistance (~ 300 ohms), and the remainder except for the output stage, are CV139 miniature pentodes ($g_m = 7.6$ ma/v.). The use of these valves gives a low input capacity at each stage of amplification and this, together with the careful choice of components has given a maximum frequency range of 1 kc/s. to 5 Mc/s. with a maximum gain of 200,000. In recording the voltage pulses the band width was set at 1 kc/s. to 1 Mc/s.

The output pulses were displayed on a cathode-ray oscilloscope, and records taken, with the time base switched off, on a Cossor continuous film camera, in which the motion of the film was at right angles to the direction of the voltage deflection. Film speeds of 800 cm/second were obtained with this camera. A timing trace was provided by the output of a square pulse generator.

The resolving time of the apparatus (6 microseconds) was found by producing regular rapid changes in flux in the search coil and examining the output pulses on the oscilloscope. The output of the square pulse generator passed through a suitable coil placed within the search coil was found to be satisfactory for this purpose.

§ 3 (iii). Results

Specimens were chosen with values of τ_1 lying within the range of the apparatus, i.e. τ_0 of the order of 100 μ seconds, and details of these are given in Table 1. The records were taken near $H = H_c$ and the values of the reversible permeability μ are given for that value of H .

Table 1

Properties of the Specimens

	Diameter (cm.)	μ_{\max}	τ_0 (10^{-6} sec.)	Composition (%)
16 s.w.G. hard drawn iron	0.162	83	177	C 0.03, Mn 0.05, Fe 99.9
16 s.w.G. annealed iron	0.162	120	250	C 0.03, Mn 0.05, Fe 99.9
20 s.w.G. large grained iron	0.046	760	123	Decarburized specimen of above (see § 4 (iii))

Unfortunately there is no means of locating the reference line mentioned in § 3(i) on the experimental records of the voltage pulses. The widths of the pulses have therefore been measured at the points where they cut the oscilloscope base line, which, because of the effect of stray capacities, occur at finite values of t .

The measurement of the pulse width on the oscilloscope base line is not entirely satisfactory as it would be expected that the size of a discontinuity (as distinct from its position in the specimen) would then affect the measured pulse width; further, because of the relatively high noise level, only the larger voltage pulses can be detected. An attempt has been made to reduce the effect of these errors by carrying out measurements on as many recorded pulses as possible, 221 in all.

The results of these measurements on the specimens are shown in Figure 7, with the measured widths multiplied by an arbitrary factor. As can be seen

there is reasonable agreement between the estimated and measured pulse width distribution. The discrepancy for high values of ξ_0 is possibly caused by the presence of two or more discontinuities so close together as to be indistinguishable; the discrepancy in the lower values is probably caused by the finite resolving time of the apparatus.

The factor by which the measured results must be multiplied may appear to be rather large, even allowing for the errors mentioned above: this is to be expected, however, since the reversible permeability used in these calculations is that for zero frequency and it is probable that the effective permeability for a rapid discontinuity is much lower.

§ 4. MEASUREMENTS ON THE CONTRIBUTION OF THE DISCONTINUOUS PROCESSES TO THE TOTAL CHANGE IN MAGNETIZATION

§ 4 (i). *Design of the Apparatus*

In this work the problems are to detect the maximum possible number of the discontinuities that occur over a given part of the magnetization curve, to measure their number and size, and to estimate their contribution to the total change in magnetization. The first requirement of the apparatus is therefore a high signal-to-noise ratio: the shape of the amplified voltage pulse is of much less importance since all that is required is that the amplitude of the output pulse shall bear some known linear relation to the change in magnetic moment in the specimen such as is expressed, for example, by equation (17 *a*) and (18 *a*). From these equations it would seem that a low value of either τ_1 or τ_2 , respectively, would give a high signal voltage, but this is offset by two other effects. Firstly the noise is then high, as the amplifier frequency bandwidth must have a finite value, which in practice tends to increase at higher frequencies. Secondly the effect of coil capacity becomes greater at higher frequencies. If the frequency of the amplifier and search coil circuit can be kept low, the frequency of the oscillatory component of the induced pulses may lie above the range of the apparatus and the resistance damping required might be appreciably reduced.

The use of a suitably low frequency has a further advantage: this is that the condition $\tau_1 \ll \tau_2$ (i.e. that the time constant of the search coil circuit and amplifier is long compared to that of a discontinuity) can be more easily fulfilled for many specimens. The amplitude of the output pulse for a given size of discontinuity is then independent of the eddy current effects in the specimen. If this condition is satisfied for a discontinuity at the axis of a specimen and at that part of the hysteresis cycle where μ is a maximum (near $H = H_c$), then the condition $\tau_1 \ll \tau_2$ will hold for all discontinuities in that specimen.

In designing the search coil its dimensions are controlled by those of the specimen which should have a reasonably small demagnetizing factor. It is desirable that the sensitivity of the coil shall be the same for all discontinuities taking place in the specimen and this can be attained by using a solenoidal coil slightly longer than the specimen. Equations (13) and (18 *a*), which hold strictly only for discontinuities at the centre of a coil, will then be reasonably accurate for all discontinuities in the specimen. The optimum number of turns is best found by trial as described in § 3 (ii).

4 (ii). *Method*

The basis of the experimental procedure, method of calibration and necessary precautions are similar to those described in paper I.

A block diagram of the apparatus is shown in Figure 1. The method of magnetizing the specimen, which is in the form of a wire 7.5 cm. long, is the same as that referred to in § 3 (ii). The search coil which was finally found to be most satisfactory was 10 cm. long with a mean diameter of 0.9 cm., wound with 52,000 turns of 47 s.w.g. copper wire. The amplifier was the same as that described in § 3 (i) with the frequency response set to limits of 1 kc/s. to 3 kc/s. The amplified voltage pulses were fed through a discriminator to a scale of 1024 (2^{10}), and a recorder of the post office type. The discriminator was used with its upper limit of discrimination set at 25 volts, which could be reduced in subdivisions of 0.1 volt.

The search coil required a parallel damping resistance of 200,000 ohms, giving a resolving time for the coil and amplifier of 300 μ sec., while the resolving time of the counting system was 100 μ sec. The noise level at the input of the amplifier with this assembly was about 1.5 μ v. (i.e. 0.3 v r.m.s. output).

In the calibration of the apparatus, the specimen was replaced by a small coil of 10 turns, 0.165 cm. mean diameter, through which current pulses of square waveform were passed. The rapid changes in current Δi in the calibrating coil simulate the rapid changes in flux in the specimen during a discontinuity, the relation being given by

$$\Delta M = \frac{qS\Delta i}{10}, \quad \dots\dots(24)$$

with q the number of turns in the calibrating coil and S the area of cross section of the calibrating coil. The discriminator was set, for each value of Δi , so that the amplified voltage pulses were just transmitted: a calibration curve was thus obtained showing the relation between discriminator setting and change in magnetic moment. The assumption that the time constant of the search coil was greater than that of the change of flux in the calibrating coil was confirmed by examining the respective waveforms of the input current and output voltage on the oscilloscope.

It should perhaps be emphasized here that although the equations (13) and (18*a*) are not used directly in the calibration of the apparatus, they are needed to show that there is a constant ratio between change in magnetic moment and the amplitude of the induced voltage pulse (discriminator setting) over the frequency range used.

The experimental procedure was as follows. The specimen was magnetized to near saturation in one direction, the field reversed several times to bring the material into a cyclic condition, and the specimen then taken through one half cycle of a hysteresis loop. With the discriminator set at a chosen level, readings of the number of discontinuities were taken at suitable values of the field. The rate of change of field was adjusted for each sample, in some cases so that a complete half cycle took up to 24 hours; the readings were repeated at each level at least three times and a mean taken. The lowest discriminator setting corresponding, in terms of ΔM , to $\Delta M = 0.3 \times 10^{-6}$ E.M.U. was above the peak noise level of the apparatus so that there was no background count. This can be compared with the sensitivity of the apparatus in paper I, where with $\Delta M = 3.0 \times 10^{-6}$ E.M.U. there was a noticeable background count.

Results.

Experiments were carried out on the specimens specified in Tables 2 and 3.

Table 2. Composition of Specimens

	Diameter (mm.)	Composition (%)
Hard drawn iron (Fe1)	0.384	C 0.03, Mn 0.05, Fe 99.9
Large grained iron (Fe2)	0.378	Decarburized specimen of above
Annealed nickel (Ni)	0.453	C 0.04, Si 0.05, Fe 0.15, Mn 0.03, Al 0.01, Mg 0.13, S 0.003, Ni balance

Table 3. Magnetic Properties of Specimens

τ_0 is calculated from equation (10), using the maximum values of reversible susceptibility κ (permeability μ) given.

Material	I_s	Maximum κ (μ)	H_0	τ_0 (10^{-6} sec.)	Average grain size (cm^3)
Hard drawn iron	1720	6.9 (87.7)	5.7	10.1	5×10^{-9}
Large grained iron	1720	32 (403)	0.39	46.0	10^{-6}
Annealed nickel	485	8.0 (102)	1.3	16.6	case 10^{-9} core 10^{-6}

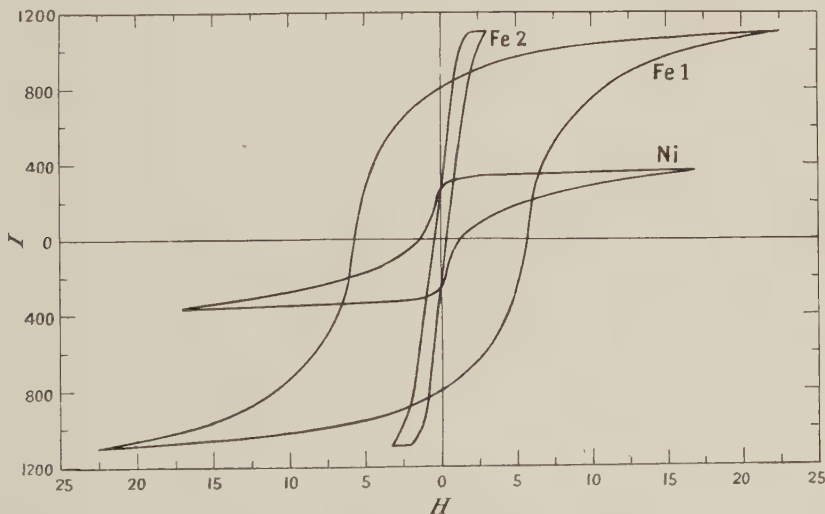


Figure 8. Hysteresis curves for hard drawn iron (Fe 1), large grained iron (Fe 2), and annealed nickel (Ni).

The large-grained iron was prepared by the method of Edwards and Pfeil (1924): a specimen of hard drawn iron was decarburized in an atmosphere of moist hydrogen for 48 hours at 950°C ., stretched by 3.5%, then annealed in dry hydrogen at 830°C . for 72 hours. The nickel was annealed in hydrogen at 930°C . for 1 hour and then allowed to cool over a period of 6 hours; this treatment is similar to that used by Bates and his collaborators. The average grain sizes shown in Table 3 were obtained from measurements on etched specimens. The hysteresis loops for the three specimens are shown in Figure 8, for which I is plotted against the applied field. For the present purpose a knowledge of

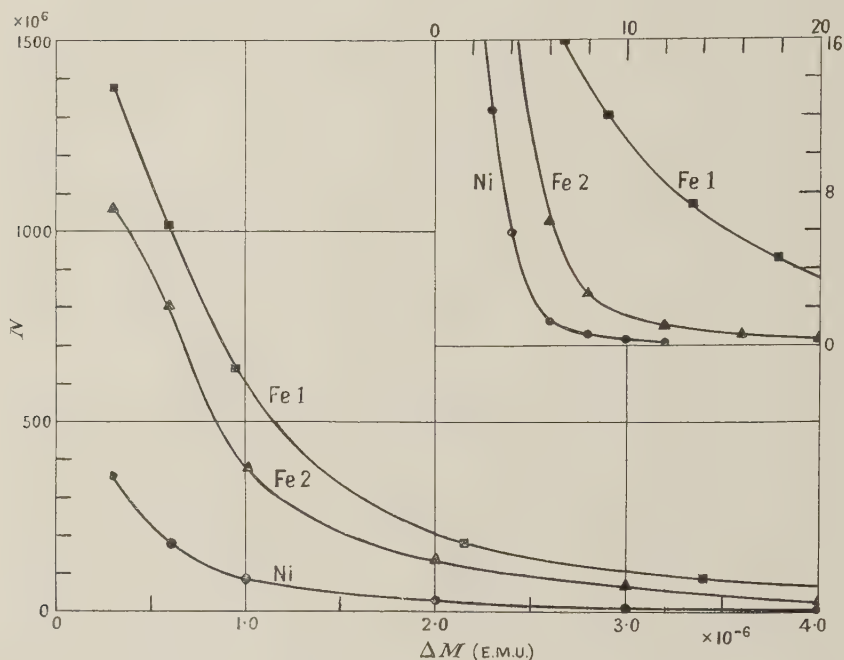


Figure 9. Number-level curves for iron and nickel, showing the number of discontinuities per cm³ with a magnetic moment greater than ΔM .

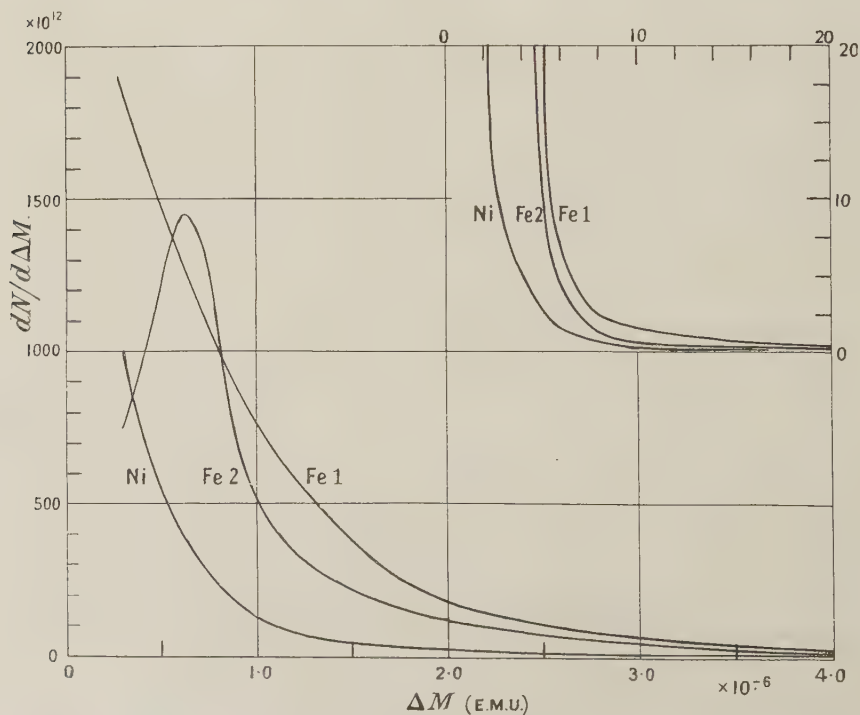


Figure 10. Distribution curves for iron and nickel. (The minimum volume associated with the change in resolved magnetic moment ΔM can be obtained by multiplying by 2.91×10^{-4} for iron and by 1.03×10^{-3} for nickel.)

the true field (i.e. corrected for demagnetization effects) is not required directly. The corrected curves do not differ greatly from those shown except for the large grained iron specimen.

From the readings taken of the number of discontinuities at each level of the discriminator, a curve was drawn for each specimen showing the number of discontinuities per cm^3 , above a given size ΔM , plotted against the corresponding discriminator setting (in terms of ΔM). Number-level curves for the three specimens are shown in Figure 9. By differentiating these curves, a (size, number) distribution curve was obtained for each specimen, i.e. $(\Delta M, dN/d\Delta M)$. These are shown in Figure 10.

Figure 11 shows the contribution per unit range of size, $\Delta M \cdot dN/d\Delta M$, to the total change in magnetization, ΔI_T , plotted against ΔM : for the purpose of comparison the ordinates have been divided by the appropriate value of ΔI_T .

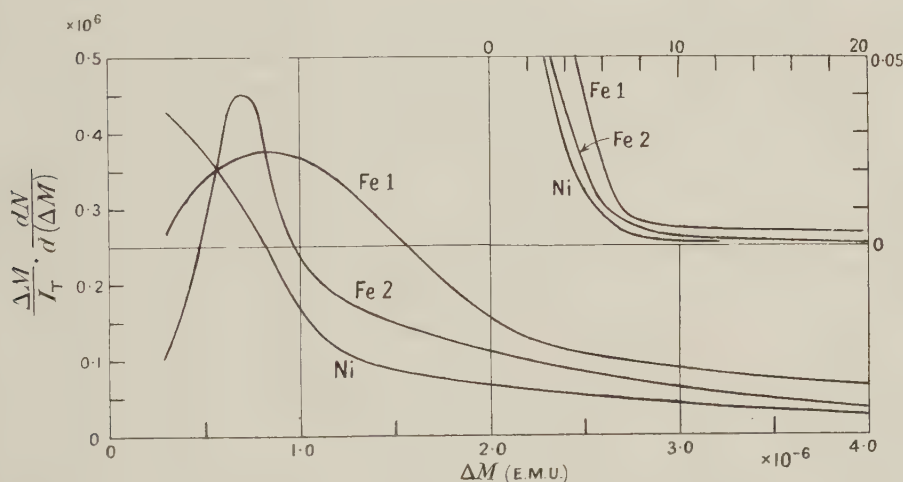


Figure 11. Contribution curves for iron and nickel showing the relative contributions to the total change in magnetization per unit range of ΔM .

The contribution of the measured discontinuities, over the measured range of ΔM , is given by the area under the contribution curve

$$\int \Delta M \frac{dN}{d\Delta M} d(\Delta M) = \int \Delta M \cdot dN,$$

with appropriate limits, which is thus the corresponding area between the number-level curve and the N axis. This is the measured change in intensity ΔI_B , produced by the Barkhausen effect, over the field limits considered. The results of this integration carried out directly on the number-level curves are shown for each specimen in Table 4.

The relative contribution of discontinuities, above a given size, to the total change in magnetization $\Delta I_B/\Delta I_T$ is shown in Figure 15, which has been obtained by integrating the area under the contribution curve above chosen values of ΔM .

An estimate has also been made of the contribution of reversible processes to the change in magnetization, by the measurement of the reversible

susceptibility, κ , at different points on the hysteresis curve. (It is hoped to publish details of this work later.) A (κ , H) curve can then be drawn and the area under this curve is given by

$$\int \kappa dH = \int \frac{dT_R}{dH} dH = \Delta I_R,$$

with appropriate limits, which can be referred to as the reversible contribution. This is also shown in Table 4, and the sum of the two contributions $\Delta I_B + \Delta I_R$ is compared with the change in intensity taken from the hysteresis loop ΔI_T . The value of $\Delta I_B + \Delta I_R$ obtained by extrapolating ΔI_B to zero ΔM is shown for the iron specimens, but this cannot be done satisfactorily for nickel as the contribution curve shows no maximum.

Table 4. Contribution of Discontinuous and Reversible Processes (ΔI_B and ΔI_R) to the Total Change in Magnetization ΔI_T

Material	Limits of field	Limits of ΔM (10^{-6} E.M.U.)	ΔI_T	dH/dt (10^{-4} oe. sec $^{-1}$)	Contribution (and percentage of total)			
					ΔI_B	ΔI_R	$\Delta I_B + \Delta I_R$	$\Delta I_B + \Delta I_R$ extrapolated
Hard drawn iron	± 18.6	0.3-35	2150	1-20	1844 (86)	180 (8.4)	2024 (94)	2109 (98)
Large grained iron	± 3.0	0.3-20	2180	0.2-4	1250 (57)	110 (4.9)	1400 (62)	1390 (64)
Annealed nickel	± 14.9	0.3-12	700	1-20	326 (47)	115 (16.4)	441 (63)	

The minimum values of v (v_m) (from equation (1b)) corresponding to $\Delta M \times 10^6 = 1$ are, for hard drawn and large grained iron ($I_s = 1720$), 2.9×10^{-10} cm 3 , and for nickel, ($I_s = 485$) $1.0_3 \times 10^{-9}$ cm 3 . The corresponding number of atoms can be readily found. The minimum values which could be detected with certainty above the noise level in the experiments, also the maximum values (as given in the results), are shown in Table 5.

Table 5. Minimum and Maximum Changes in Resolved Moment ΔM , and the Associated Minimum Volumes v_m and Numbers of Atoms n_v

	Fe 1		Fe 2		Nickel	
	Min.	Max.	Min.	Max.	Min.	Max.
$\Delta M \times 10^6$	0.30	40	0.30	20	0.3	12
$v_m \times 10^{10}$	0.87	116	0.87	58	3.1	124
$n_v \times 10^{-13}$	0.74	99	0.74	49	2.6	106

An 'average value' of ΔM (or v_m) can be calculated for each specimen by dividing the total measured contribution by the total number of measured discontinuities but, as was pointed out in I, p. 379, this value is meaningless because of the probability of a large number of much smaller discontinuities which contribute very little to the total change in magnetization. For purposes of comparison, however, an 'average value' of ΔM (or v_m) can be defined as the value above which the discontinuities account for half of the total discontinuous magnetization (i.e. $\frac{1}{2}(\Delta I_T - \Delta I_R)$). This average value, which has been calculated

from Figure 15, together with the corresponding values of v_m and n_v are shown in Table 6.

Table 6. Average Values of ΔM , v_m and n_v

	ΔM (10^{-6} E.M.U.)	v_m (10^{-10} cm ³)	n_v (10^{11} atoms)
Hard drawn iron	1.6	4.6	6.5
Large grained iron	0.7	2.0	2.8
Annealed nickel	0.4	4.1	4.8

In order to demonstrate the variation in contribution with field, curves are shown giving dI_B/dH plotted against H , compared with the corresponding curves for dI_T/dH obtained from the hysteresis loop, and with dI_R/dH , the reversible susceptibility (Figures 12-14).

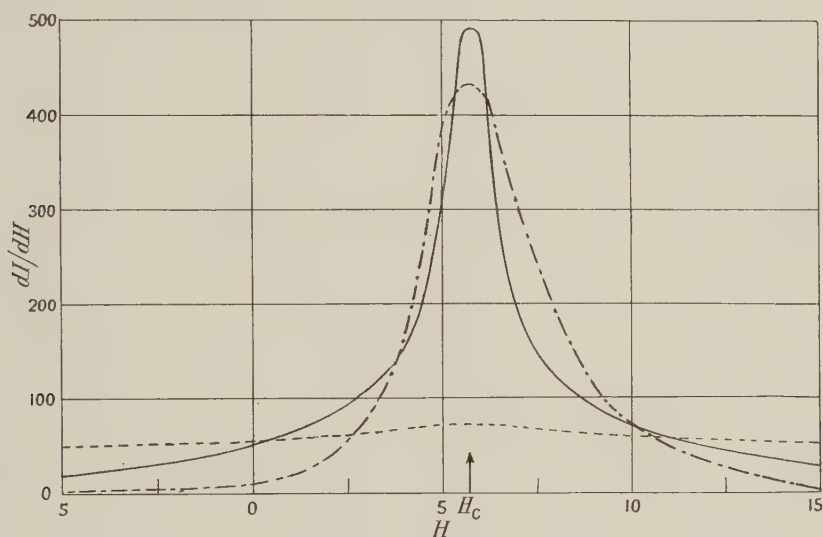


Figure 12. dI/dH curves for hard drawn iron.
— dI_T/dH . — — dI_B/dH . - - - $dI_R/dH \times 10$.

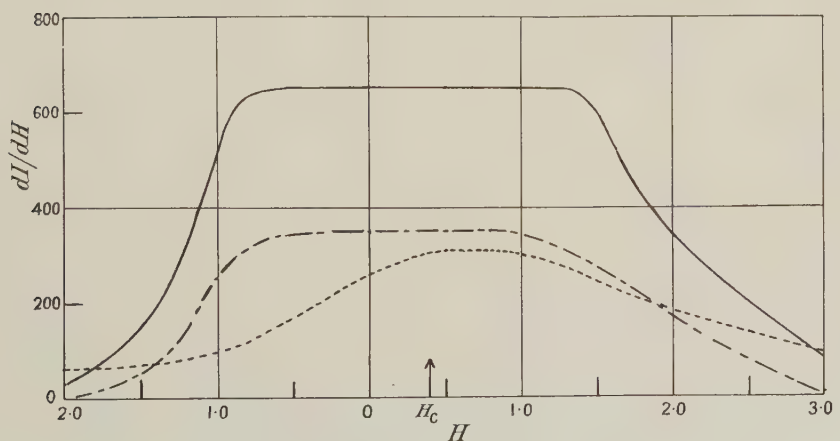


Figure 13. dI/dH curves for large grained iron.
— dI_T/dH . — — dI_B/dH . - - - $dI_R/dH \times 10$.

The measured sum $\Delta I_B + \Delta I_R$ for hard drawn iron is 94% of ΔI_T , and extrapolation of the contribution curve from $\Delta M = 0.3 \times 10^{-6}$ E.M.U. to zero accounts for another 4%, giving a total of 98%. Since the probable error in the measured Barkhausen contribution is about 5%, and the extrapolation can give only the order of magnitude of the contribution of the smaller discontinuities, the agreement is partly fortuitous and there is a possibility that there is still some further unaccounted contribution for the specimen (see also below).

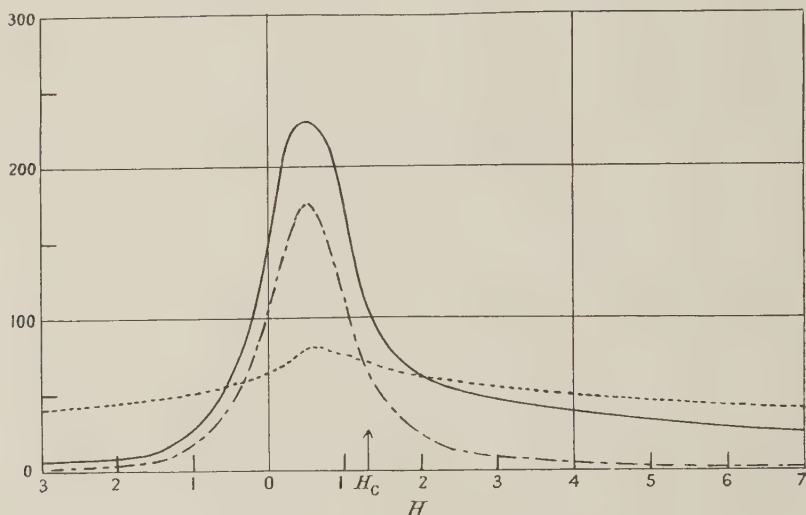


Figure 14. dI/dH curves for annealed nickel.
 — dI_T/dH . - - - dI_B/dH . - · - $dI_R/dH \times 10$.

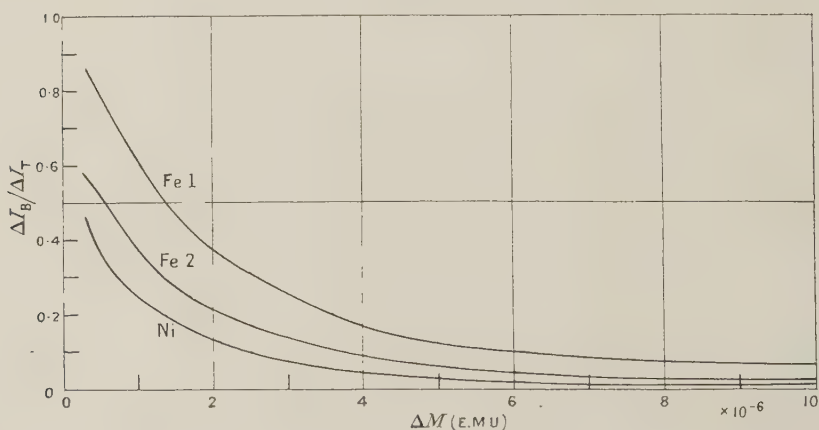


Figure 15. Fractional contribution $\Delta I_B/\Delta I_T$ of discontinuities above a given size ΔM .

The results for the large grain iron show that 38% of the total magnetization remains unaccounted for by discontinuous processes. Extrapolation below $\Delta M = 0.3 \times 10^{-6}$ E.M.U. would indicate that these smaller discontinuities can contribute to only a small proportion of this discrepancy. One possible source of error lies in the fact that the Barkhausen discontinuities do not take place at random, but tend to occur in groups, i.e. the production of one discontinuity tends to trigger a number of others. This is the main reason for the extremely

low rates of change of field (10^{-4} oersted/sec.) required in order to keep the rate of counting within the range of the apparatus and to reduce the number of coincidences between the discontinuities. In the experiments on the hard drawn iron and the annealed nickel the effect was small, but with the large grained iron the presence of the 'grouping' was still noticeable and this may be the reason for the sharp fall in contribution for low values of ΔM . The effect may be associated with the steepness of the (I, H) curve over a wide range of I , which means that at any particular (I, H) value in this range, a very small increase in H is sufficient to induce a relatively large change in I . The local change in field due to a single discontinuity may therefore be sufficient to initiate others. It is possible that the effect would be reduced by using a specimen with a higher demagnetizing factor, and experiments to test this are projected. Should this explanation be correct, the contribution of the discontinuities below the level $\Delta M = 1 \times 10^{-6}$ cm. is greater than is indicated in the results.

The lower contribution for annealed nickel (47%) is quite definite but shows a marked increase over that given in paper I, 11% for a hard drawn specimen. The percentage contribution over the steep part of the hysteresis curve appears to be somewhat greater, but it is difficult to estimate this accurately because of the rapid change in intensity over this region. Because of the absence of a maximum in the contribution curve for this specimen, it was not possible to make an accurate extrapolation over the region below $\Delta M = 0.3 \times 10^{-6}$ E.M.U., but an examination of the curve indicates that the smaller discontinuities could account for a considerable part of the discrepancy.

The results for the 'average size' of the discontinuities show that, for the hard drawn iron, half of the estimated total discontinuous change is accounted for by discontinuities for which $\Delta M > 1.6 \times 10^{-6}$ E.M.U. This value is more than twice that for the large grained specimen in which presumably flaws and inclusions are smaller. This supports the view that the larger Barkhausen discontinuities may be associated with the secondary domain structure round the imperfections in the material, as suggested by Williams and Shockley. Where the difference in the values of I_s is taken into account in estimating the average volume, there is no significant difference in the values for annealed nickel as compared with the other specimens. The order of magnitude of these average minimum volumes is about one-tenth those given in paper I, and by Bozorth and Dillinger, and this is a measure of the improvement in the sensitivity of the method.

The dI/dH curves are of interest in showing a maximum which, for a given specimen, occurs at nearly the same value of H for the Barkhausen, reversible, and total contributions. For the hard drawn iron it seems that the Barkhausen contribution may be an overestimate, where dI_B/dH is greater than dI_T/dH , but the difference is considerably greater than the experimental error, particularly as in this region the rate of counting is not very great. It is more probable that this is caused by magnetic viscosity, i.e. by the difference in the rates at which the specimen is magnetized in obtaining the hysteresis curve and in the counting experiments. The dI_B/dH and dI_T/dH curves for the large grained iron both exhibit a well defined region of constant dI/dH , corresponding to the steep part of the loop: the noticeable curvature in the dI_R/dH curve may perhaps indicate that the method of measuring reversible susceptibility is more sensitive in detecting small changes in slope on the (I, H) curve.

There is one possible source of error in any work of this nature which there seems to be no means of avoiding, except by increased sensitivity. This is that if there are a large number of small discontinuities below the noise level, these will raise the level of the noise as soon as the field is changed and discontinuities take place. The result would of course lead to an increase in the measured number of discontinuities. There was, however, no obvious increase in the noise as examined on the oscilloscope, although it would be difficult to differentiate between genuine discontinuities and an increase in the background noise, nor is there any indication, except for the hard drawn iron, Figure 12, that the measured ΔI_B is too large. It is unlikely that the steep rise in the number-level curve at low values of ΔM is caused by noise; as can be seen by comparison with the inset curves, the rise is just as pronounced at higher values of ΔM if the scale is suitably chosen.

It has been considered desirable in this work to keep the demagnetizing factor for a specimen low in order to keep the internal field uniform and so that the fields required to saturate the material would be reasonably low. Specimens with the above dimensions (7.5 cm. long and 0.376 mm. diameter) have therefore been used. This has resulted in the large number of counts which have to be taken, with the rather long time (up to 3 months) necessary to investigate a single specimen. It is proposed in any future work to use a shorter specimen about 1 cm. long, and this should reduce considerably the time taken. Because of the higher demagnetizing factors and the fact that the effective slope of the (I , H) curve will be reduced, it will only be possible to carry out experiments over a more restricted part of the magnetization curve at any one time; it will, however, have the advantages that lower effective rates of change of field will be possible and the 'grouping' of the discontinuities should be reduced. Further it will then be possible to use a shorter search coil with consequent reduction in the thermal agitation noise.

§ 4. CONCLUSION

It may be convenient to summarize some of the main results and tentative conclusions.

(1) A theory of pulse shape has been developed, with which the experimental results are in reasonable agreement.

(2) The sum of the measured Barkhausen and reversible contributions agrees quantitatively with the measured total change for hard drawn iron and the discrepancy for the large grained iron and annealed nickel can be explained.

(3) 50% of the discontinuous change in magnetization is due to individual discontinuities with $\Delta M > 1.6 \times 10^{-6}$ E.M.U., 0.7×10^{-6} E.M.U., and 0.4×10^{-6} E.M.U., for Fe 1, Fe 2, and Ni, respectively. The Barkhausen volumes ($\sim 4 \times 10^{-10}$ cm³) are in general much smaller than primary domains, at least those in single crystals, and may be attributed to localized irregularities in the displacement of primary domain boundaries.

(4) The number of larger discontinuities is greater for hard drawn iron than for a decarburized and annealed specimen but the distribution curves are not widely different. Measurement on a wider range of materials is necessary in order to see whether there are differences which can be related to the other properties of the materials.

ACKNOWLEDGMENTS

We wish to express our gratitude to Professor R. Whiddington, under whose helpful direction this work has been carried out, for his constant encouragement and advice; to Professor E. C. Stoner for the stimulating discussions and the generous help he has given in the preparation of this paper; to Mr. A. B. Gillespie, of A.E.R.E., Harwell, who gave us every help and cooperation in the construction of the amplifier; and to Dr. M. M. Nicolson, Dr. P. Rhodes, Mr. G. J. Ogilvie, and Mr. H. Partridge for their assistance.

We have also to thank the Mond Nickel Company, Messrs. Rigby and Sons Ltd., the Ministry of Supply and the Admiralty for supplying material and for the loan of apparatus.

REFERENCES

- BECKER, R., 1938, *Z. techn. Phys.*, **19**, 542.
 BOZORTH, R. M., and DILLINGER, J., 1930, *Phys. Rev.*, **35**, 733.
 BUSH, H. D., and TEBBLE, R. S., 1948, *Proc. Phys. Soc.*, **60**, 370.
 EDWARDS, C. A., and PFEIL, L. H., 1924, *J. Iron Steel Inst.*, **109**, 129.
 GILLESPIE, A. B., 1947, *Atomic Energy Research Establishment Electronics Newsletter*, **3**, 15.
 JEANS, J., 1946, *Mathematical Theory of Electricity and Magnetism* (Cambridge: University Press), p. 461.
 TERMAN, F. E., 1943, *Radio Engineers' Handbook* (New York: McGraw-Hill), p. 294.
 WILLIAMS, H. J., and SHOCKLEY, W., 1949, *Phys. Rev.*, **75**, 178.
 WSWEDENSKY, B., 1921, *Ann. Phys., Lpz.*, **64**, 609.

Domain Wall Movement in a Single Crystal

By K. H. STEWART

Cavendish Laboratory, Cambridge

Communicated by D. Shoenberg; MS. received 12th January 1950

ABSTRACT. A single crystal of silicon-iron was shaped so as to encourage the formation of large ferromagnetic domains. Its magnetization curve was found to contain a large Barkhausen jump, indicating reversal of magnetization in a volume of the order of $1/10 \text{ cm}^3$. The rate of change of magnetization was found to be proportional to the excess of the applied magnetic field over a certain critical field, and could be made very slow. It is suggested that the rate of change is controlled by the braking effect of eddy currents on the movement of domain walls.

THIS note reports some observations that have been made recently on magnetization in a single crystal of 3% silicon iron cut into the form of a hollow rectangle ('picture frame') all of whose faces were parallel to (100) planes of the lattice. Williams (Williams and Shockley 1949, Williams, Bozorth and Shockley 1949) has demonstrated the existence of remarkably simple domain arrangements in such a specimen and it was hoped that the study of magnetization changes with such a simple arrangement would give useful information about the factors controlling the movement of domain walls.

The present specimen had the dimensions shown in Figure 1. The orientations of its faces were tested by etch pit reflections and by the 'fir-tree' Bitter patterns (Williams, Bozorth and Shockley 1949), and the specimen was filed until all the faces were within 1° of (100) over most of their surface. The

characteristic domain structure found by Williams is indicated by the dotted lines in Figure 1, directions of domain magnetization being shown by arrows. The Bitter patterns formed when colloidal magnetite was applied to the present crystal revealed no such definite pattern; all that could be seen was a number of isolated 'fir-trees', on parts of the specimen where the orientation was slightly imperfect. This examination was not pressed very far as the electrolytic polishing necessary before the patterns could be seen would have consumed too much of the specimen. It may be worth recording that it was found that 'fir-tree' and straight line patterns, i.e. patterns characteristic of the true domain structure and not merely of the state of strain of the surface, could be obtained on this and other specimens if careful mechanical polishing was followed by an anneal at 1200°C . in a high vacuum ($\sim 10^{-4}$ mm. Hg). If the vacuum was less good, a film of tarnish formed on the polished surface and prevented the patterns from appearing. This method has advantages over electrolytic polishing in cases where the exact shape of surface is important.

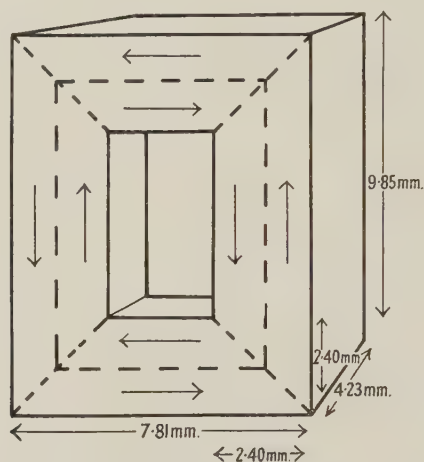


Figure 1. The single crystal specimen: domain boundaries are shown by broken lines, directions of magnetization by arrows.

The main interest of the specimen lay in its magnetization curve, which was obtained by the usual ballistic galvanometer method. The field winding consisted of six turns of 36 s.w.g. copper wire on each of the long limbs and three turns on each of the short ones. The flux coil was normally ten turns of 42 s.w.g. wire on one of the limbs. It was found that the results did not depend on the exact arrangement of these coils, in fact in some of the later experiments the eighteen-turn field winding was replaced by a single thicker wire threaded through the specimen, without affecting the results for a given magnetomotive force.

The magnetization curve is shown in Figure 2. Its chief feature is the large instability in fields of about 0.05 gauss; it can be said that almost half the total change in magnetization takes place in a single Barkhausen jump, occurring at a reproducible value of the field. Large Barkhausen jumps have been observed before, notably in the experiments of Forrer (1926) and Sixtus and Tonks (1932), but always in material subject to severe stresses and not in material where the magnetization directions are controlled by the magneto-crystalline anisotropy, a

in the present well-annealed silicon-iron crystal. The presence of such a large discontinuity in the magnetization curve suggests that very large domains are involved and that the change in magnetization occurs chiefly by the movement, perpendicular to its plane, of a single 180° wall such as that shown in Figure 1.

The 'jump' from A to B in Figure 2 took place quite slowly. It proved possible to arrest it by switching off the (negative) field as soon as movement of the galvanometer showed that the jump had begun. If the negative field was applied again gradually, the jump would re-start at a lower value of the field than the one corresponding to point A. The true hysteresis loop is therefore not the dotted curve of Figure 2, but rather the re-entrant full curve. This was at first plotted by manual control of the field as just described, but later by an automatic feedback method which adjusted the field so that there was a constant change of

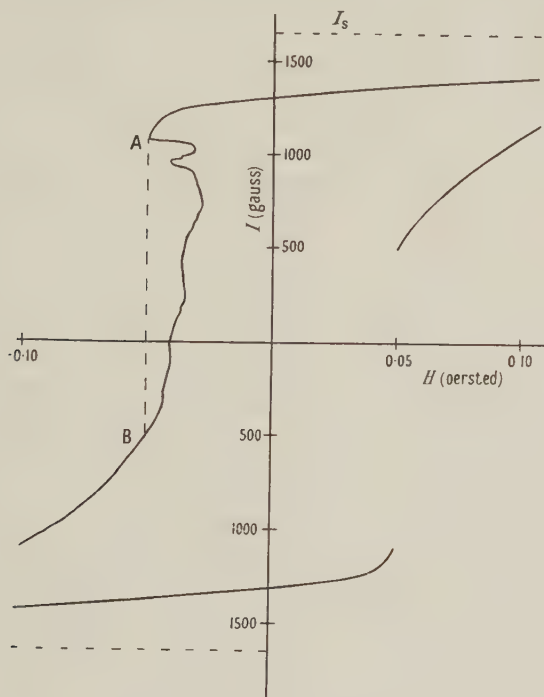


Figure 2. (I , H) curve of the specimen. The detail of the re-entrant part of the loop is taken from one 'run'; other runs give the same main features but differ in detail.

magnetization, at a very slow rate, from A to B. Figure 2 can be interpreted in terms of the movement of the 180° wall of Figure 1 if it is assumed that the movement is opposed by various obstacles such as those due to local internal stresses (Becker and Döring 1939) or inclusions of impurity (Kersten 1943). The curve suggests that there are many obstacles of about the same size in this specimen, that at A being larger than all the others as far as B. The hysteresis loss of the specimen will, of course, depend on the way in which the field is changed, being considerably larger if the dotted line AB is followed than if the field is adjusted to follow the re-entrant curve. Similar effects may well occur in more normal materials, but in these it would be very difficult to adjust the field to follow the small and rapid discontinuities.

The speed of the change from A to B was found to depend on the field strength. It was investigated by bringing the field to a point just short of A and then increasing it suddenly to some larger negative value; the subsequent changes in magnetization were measured by a photographically recording galvanometer. The results for the initial rate of change of magnetization are shown in Figure 3. If the change is interpreted as due to the movement of a single 180° wall, we obtain a linear relation between the field H , and the velocity of the wall V , given by $V = A(H - H_0)$ where A and H_0 are constants equal to 6.3 cm/sec/oersted and 0.049 oersted respectively. The experiment was repeated with the specimen cooled in liquid oxygen and the lower line of Figure 3 was obtained, with $A = 5.7$ cm/sec/oersted, $H_0 = 0.056$ oersted.

These values of wall velocity are much lower than those that must occur in ordinary polycrystalline silicon-iron, since such low values would give rise to viscosity effects much larger than those commonly observed. Various effects have been suggested as controlling the speed of wall movement (Snoek 1938, 1947)

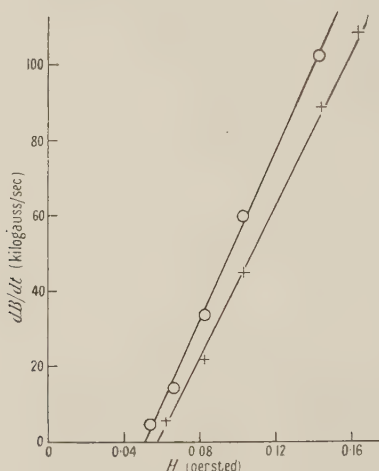


Figure 3. Rate of change of flux density as a function of field strength at room temperature (circles) and at the temperature of liquid oxygen (crosses).

but the only one which provides a ready explanation for the very slow movement in the present specimen is the control by eddy currents. Since eddy current effects depend markedly on dimensions, the present very large wall would be expected to move much more slowly than the usual small ones. A rough calculation, assuming that the wall moves as a rigid plane and induces the same eddy currents as would an infinite plane wall, gives a value of A of 1.0 cm/sec/oersted for the specimen of Figure 1. This is only one sixth of the value found from Figure 3, but the very rough assumptions of the calculation would certainly lead to an underestimate of A , so that the discrepancy is not serious. The idea that A is determined by eddy current effects is supported by its variation with temperature. If the speed of movement were controlled by effects such as the relief of elastic strains, it should have a very large temperature dependence; if by eddy currents, then the speed should be proportional simply to the resistivity of the material. In fact, Figure 3 shows that A decreases by 10% when the specimen is cooled from room temperature to liquid oxygen temperature, while the measured decrease in

resistivity for a strip sample of the same material cooled in the same way was 18%. In view of various experimental inaccuracies this order-of-magnitude agreement seems to support the eddy current hypothesis.

The linear relation between V and H shown in Figure 3 is similar to that found by Sixtus and Tonks (1932) in their experiments on stretched nickel-iron wires, but in their case the values of the constant A were much greater, of the order of 10,000 cm/sec/oersted. Their original interpretation of the results suggested that A was determined by eddy currents, but Snoek (1947) has shown that this is probably incorrect and that some additional 'frictional' mechanism must be present. In the single crystal specimen it is apparently unnecessary to postulate such a mechanism to account for the observed effects; if it exists it is masked by the much larger 'friction' provided by eddy currents.

Further experiments on various phenomena in the crystal would have been desirable, but unfortunately it was destroyed while being annealed in an attempt to improve its properties.

ACKNOWLEDGMENT

This work forms part of a programme of research sponsored by the Electrical Research Association; the author is indebted to the Association for permission to publish.

REFERENCES

- BECKER, R., and DÖRING, W., 1939, *Ferromagnetismus* (Berlin : Springer), Ch. 15.
FORRER, R., 1926, *J. Phys. Radium* (6), **7**, 109.
KERSTEN, M., 1943, *Grundlagen einer Theorie der Ferromagnetischen Hysterese und der Koerzitivkraft* (Leipzig : Hirzel).
SIXTUS, K., and TONKS, L., 1932, *Phys. Rev.*, **42**, 419.
SNOEK, J. L., 1938, *Physica*, **5**, 663; 1947, *New Developments in Ferromagnetic Materials* (Amsterdam : Elsevier).
WILLIAMS, H. J., BOZORTH, R. M., and SHOCKLEY, W., 1949, *Phys. Rev.*, **75**, 178.
WILLIAMS, H. J., and SHOCKLEY, W., 1949, *Phys. Rev.*, **75**, 155.

Sommerfeld's Polynomial Method Simplified

BY A. RUBINOWICZ

Institute of Theoretical Mechanics, University of Warsaw

MS. received 30th September 1949

ABSTRACT. From two earlier papers by the author it follows that eigenfunctions obtainable by Sommerfeld's polynomial method contain either a Riemann P -function or a degenerate form of it when the fundamental interval is either finite or infinite respectively. Comparing the differential equation for the P -function or its degenerate form with the differential equation which we get for P from the original differential equation of the eigenvalue problem, we obtain standard formulae for the constants determining the eigenvalues and eigenfunctions. The calculations necessary to give the complete solution of an eigenvalue problem, which can be treated by Sommerfeld's polynomial method, are thus reduced to a minimum of differentiations and simple algebraic operations. It is also possible using appropriately chosen P -functions to obtain the eigenfunctions directly in the required form. The method yields also eigenfunctions for eigenvalues in the continuous spectrum.

§ 1. INTRODUCTION

IN two earlier papers (Rubinowicz 1949 a, b) it was shown that the solutions of the eigenvalue problem belonging to the self-adjoint differential equation

$$\frac{d}{dx} \left(p \frac{df}{dx} \right) - (q - \lambda \rho) f = 0 \quad \dots\dots (1)$$

and obtainable by Sommerfeld's (1939) polynomial method are given by

$$f = p^{-1/2} P. \quad \dots\dots (2)$$

The function P is here either of the form

$$(I) \quad P = \xi^\alpha (1 - \xi)^\gamma F(a, b, c, \xi)$$

or of the form

$$(II) \quad P = \xi^\alpha \exp(-\xi/2) F_1(a', c', \xi),$$

where

$$\xi = \kappa x^h. \quad \dots\dots (3)$$

F and F_1 are the ordinary and the confluent hypergeometric functions and h is a positive integer. We use function (I) where the fundamental interval of the eigenvalue problem (bounded by two singular points of the equation (1)) is finite and its boundary points are given by $\xi = 0$ and $\xi = 1$, and function (II) when this interval is infinite and bounded by $\xi = 0$ and $\xi = +\infty$. But if h is an even integer and $x = \xi = 0$ is not a singular point of the differential equation (1) the boundaries of the fundamental intervals will be given in the two cases (I) and (II) only by $\xi = 1$ and $\xi = +\infty$ respectively.

In this paper the above results will be used to show that we can obtain the eigenfunctions and eigenvalues quite simply in all cases where Sommerfeld's polynomial method can be applied. The same procedure can also of course be used independently of its connection with Sommerfeld's polynomial method.

The starting point of our considerations is the remark that the function P is in case (I) a Riemann P -function and in case (II) obviously a confluent form of it.

§ 2. GENERAL RELATIONS

Inserting the function f as defined by (2) into the differential equation (1) we get for P , as a function of the variable ξ defined in equation (3), the differential equation

$$\frac{d^2 P}{d\xi^2} + \frac{h-1}{h} \frac{1}{\xi} \frac{dP}{d\xi} + \frac{1}{h^2} \frac{x^2}{\xi^2} \left[\left(\frac{1}{2p} \frac{dp}{dx} \right)^2 - \frac{1}{2p} \frac{d^2 p}{dx^2} - \frac{q-\lambda p}{p} \right] P = 0. \quad \dots\dots(4)$$

In case (I) P is a Riemann P -function and therefore a solution of the differential equation

$$\frac{d^2 P}{d\xi^2} + \left(\frac{1-\alpha-\alpha'}{\xi} - \frac{1-\gamma-\gamma'}{1-\xi} \right) \frac{dP}{d\xi} + \left(\frac{\alpha\alpha'}{\xi} + \frac{\gamma\gamma'}{1-\xi} - \beta\beta' \right) \frac{1}{\xi(1-\xi)} P = 0, \quad \dots\dots(5)$$

where $\alpha + \alpha' + \beta + \beta' + \gamma + \gamma' = 1. \quad \dots\dots(5a)$

The constants a, b, c in (I) are then given by

$$a = \alpha + \beta + \gamma; \quad b = \alpha + \beta' + \gamma; \quad c = 1 + \alpha - \alpha'. \quad \dots\dots(5b)$$

Comparing the coefficients of $dP/d\xi$ in (4) and (5) we get $(h-1)/h = 1 - \alpha - \alpha'$, $0 = 1 - \gamma - \gamma'$ and hence from (5a)

$$\alpha + \alpha' = 1/h, \quad \beta + \beta' = -1/h, \quad \gamma + \gamma' = 1. \quad \dots\dots(6)$$

Comparing coefficients of P in (4) and (5), multiplying by $h^2 \xi^2$ and resolving into partial fractions in ξ , we finally obtain our standard formula for case (I)

$$\begin{aligned} x^2 \left[\left(\frac{1}{2p} \frac{dp}{dx} \right)^2 - \frac{1}{2p} \frac{d^2 p}{dx^2} - \frac{q-\lambda p}{p} \right] \\ = h^2 \left[- \frac{\gamma(\gamma-1)}{(1-\xi)^2} + \frac{-\alpha(\alpha-1/h) + \beta(\beta+1/h) + \gamma(\gamma-1)}{1-\xi} + \beta(\beta+1/h) \right]. \end{aligned} \quad \dots\dots(7)$$

In order to apply the same procedure in case (II) we remark that the confluent form (II) of the P -function is obtained in the limit $\epsilon \rightarrow 0$ if in (I) we put

$$\left. \begin{aligned} \xi &= \frac{\epsilon}{2} \xi_1' & \beta &= \beta_0 + 1/\epsilon, & \gamma &= \gamma_0 + 1/\epsilon, \\ & & \beta' &= \beta_0' - 1/\epsilon, & \gamma' &= \gamma_0' - 1/\epsilon. \end{aligned} \right\} \quad \dots\dots(8)$$

For the coefficients a', c' in (II) we then get

$$a' = \alpha + \beta_0' + \gamma_0, \quad c' = 1 + \alpha - \alpha', \quad \dots\dots(9)$$

and writing ξ instead of ξ' we obtain for the function P in case (II) the differential equation

$$\frac{d^2 P}{d\xi^2} + \frac{1-\alpha-\alpha'}{\xi} \frac{dP}{d\xi} + \left(\frac{\alpha\alpha'}{\xi^2} + \frac{\beta_0-\beta_0'-\gamma_0+\gamma_0'}{2\xi} - \frac{1}{4} \right) P = 0. \quad \dots\dots(10)$$

From (4) and (10) follows

$$\alpha + \alpha' = 1/h \quad \dots\dots(11)$$

and therefore also the standard formula for case (II)

$$x^2 \left[\left(\frac{1}{2p} \frac{dp}{dx} \right)^2 - \frac{1}{2p} \frac{d^2p}{dx^2} - \frac{q - \lambda p}{p} \right] = h^2 \left[-\alpha(\alpha - 1/h) + \left(\alpha - \alpha' + \frac{1}{2} - \frac{1}{2h} \right) \xi - \frac{1}{4} \xi^2 \right]. \quad \dots\dots(12)$$

In deriving (12) we have used the fact that $\beta_0 - \beta'_0 - \gamma_0 + \gamma'_0 = 2(\alpha - \alpha') + 1 - 1/h$ which follows from (5a), (8), (9) and (11).

For $h = 1$ equation (10) is identical with the differential equation for Whittaker's confluent P -function W .

When, using Sommerfeld's polynomial method, we obtain a solution of an eigenvalue differential equation of the form (1), its coefficients p , q and ρ must be such that they identically satisfy equation (7) for case (I), and equation (12) for case (II). If we split the left-hand side of (7) or (12) into partial fractions and equate the two sides of the equation in question, using (3), we obtain the value of h , and in case (I) also that of κ . Further, since in both these equations we have three terms on the right hand side, we obtain three equations for the six constants (κ , h , α , β , γ , λ) involved in case (I) and for the five constants (κ , h , α , α' , λ) in case (II). These equations are quadratic in α and in case (I) also in β and γ , being of the form $\alpha(\alpha - 1/h) = A$, $\beta(\beta + 1/h) = B$ and $\gamma(\gamma - 1) = C$. Generally we have therefore two values of α , β , γ at our disposal. For discrete eigenvalues these constants must have fixed values or values which depend upon a quantum number. In both our cases we still need for this purpose one equation corresponding to Sommerfeld's condition for the breaking off of the power series and containing the quantum number. This equation we get, possibly together with inequalities for our constants, by investigating the behaviour of the eigenfunctions at the boundary points of the fundamental interval. In case (I) these points coincide with $\xi = 0$ and $\xi = 1$ and in case (II) with $\xi = 0$ and $\xi = +\infty$. The convergence of the normalization and orthogonality integrals

$$\int f_1^* f_2 \rho dx = \int P_1^* P_2 \frac{\rho}{p} dx \quad \dots\dots(13)$$

at the point $x = \xi = 0$ depends, in both cases (I) and (II), upon the factor $\xi^\alpha (\rho/p)^{1/2}$ (also if $x = 0$ is an inner point). This factor may suppress one of our two α -values. One at least of the boundary points is given in case (I) by $\xi = 1$ and in case (II) by $\xi = +\infty$. In case (I) the convergence of (13) at $\xi = 1$ depends upon the factor $(1 - \xi)^\gamma (\rho/p)^{1/2}$ if $F(a, b, c, \xi)$ converges for $\xi = 1$. This factor can cause a suppression of one of our two γ -values given by $\gamma = \frac{1}{2} + (C + \frac{1}{4})^{1/2}$ and $\gamma = \frac{1}{2} - (C + \frac{1}{4})^{1/2}$. But if a or b is not a negative integer the hypergeometric series $F(a, b, c, \xi)$ does not terminate and converges for $\xi = 1$ only if $\text{Re}(a + b - c) < 0$, i.e. from (5b) and (6), if $\text{Re}(\gamma) < \frac{1}{2}$. In every special case in which we are concerned with discrete eigenvalues it must be impossible to fulfil this inequality so that we must choose for a or b a negative integer $-n$ ($n = 0, 1, 2, \dots$). Otherwise we would not have a quantum number. For $a = -n$ we obtain according to (5b) and (6)

$$\beta = -n - \alpha - \gamma, \quad \beta' = n + \alpha + \gamma - 1/h \quad \dots\dots(14a)$$

and for $b = -n$

$$\beta = n + \alpha + \gamma - 1/h, \quad \beta' = -n - \alpha - \gamma. \quad \dots\dots(14b)$$

Since the constants β and β' enter symmetrically in our formulae we get the same final results for both the cases $a = -n$ and $b = -n$.

We must apply a similar procedure in case (II). Here the behaviour of $F_1(a', c', \xi)$ for $\xi \rightarrow +\infty$ is given by the semiconvergent expansion (Sommerfeld 1939)

$$F_1(a', c', \xi) = \frac{\Gamma(c')}{2\Gamma(c' - a')} (-\xi)^{a'} G(a', c' - a' - 1, 1/\xi) \\ + \frac{\Gamma(c')}{2\Gamma(a')} \xi^{a' - c'} e^{\xi} G(a' - 1, c' - a', -1/\xi),$$

where $G(a, b, \xi) = 1 + \frac{ab}{1!} \xi + \frac{a(a+1)b(b+1)}{2!} \xi^2 + \dots$

In order that the integrals (13) may converge for real values of ξ , we must therefore assume $a' = -n$ which gives us a discontinuous eigenvalue spectrum. In the case of continuous eigenvalues the variable ξ and hence also κ must be imaginary. In § 4 we shall show by an example how to treat such a case.

We can use formulae (7) and (12) also for the determination of the limits of applicability of Sommerfeld's polynomial method (cf. Rubinowicz 1949 a). Having given p and ρ we can determine, from these formulae, the functions q for which an eigenvalue problem (1) can be solved.

Finally we remark that, instead of the special functions (I) and (II) suggested by Sommerfeld's original method, we can also take for P other solutions of the differential equations (5) or (10). Such a procedure of course cannot change the equations for our constants but it will in general require us to take other values of the solutions of these equations in order that the integrals (13) may be convergent. It will also be necessary to replace the equations (14) or the equation $a' = -n$ by other equations representing Sommerfeld's condition for the breaking off for the special P -functions we use.

It is clear that for non-degenerate eigenvalues we obtain, by this method, the same eigenfunction for a given eigenvalue as in the case of the P -functions (I) or (II), since according to our assumptions these functions are uniquely determined. The advantage of using P -functions other than (I) or (II) is that we can obtain the eigenfunctions in different forms containing, for example, a polynomial in descending powers of ξ .

§ 3. ASSOCIATED LEGENDRE FUNCTIONS

An example of an eigenvalue problem in a finite fundamental interval (case (I)) is that for the associated Legendre functions. Its differential equation is given by

$$\frac{d}{dx} \left((1-x^2) \frac{df}{dx} \right) - \left(\frac{m^2}{1-x^2} - \lambda \right) f = 0,$$

where m is an integer. We have therefore here the differential equation (1) with

$$p = 1 - x^2, \quad \rho = 1, \quad q = m^2/(1-x^2). \quad \dots\dots (15)$$

The boundary points of the fundamental interval of this eigenvalue problem are the singular points of our differential equation situated at $x = \pm 1$.

If we put (15) into equation (7) and split into partial fractions in the variable x , we get

$$-\frac{m^2-1}{(1-x^2)^2} + \frac{m^2+\lambda-1}{1-x^2} - \lambda \\ = h^2 \left[-\frac{\gamma(\gamma-1)}{(1-\xi)^2} + \frac{-\alpha(\alpha-1/h) + \beta(\beta+1/h) + \gamma(\gamma-1)}{1-\xi} - \beta(\beta+1/h) \right].$$

Hence using (3) we have $\xi = x^2$ so that

$$h=2, \quad \kappa=1 \quad \dots\dots(16)$$

and therefore

$$\begin{aligned} 4\gamma(\gamma-1) &= m^2-1, & 4\beta(\beta+\tfrac{1}{2}) &= \lambda, \\ 4[-\alpha(\alpha-\tfrac{1}{2}) + \beta(\beta+\tfrac{1}{2}) + \gamma(\gamma-1)] &= m^2 + \lambda - 1. \end{aligned}$$

From these equations it follows that

$$\alpha(\alpha-\tfrac{1}{2})=0 \text{ so that } \alpha=0 \text{ or } \alpha=\tfrac{1}{2}, \quad \dots\dots(17a)$$

$$\lambda=l(l+1) \text{ if we put } 2\beta=l, \quad \dots\dots(17b)$$

$$\gamma=(m+1)/2 \text{ for } m \geq 0, \quad \dots\dots(17c)$$

because $\gamma=(-m+1)/2$ with $m>0$ would yield a function f with singular points at $x=\pm 1$ and hence an infinite normalization integral (13).

Since, according to (17a) and (17c), α and γ are integers or half odd integers and n is an arbitrary integer, the numbers $l=2\beta$ are, according to (14b), arbitrary integers. Hence the eigenvalues $\lambda=l(l+1)$ are determined.

In order to get the eigenfunctions we must calculate the constants a, b, c . From (5b), (16) and (17) it follows that

$$a=(l+m+1)/2+\alpha, \quad b=-(l-m)/2+\alpha, \quad c=2\alpha+\tfrac{1}{2}.$$

According to (2), (I) and (15) we obtain therefore the eigenfunctions

$$f=x^{2\alpha}(1-x^2)^{m/2}F\left(\frac{l+m+1}{2}+\alpha, -\frac{l-m}{2}+\alpha, 2\alpha+\tfrac{1}{2}, x^2\right) \quad \dots\dots(18)$$

where α is equal to 0 or $\frac{1}{2}$ according as $(l-m)$ is an even or odd integer. We obtain (17b) and (18) also, if we put $2\beta=-l-1$.

Equation (18) represents the associated Legendre functions apart from a constant factor. We can see this by using the relation

$$\begin{aligned} F(a, b, c, z) &= \frac{\Gamma(c)\Gamma(a-b)}{\Gamma(b)\Gamma(a-c)} (-z)^{-a} F(a, 1-c+a, 1-b+a, 1/z) \\ &+ \frac{\Gamma(c)\Gamma(b-a)}{\Gamma(a)\Gamma(b-c)} (-z)^{-b} F(b, 1-c+b, 1-a+b, 1/z) \quad \dots\dots(19) \end{aligned}$$

which, when a or b is a negative integer (when $\Gamma(a)$ or $\Gamma(b)=\infty$) transforms a hypergeometric polynomial in ascending powers into one in descending powers. Applying (19) to (18), we get the well-known formula

$$P_l^m(x) = \frac{(-1)^m(2m)!}{2^l l! (l-m)!} x^{l-m} (1-x^2)^{m/2} F\left(-\frac{l-m}{2}, -\frac{l-m-1}{2}, -l+\tfrac{1}{2}, 1/x^2\right)$$

for the Legendre functions.

We can also obtain this expression directly if we put the values (16) and (17) for our constants into the P -function

$$P=\xi^{-\beta'-\gamma}(1-\xi)^\gamma F(\alpha+\beta'+\gamma, \alpha'+\beta'+\gamma, 1+\beta'-\beta, 1/\xi).$$

This is possible because either $\alpha+\beta'+\gamma$ or $\alpha'+\beta'+\gamma$ is in our case a negative integer and therefore the above P -function is regular in the fundamental interval given by $\xi=x^2=1$. The fact that the same values of the constants which we used formerly are applicable also in case of our new P -function is due to its special choice.

§ 4. RADIAL FUNCTIONS OF A NON-RELATIVISTIC ONE-ELECTRON ATOM

This is an example of an infinite fundamental interval. Equation (1) is here given by

$$\frac{1}{x^2} \frac{d}{dx} \left(x^2 \frac{df}{dx} \right) + \left[\frac{2m}{\hbar^2} \left(E + \frac{Ze^2}{x} \right) - \frac{l(l+1)}{x^2} \right] f = 0, \quad \dots\dots (20)$$

Since $x=0$ is a singular point of (20) we must take the fundamental interval from $\xi=0$ to $\xi=+\infty$.

A comparison of (20) with (1) gives

$$p = \rho = x^2, \quad \lambda = \frac{2m}{\hbar^2} E, \quad q = -2x/a_1 + l(l+1), \quad \dots\dots (21)$$

where $a_1 = \hbar^2/m\mathbf{e}^2Z$ is the radius of the first Bohr orbit.

With regard to (12) we have therefore

$$-l(l+1) + 2x/a_1 + \lambda x^2 = \hbar^2 \left[-\alpha(\alpha-1/\hbar) + (\alpha - a' + \frac{1}{2} - 1/2\hbar)\xi - \xi^2/4 \right].$$

Hence in accordance with (3)

$$h = 1, \quad \xi = \kappa x,$$

and therefore

$$l(l+1) = \alpha(\alpha-1), \quad \dots\dots (22 a)$$

$$2/a_1 = (\alpha - a')\kappa, \quad \dots\dots (22 b)$$

$$\lambda = -\kappa^2/4. \quad \dots\dots (22 c)$$

From (22 a) it follows that $\alpha = l+1$ so that, since $a' = -n$, we have $\alpha - a' = n + l + 1$. We get, therefore, according to (22 b),

$$\kappa = 2/(n + l + 1)a_1. \quad \dots\dots (23)$$

For the eigenvalues of E we thus obtain, using (21) and (22 c), the well-known Balmer formula. The eigenfunctions of (20) are given according to (II), (9), $a' = -n$, $\alpha = l+1$ and $h=1$ by

$$f = x^l \exp(-\kappa x/2) F_1(-n, 2l+2, \kappa x)$$

where κ is given by (23).

In order to get positive values for E and λ the constant κ must, by (22 c) be imaginary. If we put $\kappa = \pm 2ik$ then according to (22 b) we have $\alpha - a' = \mp i/ka_1$ and hence using $\alpha = l+1$ we have $a' = l+1 \pm i/ka_1$. We get therefore for the eigenfunctions f in the continuous eigenvalue spectrum the expression

$$f = x^l \exp(\mp ikx) F_1(l+1 \pm i/ka_1, 2l+2, \pm 2ikx),$$

$k/2\pi$ being the wave number at infinity.

REFERENCES

- RUBINOWICZ, A., 1949 a, *Proc. Acad. Amsterdam*, **52**, 351, or *Indagationes Math.*, **11**, 125;
1949 b, *Proc. Phys. Soc. A*, **62**, 736.
SOMMERFELD, A., 1939, *Atombau und Spektrallinien*, Bd. II (Braunschweig: Vieweg und Sohn).

Investigation of the Spectrum of the High Voltage Arc in Carbon Dioxide: the CO Flame Spectrum

BY M. W. FEAST*
Imperial College, London

MS. received 21st December 1949

ABSTRACT. The spectrum emitted by a high voltage arc in CO_2 at atmospheric pressure has been investigated in the region 2000 Å. to 9000 Å. It was found to consist, mainly, of a continuum and the 'CO flame bands'. A study of the spectrum at different dispersions and on photographic plates of various kinds shows that although the Schumann-Runge O_2 bands do form a part of the spectrum they are relatively weak compared with the bands attributed to CO_2 . The excitation of the Schumann-Runge O_2 system in flames is discussed.

§ 1. INTRODUCTION

AN earlier paper (Feast 1949) described a high voltage, low current arc and also discussed the use of this source in the investigation of the spectrum of the O_2 molecule. More recently the arc source has been used in the investigation of other gases, viz. N_2 , H_2 , $\text{N}_2\text{-H}_2$ mixtures, and NH_3 (Feast 1950). In continuation of these investigations the spectrum emitted by carbon dioxide in the arc source has now been studied and the results obtained are discussed in the present paper. Experiments on carbon dioxide are of particular interest at this time as there is some controversy over the question of the identity of the spectrum emitted by the CO-O_2 flame. This spectrum has usually been attributed to CO_2 (see Gaydon 1948 and references given there). Recently, however, it has been suggested that the major part, if not the whole, of this spectrum may simply be the emission Schumann-Runge O_2 band system (Hornbeck 1948, Hornbeck and Hopfield 1949). The fact that the Schumann-Runge bands were found to be so easily excited in the high voltage arc in oxygen at atmospheric pressure and to be so sensitive to the pressure of the gas (Feast 1949) made a study of carbon dioxide in this source even more interesting.

§ 2. EXPERIMENTAL

The arc source used in the investigation of oxygen was again used in these experiments. The arc was struck between wires of a platinum-rhodium alloy in a litre 'Pyrex' flask containing the gas. Small dispersion spectrograms of the arc in CO_2 at atmospheric pressure were taken on medium contrast plates with a Hilger E.3 spectrograph. Apart from some weak CO Third Positive bands and a few lines (oxygen, carbon, platinum and rhodium) the spectrum consisted solely of an apparent continuum stretching from the ultra-violet region to the infra-red region. By using a prism-grating spectrograph it was possible to follow the continuum as far as 9000 Å. When photographic plates of higher contrast were employed it was found that in the region 3000 Å. to 5000 Å. there

* Now at the National Research Council, Ottawa, Canada.

was a large number of bands superimposed on the continuum. By a comparison with Gaydon's published spectrograms they were identified as the CO flame bands. An investigation of the spectrum at various pressures showed that the flame bands decreased rapidly in intensity as the gas pressure was reduced and that they gave way to the normal low pressure discharge type CO spectrum. It should be noted that the appearance of the CO flame spectrum thus found is very different from the appearance of the Schumann-Runge O₂ bands photographed with the same spectrograph from the arc in oxygen.

Following on the low dispersion work the region 3000 Å. to 5000 Å. was investigated with a 10 ft. Eagle Mounting grating. Using high contrast (process) plates the Schumann-Runge bands were found and nothing else appeared to be present. These bands were easily identified by comparison with those obtained in the oxygen investigation. However, using low contrast plates (Ilford Zenith) the band lines were lost in continuum.

§ 3. DISCUSSION OF OBSERVATIONS

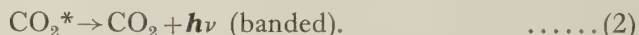
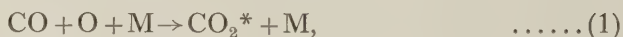
In order to discuss these observations it is necessary first to review briefly the present state of the work on the CO flame bands. These bands have usually been studied in the spectrum of the CO-O₂ flame. A summary of all but the most recent work on these bands is given by Gaydon (1948). The conclusion reached by Gaydon and others was that the bands were to be attributed to a CO₂ electronic band system. However the analysis of the band system could not be made with sufficient accuracy for this assignment to be quite definite. Other possible emitters such as C₃O₂ and CO₃ were considered unlikely whilst the spectrum appeared too complex to be assigned to any diatomic emitter. Quite recently, on the other hand, it has been suggested (Hornbeck 1948, Hornbeck and Hopfield 1949) that the major part if not all of the flame bands are to be attributed to the Schumann-Runge O₂ band system. High dispersion spectrograms of CO-O₂ flames and explosions have revealed the emission Schumann-Runge bands and also (in the infra-red region) emission bands belonging to the the same system as the O₂ atmospheric absorption bands.

The present low dispersion spectrograms of CO₂ in the high voltage arc show little or no resemblance to the Schumann-Runge bands emitted by O₂ in the same source. Besides the other differences in the two spectra it is important to notice that though the rotational line structure of the Schumann-Runge bands is reasonably clear even on Hilger E.3 spectrograms, the flame bands are diffuse and without trace of fine structure. Hence if the Schumann-Runge system is emitted even weakly by the arc in CO₂ it will dominate the spectrum at high dispersion (especially with high contrast plates) for, as is well known, the apparent intensity of a continuum or quasi-continuum falls rapidly compared with the apparent intensity of a resolved line as the dispersion of the spectrum is increased. It should be noted that the differences between the high voltage arc spectra of O₂ and CO₂ cannot be attributed to differences in rotational or vibrational intensity distributions in the two cases since the high dispersion work shows that the structure of the Schumann-Runge bands is the same in the two spectra.

Gaydon and Wolfhard (1949) state that the CO flame spectrum is emitted from a different part of the CO-O₂ flame from the Schumann-Runge bands. In the arc however no such separation of the various spectra was observed.

§ 4. EMISSION MECHANISMS FOR THE CO FLAME AND THE SCHUMANN-RUNGE BANDS

In attributing the CO flame bands to CO₂ Gaydon has suggested a mechanism for their emission. The normal state of CO₂ is not formed from CO and O in their ground states CO(¹Σ) and O(³P) but probably from CO(a³Π) and O(³P). Since there is no evidence for excited states of CO in flames, Gaydon concludes that the CO₂ is formed from normal CO(¹Σ) and O(³P) giving an excited state of CO₂. The transition from this excited state to the ground state gives the flame bands according to this theory. Thus if M is a third body we have :



There is nothing in this theory to disagree with the present observations on the high voltage arc. Indeed the flame bands would be expected to occur quite strongly in the arc since this mechanism is very similar to the one used to explain the pressure dependence of the Schumann-Runge bands (Feast 1949). The fact that a similar pressure sensitivity has been found for the flame bands indicates a similarity in excitation mechanism and tends to strengthen both theories.

It may be noted that the presence of the Schumann-Runge bands in flame spectra may be expected if the emission process for the system is considered. The emission mechanism suggested by the author involves a three-body collision resulting in the recombination of an O(³P) atom with a O(¹D) atom into the upper state of the band system. Since it is known that there is a considerable concentration of oxygen atoms in flames (Gaydon 1948) it seems likely that some proportion of these will be in the O(¹D) state. This state is metastable and hence there will be only a very small depopulation of the state due to radiative return to the ground state. Furthermore, the state is only 1.96 ev. above the ground state. Thus the excitation of the system by this mechanism does not require the large amount of energy (6.09 ev.) needed if the system is directly excited and hence the appearance of the system in a source of low excitation such as a flame is more readily understood. This process is further supported by the fact that since Gaydon and Wolfhard (1949) find the Schumann-Runge bands in H₂-O₂ flames also, it must be concluded that only oxygen is involved in the emission mechanism.

ACKNOWLEDGMENTS

The author wishes to express his sincere thanks to Professor R. W. B. Pearse for his helpful interest in this problem. The work was made possible by the award of a grant from the Department of Scientific and Industrial Research.

REFERENCES

- FEAST, M. W., 1949, *Proc. Phys. Soc. A*, **62**, 114; 1950, *Ibid.*, **63**, 563.
 GAYDON, A. G., 1948, *Spectroscopy and Combustion Theory* (London : Chapman and Hall).
 GAYDON, A. G., and WOLFARD, H. G., 1949, *Nature, Lond.*, **164**, 22.
 HORNBECK, G. A., 1948, *J. Chem. Phys.*, **16**, 845, 1005.
 HORNBECK, G. A., and HOPFIELD, H. S., 1949, *J. Chem. Phys.*, **17**, 982.

LETTERS TO THE EDITOR

Radioactive ^{165}Er

There is no stable erbium isotope of mass number 165. Pool and Quill (1938) bombarded erbium with fast neutrons and found a positron activity with a half-life of 1.1 min., for which a tentative assignment to ^{165}Er was suggested. There was, however, no direct evidence for the chemical identity or mass number.

To prepare ^{165}Er by the reaction $^{165}\text{Ho}(p, n)^{165}\text{Er}$, 5 mg. of holmium oxide of over 99.97% purity was bombarded with 10 mev. protons. Erbium carrier was then added and a chemical purification of the rare earth mixture from radioactive contaminants made. The erbium was then isolated by means of an ion-exchange column of the type described by Ketelle and Boyd (1947).

The radioactivity of the erbium decayed entirely with a half-life of 10.0 ± 0.1 hrs. The decay was measured, by means of a thin window (1.9 mg. cm^{-2}) Geiger counter, over a period of ten half-lives.

Experiments in a magnetic deflection device failed to indicate any electrons or positrons in the radiation, which was entirely electromagnetic.

Measurements of the absorption of the electromagnetic radiation in aluminium showed two components with energies of 6.6 kev. and 52 kev. Absorption measurements of the harder component in copper gave a value of 47 kev. These values agree well with those for the L and K x-radiations of holmium. There was no harder gamma-radiation. The isotope ^{165}Er therefore decays purely by orbital electron capture.

The author wishes to thank the members of the Cyclotron Group for carrying out the irradiation.

Atomic Energy Research Establishment,
Harwell, Berks.
7th May 1950.

F. D. S. BUTEMENT.

KETELLE, B. H., and BOYD, G. E., 1947, *J. Amer. Chem. Soc.*, **69**, 2800.
POOL, M. L., and QUILL, L. L., 1938, *Phys. Rev.*, **53**, 437.

Proton Capture Radiation of Fluorine-19

When ^{19}F captures a proton of low energy, it is well known that the compound nucleus of ^{20}Ne which is formed has an excess energy of 13 to 14 mev. which may be emitted in the form of gamma-radiation. The most probable process, however, for the decay of this excited nucleus is the emission of an alpha-particle. This process usually leaves the residual ^{16}O nucleus in an excited state which subsequently emits gamma-radiation of about 6 mev. The yield of gamma-radiation due to the decay of ^{20}Ne to the ground state is likely to be small compared to that of 6 mev. radiation, and Walker and McDaniel (1948), who searched for energetic gamma-rays with a pair spectrometer, were unable to detect any such hard radiation. They stated that this radiation, if it existed, had an intensity of less than 0.3% of that of the 6 mev. gamma-rays accompanying the alpha-decay for a thick target bombarded with protons of energy 1,150 kev.

Devons and Hereward (1948) made a search for this hard gamma-radiation, using the photo-nuclear effect in ^{63}Cu , which has a threshold at about 11 mev., and found that gamma-rays having energy sufficient to activate the Cu were emitted at a proton bombarding energy of 660 kev., a value agreeing with that for the short-range alpha-particle resonance. These authors, who were using a thick target, found that the intensity of the hard radiation increased only very slowly as the bombarding energy was increased from 700 to 960 kev., and certainly possessed no further detectable resonances in this region. They estimated the intensity of the radiation from the 660 kev. resonance, which they assumed to be of energy 13.4 mev., corresponding to a transition to the ground state of ^{20}Ne , to be $2.2 \pm 0.8\%$ of the intensity of the 6 mev. radiation from that resonance.

In view of the results of Devons and Hereward, we have used a pair spectrometer to search for hard gamma-rays from this reaction using a thinner target than that of Walker

and McDaniel, and a proton bombarding energy corresponding to the 660 kev. resonance. The H.T. set at Glasgow consists of an 800 kev. cascade generator, with an accelerator tube and a high-frequency ion source. Magnetically resolved proton beams of about $100\ \mu\text{a}$. were used. The targets had a stopping power of about 50 kev. and were prepared by

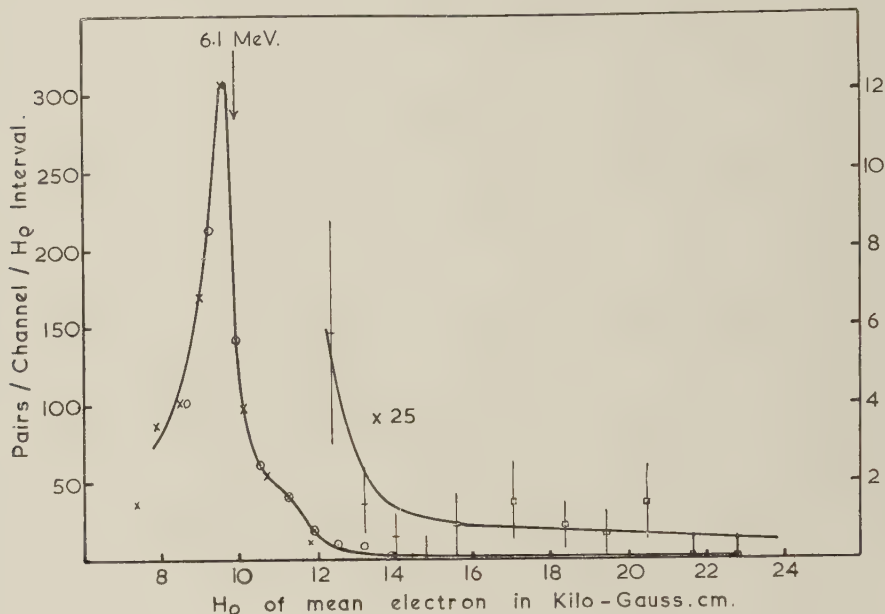


Figure 1. Gamma-rays from $^{19}\text{F} + \text{p}$, 340 kev. resonance.

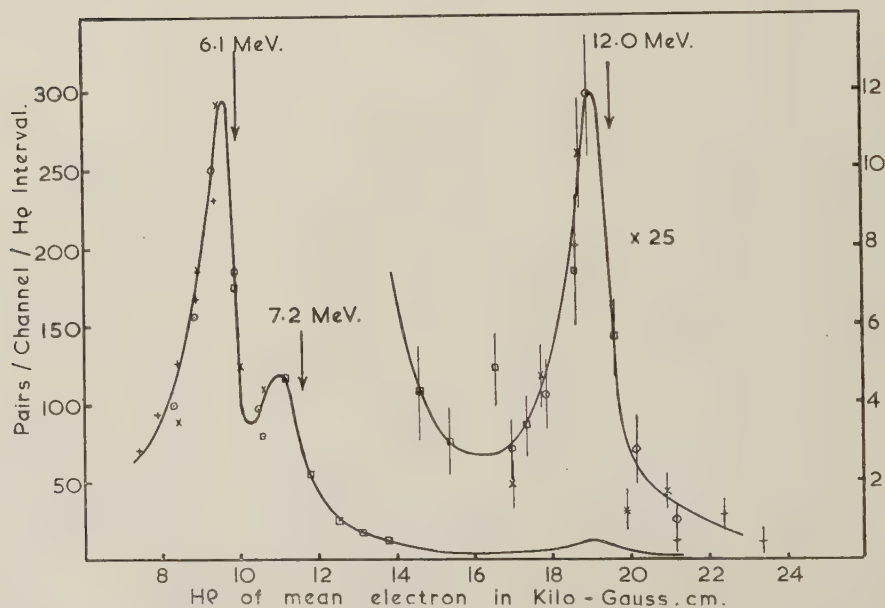


Figure 2. Gamma-rays from $^{19}\text{F} + \text{p}$, 660-kev. resonance.

evaporation of calcium fluoride on to a brass plate. Energy measurements were made with a pair spectrometer which is similar to that described by Walker and McDaniel, but which has ten counters placed in the field of a twelve-inch electromagnet. The electron pairs were produced in a lead sheet of thickness 0.0015 inch. Typical spectra obtained under these conditions are shown in Figures 1 and 2. At the 340 kev. resonance (Figure 1) it will be

seen that there is a strong gamma-ray component having an energy of about 6 mev. together with a very weak component at about 7 mev. Above this energy no further gamma-ray lines are evident. Figure 2 shows the spectrum of the radiation emitted at the 660 kev. resonance, and here it will be seen that the 7 mev. component has become appreciable, and that there has also appeared a weak line having an energy which has been determined as 12.0 ± 0.2 mev. by comparison with the ${}^7\text{Li}(p, \gamma)$ radiation. The intensity of the 12 mev. line has been estimated as 2% of that at 6 mev., which is in good agreement with the results of Devons and Hereward. It should also be noted that this value is not in contradiction with the findings of Walker and McDaniel, since their value of less than 0.3% of the intensity of the 6 mev. radiation was determined for a bombarding energy of 1,150 kev. With this high bombarding energy and a thick target, the intensity of the 6 mev. radiation would be about 15 times as great as that due to the 660 kev. resonance alone (Bonner and Evans 1948), while the intensity of the capture radiation is known to increase very little when the bombarding energy is increased from 700 to 960 kev. (Devons and Hereward 1948). For bombarding energies between 960 and 1,150 kev. there are two weak gamma-ray resonances which contribute only about 1.5% to the total output of gamma-rays (Bonner and Evans), and so unless these two resonances produce a high proportion of capture radiation, it is unlikely that its intensity, for a bombarding energy of 1,150 kev., exceeds the figure of 0.3% given by Walker and McDaniel.

The most interesting feature of the present experiment, however, is the determination of the energy of the capture radiation as 12.0 mev. This suggests that the radiation is not due to a transition to the ground state of ${}^{20}\text{Ne}$ as supposed by Devons and Hereward, but is emitted during a transition to some intermediate level which is about 1.4 mev. above the ground state as shown in Figure 3. There seem to be good grounds for this interpretation

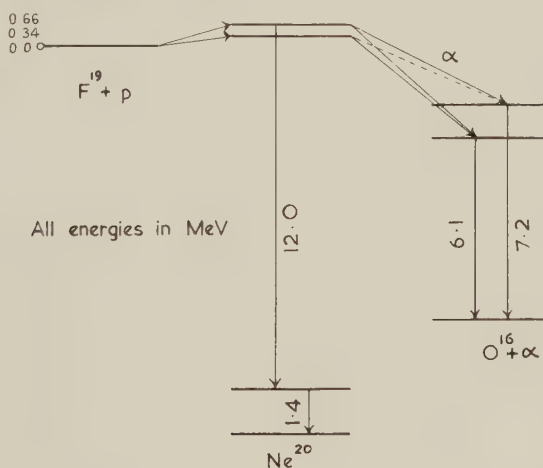


Figure 3. Energy-level diagram, ${}^{19}\text{F} + p$.

of the experimental results, for such a state has already been detected as a result of the study of other reactions (Curran and Strothers 1940, Powell 1943, Powell, May, Chadwick and Pickavance 1940).

Department of Natural Philosophy,
University of Glasgow.
26th April 1950.

E. R. RAE.
J. G. RUTHERGLEN.
R. D. SMITH.

- BONNER, T. W., and EVANS, J. E., 1948, *Phys. Rev.*, **73**, 666.
CURRAN, S. C., and STROTHERS, J. E., 1940, *Proc. Camb. Phil. Soc.*, **36**, 252.
DEVONS, S., and HEREWARD, H. G., 1948, *Nature, Lond.*, **162**, 331.
POWELL, C. F., 1943, *Proc. Roy. Soc. A*, **181**, 344.
POWELL, C. F., MAY, A. N., CHADWICK, J., and PICKAVANCE, T. G., 1940, *Nature, Lond.*, **145**, 893.
WALKER, R. L., and MCDANIEL, B. D., 1948, *Phys. Rev.*, **74**, 315.

Isotope Effect in Superconductivity

In a paper recently submitted for publication it has been shown that investigation of the 'self-energy' of the free electrons of a metal in the vibrational field of the lattice leads to a quantitative understanding of superconductivity. So far the theory has been developed for the absolute zero of temperature only; there the energy difference between the superconducting and the normal state is

$$|S| = c_1 \frac{C^2 m n_{el}}{\zeta M},$$

where $c_1 \simeq 0.1$, m and M are the electronic and ionic mass respectively, ζ is the kinetic energy of the fastest of the n_{el} free electrons and C is an energy connected with the interaction between an electron and the displaced lattice. Using the empirical fact that apart from a numerical factor $|S|$ is equal to the thermal energy of the free electrons in the normal state at the transition temperature T_0 , i.e.

$$|S| = \frac{c_2 (kT_0)^2 n_{el}}{\zeta}$$

(c_2 is a numerical constant), it follows that

$$kT_0 = \left(\frac{m}{M} \frac{c_1}{c_2} \right)^{1/2} C.$$

For different isotopes of the same element C has the same value, so that $kT_0 \propto 1/\sqrt{M}$. This is in excellent agreement with the experiments by Reynolds *et al.* (1950) and Maxwell (1950) on mercury which have just come to my notice. This agreement forms a direct check on the basic idea of the theory: interaction between electrons and lattice vibrations.

Department of Theoretical Physics,
University of Liverpool.
19th May 1950.

H. FRÖHLICH.

MAXWELL, E., 1950, *Phys. Rev.*, **78**, 477.

REYNOLDS, C. A., SERIN, B., WRIGHT, W. H., and NESBITT, L. B., 1950, *Phys. Rev.*, **78**, 487.

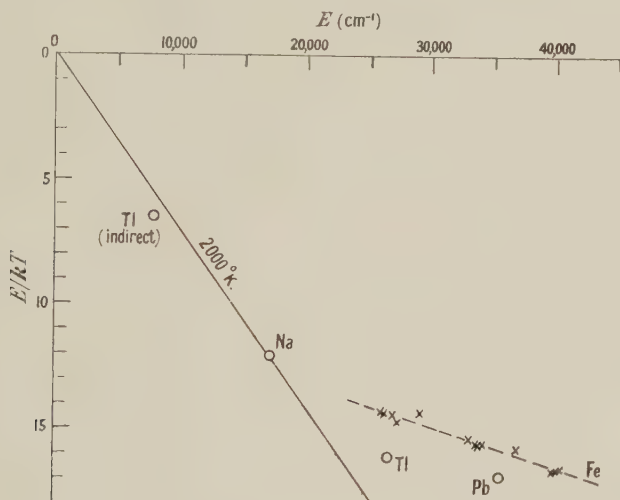
Excitation of Spectra in the Inner Cones of Flames

Flames of most organic compounds premixed with air or oxygen show a relatively bright inner cone, corresponding to the reaction zone of the flame. The luminosity is no doubt partially confined to this region because active radicals emitting the light, such as C_2 and CH , are only present here, and also in some cases molecules may be formed in electronically excited states by the chemical processes. However, we have recently accumulated evidence showing that there is some active species present in the reaction zone which causes abnormally high excitation of inert atoms introduced into the flame.

We have studied the effect by means of the spectrum-line reversal method, using a carbon arc with adjustable sector as background. Most of the work has been done on flames at very low pressure, because these can be made to give a thick flat reaction zone (Gaydon and Wolfhard 1948, 1949). When a metal vapour such as Fe (as iron carbonyl) or Pb (as lead ethyl) is introduced it is found that most of the lines of the spectrum are obtained in emission even against the background of the full light of the arc (around 3,800° K.), but that resonance lines may be reversed. The reversal temperatures are usually much higher than the expected flame temperature, and lines of short wavelength give higher temperatures than lines of longer wavelength. Results for various resonance lines for an acetylene-air flame at 24 mm. Hg pressure are tabulated.

Line	Reversal temp. ($^{\circ}$ K.)	E/kT	Line	Reversal temp. ($^{\circ}$ K.)	E/kT
Na 5890.6	2010	12.1	Fe 2983.5	3050	15.7
Fe 3859.9	2565	14.4	Fe 2966.9	3068	15.7
Fe 3824.4	2580	14.45	Fe 2936.9	3100	15.7
Tl 3775.7	2350	16.2	Pb 2833.0	2970	17.0
Fe 3719.9	2650	14.5	Fe 2719.0	3310	15.9
Fe 3679.9	2630	14.8	Fe 2522.8	3365	16.8
Fe 3440.6	2880	14.4	Fe 2501.1	3410	16.75
Fe 3020.6	3058	15.5	Fe 2483.3	3450	16.7

The actual observation is of the effective temperature corresponding to the ratio of the populations of atoms in the ground and excited electronic states. This may be represented by the value of $-E/kT$, which is equal to the natural logarithm of the ratio of populations in the ground state and excited states; E is the energy of the excited state expressed in cm^{-1} , and k is the Boltzmann constant. In the Figure the values of E/kT are plotted against E .



For equilibrium the points should lie on a straight line passing through the origin, the slope giving the temperature. Clearly there is a major departure from equilibrium. The actual flame temperature from reversal measurements just above the reaction zone appears to be about $2,000^{\circ}$ K. For energies below about $18,000 \text{ cm}^{-1}$ the excitation may be mainly due to thermal causes, but at higher energy the population is much higher than could be accounted for thermally, and indeed the value of E/kT for the Fe lines varies surprisingly little with E . The extent of the abnormal excitation appears to vary from element to element, Pb and Tl being less highly excited than Fe. The low slope of the graph at high E explains the extremely high apparent temperatures for non-resonance lines. The Tl green line at 5350 \AA , which is not a true resonance line, reverses at $2,750^{\circ}$ K.; by combining this value with that for Tl 3775, which has the same initial level, we obtain E/kT for the lower level of the $5,350$ line at 7793 cm^{-1} .

The amount of energy available for the abnormal excitation in these flames is surprisingly high. The emission lines of Fe I from the flames of C_2H_2 , C_2H_6 and CH_3OH have an intensity distribution very similar to that in an iron arc. Lines requiring an excitation energy up to at least $60,757 \text{ cm}^{-1}$ occur, corresponding to 174 kcal/mole . It is very difficult to find any chemical reaction liberating this amount of energy. No lines of Fe II have been observed.

The effect is shown by the reaction zones of all the organic flames we have studied (C_2H_2 , C_2H_6 , CH_4 , CH_3OH) except formaldehyde. Flames of hydrogen and carbon monoxide do not show abnormally high excitation. Flames of organic compounds supported by N_2O show the effect, but not as strongly as flames with air or O_2 . The effect occurs at atmospheric as well as at low pressure, although we have not succeeded in making

quantitative measurements at 1 atmosphere; the measured reversal temperatures do not vary much with pressure in the range 10 to 200 mm. Hg. Diffusion flames of the type studied by Wolfhard and Parker (1949) at atmospheric pressure do not show abnormally high excitation; at very low pressure even diffusion flames show high excitation, probably because of the rapid mixing by diffusion under these conditions. In the pre-mixed flames the effect is most pronounced for slightly rich mixtures, but it decreases surprisingly slowly on the side of lean mixtures.

Imperial College,
London, S.W. 7.
5th May 1950.

A. G. GAYDON.
H. G. WOLFHARD.

GAYDON, A. G., and WOLFHARD, H. G., 1948, *Proc. Roy. Soc. A*, **194**, 169; 1949, *Ibid.*, **199**, 89.
WOLFHARD, H. G., and PARKER, W. G., 1949, *Proc. Phys. Soc. A*, **62**, 722.

CORRIGENDA

"The Angular Distribution of Synchrotron Target Radiation: A Preliminary Experimental Study", by J. D. LAWSON (*Proc. Phys. Soc. A*, 1950, **63**, 653).

Page 654, line 25 should begin $\sqrt{2\mu/E}$ instead of $\sqrt{z\mu/E}$.

Page 659, equation (1) should read

$$F(t, \theta) = \frac{E^2}{440\pi t} \exp(-E^2\theta^2/440t).$$

Insert under Figure 1:

The values of t shown on the diagram should be multiplied by 2.

REVIEWS OF BOOKS

Ions, Electrons and Ionizing Radiations, by J. A. CROWTHER. Pp. ix+322+7 plates. 8th Edition. (London: Edward Arnold and Co., 1949.) 21s.

The preface to the eighth edition of this well-known book states that it is intended to be "a textbook from which students who have been grounded in the more elementary portions of physics might obtain a systematic knowledge of its later developments"; the level of the students is said to be that of the second year of a pass degree course. The previous editions have introduced to a whole generation of students the subjects of Atomic and Nuclear Physics and the book has been deservedly popular with this past generation because of the clear style in which it is written and the interesting manner of presentation. These characteristics of Professor Crowther's writings are, of course, present in the new edition, but the present reviewer considers that the book does not fulfil its stated purpose for the new, post-war, generation of students.

One, to some extent, admirable feature of the book is the description of 'classical' experiments and apparatus. However, this is grossly overdone; it should be possible to retain the more important of these descriptions while giving accounts of modern apparatus and methods, which are just as easy to understand. This would give a much better balance between a historical description of the subject and a logical one—that is, a better balance judged from the standpoint of our present knowledge of Atomic and Nuclear Physics. Another modification which is necessary in order to achieve this better balance is in the amount of space allotted to the various subjects. Too much space is devoted to a subject like 'the conduction of electricity in gases', whose importance is historical and technical,

and too little is given to such fundamental topics as 'the structure of the atom' and 'the physics of the nucleus'. The present reviewer believes that the book would be improved if it were substantially revised so as to strike a new balance along the lines indicated above.

There are also many serious errors and misleading accounts, particularly in the chapters on the nucleus and related subjects. Professor Crowther describes the Geiger counter for detecting single β -particles as a 'point' counter. If the neutrino is to be discussed, it is surely possible in a book written in 1949 to give a brief account of the experiments of Sherwin and of Allen, rather than mention only the twelve-year-old cloud chamber work of Crane and Halpern, which Professor Crowther describes as recent. The section on the properties of the meson could have been written much better in 1949. It is certainly not correct to describe the ${}^2_1\text{D}(d, n){}^3_2\text{He}$ reaction as "by far the most prolific source of neutrons". Professor Crowther should have known that the 184 m. cyclotron at Berkeley has been working for two years now, and that the difficulties associated with variation of mass with velocity have been overcome by frequency modulation and not, as he implies, by shaping the pole pieces of the cyclotron magnet. Another error which is inexcusable is the statement that the half-value periods of RaC' , ThC' and AcC' are 10^{-8} second or less. It has been known for at least ten years that the half-value periods are 1.5×10^{-4} sec., 3×10^{-7} sec., and 5×10^{-8} sec., respectively.

This is only a small selection of the errors and misleading accounts in which the book abounds. Most of them occur in the sections on more recent work and the net result is to give the impression that there has been no serious attempt to bring the book up to date. It is, therefore, with regret that the present reviewer feels that he cannot recommend the eighth edition of this book.

J. DAINTY.

Materiewellen und ihre Interferenzen, by M. VON LAUE. Pp. 392. Second Edition. (Leipzig: Akademische Verlagsgesellschaft Geist and Portig K-G., 1948.)

Only a few copies of the first edition of Professor von Laue's book, published in 1943, reached this country. The second edition is therefore all the more welcome. The development of theoretical aspects of electron diffraction is due, in no small degree, to Professor von Laue and his collaborators, and all physicists interested in this subject are greatly indebted to the author for his masterly and comprehensive treatise.

The publication comes at a particularly appropriate time as experimental work is in full swing again after a lapse during the war years, and a survey of the outstanding problems will be a great help to the experimental physicist. It is also some ten years since the only other textbook on this subject was published, and an up-to-date account of all theoretical developments will satisfy a definite need.

The subject matter of the book can be divided into three main parts, an historical and a theoretical introduction, an account of the geometrical theory of the diffraction of electrons by crystals, and a study of the dynamical theory of diffraction. The diffraction of molecular rays and of neutrons is treated in a separate chapter. In the main the practical applications of electron diffraction are not dealt with—experimental results are considered only in so far as they have theoretical significance.

The preliminary sections, apart from an excellent historical survey, are concerned chiefly with quantum mechanics (Schrödinger theory and Dirac theory of the electron), and in particular with the Born theory of elastic and inelastic collisions. It is rather striking that the theory of inelastic collisions should have so little quantitative information to offer as to the probability of small energy losses, which are of particular interest, for example, in connection with the origin of Kikuchi lines or the intensity of the background in electron diffraction photographs. The position is unsatisfactory enough as regards atoms—where solids are concerned there seems to be no position at all. However, von Laue draws attention to some very interesting experiments on discrete energy losses of cathode rays after passing through thin films of solids, and it is from experiments of this type that one can hope to obtain the necessary information.

The section on the geometrical theory of diffraction contains a complete account of reciprocal lattice theory, effects of structure factor etc. The most important feature is a

comprehensive discussion of the effect of the external form of a small crystal on the structure of the intensity pattern in the reciprocal lattice. The theory of these 'shape factors', due to von Laue, has been of material assistance in the interpretation of electron diffraction patterns and will prove increasingly useful as the study of surface structure proceeds. The influence of crystal deformations on the diffraction pattern is also discussed, though somewhat briefly; it seems likely that such features, hitherto rather neglected, would be well worth further consideration.

Almost half the subject matter of the book is devoted to a discussion of the interaction of diffracted rays inside a crystal—the dynamical effects. The two-ray problem is worked out in detail, and a complete account is given of the many-ray problem. The use of the dynamical theory is well illustrated in a detailed discussion of the experiments of Kossel and Möllenstedt, in which special types of interference patterns are obtained in transmission (using convergent beams) through thin films of single crystals such as mica. Apart from checking many theoretical points, these experiments lead to the determination of the coefficients of the Fourier expansion of the potential of the crystal.

The last sections contain an account of the theory of Kikuchi lines developed by von Laue, together with an interpretation of the features of the structure of Kikuchi lines and bands. It appears from the discussion that there are still little-understood features, including, for example, the relative intensity of bands at widely separated angles.

From the point of view of experimental work on electron diffraction, the discussion of the mean electrostatic potential or 'inner potential' of a crystal is of particular interest. There are numerous experimental measurements of this quantity. von Laue shows that, ignoring surface effects, the potential inside a crystal is not constant except where there are special symmetry properties, e.g. for cubic crystals. The potential is shown to be determined by the components of the quadrupole moment tensor of the cell unit. What is however not made clear, is how large the deviations from a constant value are likely to be. This information might be obtained from the diamagnetic susceptibility of a solid, in certain cases, as the same tensor is formally involved here. In the case of quartz, for instance, the diamagnetic susceptibilities, parallel and perpendicular to the principal axis, do not differ by more than one per cent, and one would not expect appreciable variations of the 'inner potential'.

However, even in the case of cubic crystals, the surface distortions may, in von Laue's opinion, produce appreciable electrostatic fields. In fact, one might draw the conclusion that the experimental measurements of 'inner potential' have very little meaning, and the discrepancies in published values of the 'inner potential' for a given crystal are taken as evidence on this point. This is rather unfair to the experimental physicist, as the early—admittedly rough—values are given the same weight as later values. In particular, care has been taken in recent experiments using cathode rays to avoid conditions in which strong rays, other than the one used for the measurement, appear in the diffraction pattern—which covers one of the criticisms of the experimental work made by von Laue. All recent experimental values of the 'inner potential' of rocksalt, for instance, agree extremely well. The points raised by von Laue, particularly those on surface effects, do however need careful consideration by experimental workers, and further work will be required to see how important they are in practice.

Physicists concerned with electron diffraction will find Professor von Laue's book an indispensable guide to the theory. It possesses, in addition, the very rare feature of suggesting experiments on almost every aspect of the theory.

M. BLACKMAN.

CONTENTS FOR SECTION B

	PAGE
Prof. G. I. FINCH. The Sliding Surface (34th Guthrie Lecture)	465
Mr. J. CRANK. The Influence of Concentration-Dependent Diffusion on Rate of Evaporation	484
Mr. C. R. BARBER. The E.M.F.-Temperature Calibration of Platinum, 10% Rhodium-Platinum and Platinum, 13% Rhodium-Platinum Thermocouples over the Temperature Range 0°-1,760° C.	492
Dr. J. ASHMEAD. A Joule-Thomson Cascade Liquefier for Helium	504
Dr. R. STREET and Mr. J. C. WOOLLEY. Time Decrease of Magnetic Permeability in Alnico	509
Prof. L. F. BATES and Mr. J. R. MALLARD. The Magnetic Properties of Uranium and Uranium-Iron Alloys	520
Dr. E. H. LINFOOT. On Phase-Contrast Testing with a Slit Source	527
Letters to the Editor :	
Mr. P. C. BANBURY and Dr. H. K. HENISCH. On the Frequency Response of PbS Transistors	540
Reviews of Books	541
Contents for Section A	542
Abstracts for Section A	542

ABSTRACTS FOR SECTION B

The Sliding Surface (34th Guthrie Lecture), by G. I. FINCH.

The Influence of Concentration-Dependent Diffusion on Rate of Evaporation, by J. CRANK.

ABSTRACT. It has been suggested that evaporation through a membrane or from a polymer film has a characteristic behaviour different from that commonly associated with a free liquid surface. In particular it is claimed that an increase in surface humidity produces an increased rate of evaporation through a membrane, though the opposite effect is well known for a liquid surface. This behaviour is said to be observed when diffusion within the membrane or film is the rate controlling process in systems for which the diffusion coefficient increases with increasing concentration.

In this paper the behaviour of such diffusion-controlled evaporation processes is examined from the point of view of the diffusion equations and it is found that there is no theoretical reason to expect such processes to show anomalous behaviour.

It is seen that when the experimental data for evaporation through a membrane are correctly interpreted they are in agreement with theoretical prediction.

The so-called 'skin effect' in the dry spinning of fibres is examined and appears to be due to complicating features other than diffusion.

The E.M.F.-Temperature Calibration of Platinum, 10% Rhodium-Platinum and Platinum, 13% Rhodium-Platinum Thermocouples over the Temperature Range 0°-1,760 °C., by C. R. BARBER.

ABSTRACT. E.M.F. temperature reference tables are given for platinum, 10% rhodium-platinum and platinum, 13% rhodium-platinum thermocouples over the range from 0° to 1,750° C. The tables are based on the calibration of twelve thermocouples of each kind, six from each of two manufacturers. Each set of six thermocouples comprised two samples from each of three batches of wire. The calibrations are in terms of the International Temperature Scale as revised at the Ninth General Conference of Weights and Measures held in Paris in October 1948.

The methods of intercomparison between the thermocouples and the various interpolation instruments specified in the International Temperature Scale are described. It is shown that the differences between the new tables and the old are mainly due to changes in the International Temperature Scale, and that the new tables represent the shape of the E.M.F.-temperature characteristics of the thermocouples of either make sufficiently closely to give interpolation between calibration points with accuracy within $\pm 1^\circ \text{C.}$ up to $1,063^\circ \text{C.}$, $\pm 2^\circ \text{C.}$ up to $1,550^\circ \text{C.}$, and $\pm 3^\circ \text{C.}$ above this temperature.

A Joule-Thomson Cascade Liquefier for Helium, by J. ASHMEAD.

ABSTRACT. A helium liquefier has been constructed with an output of 3.8 litres per hour and a starting time of 70 minutes. The liquid hydrogen needed to cool the helium below its inversion temperature is provided continuously by a hydrogen liquefier within the same machine. The advantages of the machine are (i) short starting time, (ii) simplicity of operation and ease of servicing, (iii) closed hydrogen circuit.

Time Decrease of Magnetic Permeability in Alnico, by R. STREET and J. C. WOOLLEY.

ABSTRACT. The formal theory, based on the concept of thermal activation of domain processes, previously proposed to account for the phenomenon of magnetic viscosity, has been extended to describe time decrease of permeability. Within certain limits the predictions of the theoretical analysis are verified by measurements made on time decrease of permeability using an alnico rod specimen. It is shown that the quantitative results of these measurements are in good agreement with those obtained from the magnetic viscosity experiments. The possible physical mechanisms responsible for both magnetic viscosity and time decrease of permeability in alnico are discussed.

The Magnetic Properties of Uranium and Uranium-Iron Alloys, by L. F. BATES and J. R. MALLARD.

ABSTRACT. Measurements have been made of the magnetic susceptibility of fairly pure uranium and of 5 and 10 atomic per cent alloys of iron with uranium. Using a modification of the Curie method, with special pole-pieces and electromagnetic dynamometer control, the specimens were found to be paramagnetic with no trace of ferromagnetism in the temperature range 20° to 350°C. At 20°C. the susceptibility of pure uranium is $+1.740 \times 10^{-6}$ E.M.U. per gm., increasing to $+1.804 \times 10^{-6}$ at 350°C. ; the results fit the equation

$$\chi_U = 32 \times 10^{-11} T + 1.564 \times 10^{-6} + 24.0 \times 10^{-6} / T.$$

Assuming that the iron is present in form of the compound U_6Fe , it is found that the latter has a susceptibility of $+2.036 \times 10^{-6}$ E.M.U. per gm. at 20°C. , which remains practically constant with temperature.

On Phase-Contrast Testing with a Slit Source, by E. H. LINFOOT.

ABSTRACT. In the standard form of the phase contrast test, the light-source is a pinhole comparable in size with the Airy disc of the system under test. As a consequence, it is difficult to obtain enough light through the pinhole to carry out the test with full efficiency. If a slit source and a phase-changing strip are used this difficulty is overcome, but the properties of the test are altered; for example, the brightness distribution seen on the surface of a true mirror under the test is no longer radially symmetrical.

In the present paper the properties of the phase-strip test are examined in the mathematically simplest case where the light-source is a slit of negligible width, passing monochromatic light, and it is concluded that the test can safely be used in figuring an optical surface to an accuracy of about one twentieth of a fringe. Below this limit, the systematic error inherent in the usual interpretation of the test begins to be appreciable in the case of slow errors, though rapid local errors are correctly seen right up to the limit of sensitivity of the test.

PHYSICAL SOCIETY PUBLICATIONS

Fellows and Student Members of the Society may obtain ONE copy of each publication at the price shown in brackets. In most cases the cost of postage and packing is extra.

- Noise and Sound Transmission.* Report of the 1948 Summer Symposium of the Acoustics Group of the Physical Society. Pp. 200. In paper covers. 17s. 6d. (10s. 6d.) Postage 6d.
- Resonant Absorbers and Reverberation.* Report of the 1947 Summer Symposium of the Acoustics Group of the Physical Society. Pp. 57. In paper covers. 7s. 6d. (5s.) Postage 6d.
- The Emission Spectra of the Night Sky and Aurorae, 1948.* Papers read at an International Conference held under the auspices of the Gassiot Committee in London in July 1947. Pp. 140. In paper covers. 20s. (12s. 6d.) Postage 6d.
- The Strength of Solids, 1948.* Report of Conference held at Bristol in July 1947. Pp. 162. In paper covers. 25s. (15s. 6d.) Postage 8d.
- Report of International Conference on Fundamental Particles (Vol. I) and Low Temperatures (Vol. II), 1947.* Conference held at Cambridge in July 1946. Pp. 200 (Vol. I), pp. 184 (Vol. II). In paper covers. 15s. each vol. (7s. 6d.) Postage 8d.
- Meteorological Factors in Radio-Wave Propagation, 1947.* Report of Conference held jointly with the Royal Meteorological Society in April 1946. Pp. 325. In paper covers. 24s. (12s. + postage 1s.)
- Handbook of the 34th Exhibition of Scientific Instruments and Apparatus, 1950.* Pp. xii + 266. In paper covers. 5s. (2s. 6d.) Postage 1s.
- Handbook of the 33rd Exhibition of Scientific Instruments and Apparatus, 1949.* Pp. 272. In paper covers. 5s. (2s. 6d.) Postage 1s.
- Catalogue of the 32nd Exhibition of Scientific Instruments and Apparatus, 1948.* Pp. 288. In paper covers. 5s. (2s. 6d.) Postage 1s. (Half price from 5th April 1949).
- Catalogue of the 31st Exhibition of Scientific Instruments and Apparatus, 1947.* Pp. 298. In paper covers. 2s. 6d. (1s. 6d.) Postage 1s.
- Report on Colour Terminology, by a Committee of the Colour Group.* Pp. 56. In paper covers. 7s. (3s. 6d.)
- Report on Defective Colour Vision in Industry, by a Committee of the Colour Group. 1946.* Pp. 52. In paper covers. 3s. 6d. (1s. 9d. + postage 4d.)
- Science and Human Welfare.* Conference held by the Association of Scientific Workers, Physical Society and other bodies. 1946. Pp. 71. In paper covers. 1s. 6d. (9d.) Postage 4d.
- Report on the Teaching of Geometrical Optics, 1934.* Pp. 86. In paper covers. 6s. 3d. Postage 6d.
- Report on Band Spectra of Diatomic Molecules, 1932.* By W. JEVONS, D.Sc., Ph.D. Pp. 308. In paper covers, 25s.; bound in cloth, 30s. (15s.) Postage 1s.
- Discussion on Vision, 1932.* Pp. 327. In paper covers. 6s. 6d. (3s. 3d.) Postage 1s.
- Discussion on Audition, 1931.* Pp. 151. In paper covers. 4s. (2s.) Postage 1s.
- Discussion on Photo-electric Cells and their Application, 1930.* Pp. 236. In paper covers. 6s. 6d. (3s. 3d.) Postage 8d.
- The Decimal Bibliographic Classification (Optics, Light and Cognate Subjects), 1926.* By A. F. C. POLLARD, D.Sc. Pp. 109. Bound in cloth. 4s. (2s.) Postage 8d.
- Motor Headlights, 1922.* Pp. 39. In paper covers. 1s. 6d. (9d.) Postage 4d.
- Report on Series in Line Spectra, 1922.* By A. FOWLER, C.B.E., Sc.D., F.R.S. Pp. 182. In paper covers. 30s. (15s.) Postage 8d.
- A Discussion on the Making of Reflecting Surfaces, 1920.* Pp. 44. In paper covers. 2s. 6d. (1s. 3d.) Postage 4d.
- Reports on Progress in Physics.* Vol. XIII (1949-50). Bound in cloth. 50s. (25s.) Postage 1s.
- Reports on Progress in Physics.* Vol. XII (1948-49). Pp. 382. Bound in cloth. 42s. (25s.) Postage 1s.
- Reports on Progress in Physics.* Vol. XI (1946-48). Pp. 461. Bound in cloth. 42s. (25s.) Postage 1s.
- Reports on Progress in Physics.* Vols. IV (1937, reprinted 1946) and X (1944-45). Bound in cloth. 30s. each. (15s.) Postage 1s.
- The Proceedings of the Physical Society.* From Vol. I (1874-75), excepting a few parts which are out of print. Prices on application to Messrs. Wm. Dawson Ltd., 102 Wigmore St., London W.1.
- The Transactions of the Optical Society.* Vols. 1 (1899-1900) - 33 (1931-32), excepting a few parts which are out of print. Prices on application to Messrs. Wm. Dawson Ltd., 102 Wigmore St., London W.1.

Orders, accompanied by remittances, should be sent to

THE PHYSICAL SOCIETY

1 Lowther Gardens, Prince Consort Road, London S.W.7

The PHILOSOPHICAL MAGAZINE

(First Published 1798)

*A Journal of
Theoretical, Experimental
and Applied Physics*

EDITOR:
PROFESSOR N. F. MOTT,
M.A., D.Sc., F.R.S.

EDITORIAL BOARD:
SIR LAWRENCE BRAGG,
O.B.E., M.C., M.A., D.Sc., F.R.S.

ALLAN FERGUSON,
M.A., D.Sc.

SIR GEORGE THOMSON,
M.A., D.Sc., F.R.S.

PROFESSOR A. M. TYNDALL,
C.B.E., D.Sc., F.R.S.



Established 150 Years

ANNUAL SUBSCRIPTION

£5 2s. 6d.

OR

10s. 6d.
EACH MONTH
POST-FREE

Contents for July 1950

C. G. B. GARRETT (Royal Society Mond Laboratory, Cambridge). "The Thermal Conductivity of Potassium Chrome Alum at Temperatures below One Degree Absolute".

VERA DANIEL (British Electrical Research Association). "The Crystallography and Thermodynamics of Order-Disorder Transitions in certain Mixed Ketones".

W. THIRRING (Dublin Institute for Advanced Studies). "On a Fourth-Order Meson-Equation".

H. JONES (Mathematics Department, Imperial College, London). "The Effect of Electron Concentration on the Lattice Spacings in Magnesium Solid Solutions".

L. BOURNE & R. HILL (Metal Flow Research Laboratory, Sheffield). "On the Correlation of the Directional Properties of Rolled Sheet in Tension and Cupping Tests".

J. S. GREENHOW (University of Manchester). "The Fluctuation and Fading of Radio Echoes from Meteor Trails".

C. D. ELLYETT (University of Manchester). "The Influence of High Altitude Winds on Meteor Trail Ionization".

A. G. CARLSON, J. E. HOOPER & D. T. KING (The H. H. Wills Physical Laboratory, University of Bristol). "Nuclear Transmutations produced by Cosmic-Ray Particles of Great Energy.—Part V. The Neutral Mesons".

CORRESPONDENCE:

P. E. HODGSON. "Gap Measurement as a Method of Analysing Cosmic Ray Stars in Emulsions".

C. B. DAISH, D. H. FENDER & A. J. WOODALL (Military College of Science, Physics Branch). "A Note on the Use of Resistance Thermometers for Measurement of Rapidly Changing Temperatures".

BOOK REVIEWS.

TAYLOR & FRANCIS LTD., Red Lion Court, Fleet St., LONDON, E.C.4

Printed by TAYLOR AND FRANCIS, LTD., Red Lion Court, Fleet Street, London E.C.4